THE MECHANISM OF ACTION OF ISOPRENE IN PLANTS

By

Christopher M. Harvey

A DISSERTATION

Submitted to
Michigan State University
in partial fulfillment of the requirements
for the degree of

Biochemistry and Molecular Biology–Doctor of Philosophy

2015

ABSTRACT

THE MECHANISM OF ACTION OF ISOPRENE IN PLANTS

By

Christopher M. Harvey

Isoprene is a five carbon volatile hydrocarbon that is synthesized in the chloroplasts of some but not all plant species. Isoprene is produced from the end product of a stroma-localized metabolic pathway which draws upon metabolites produced from photosynthesis. It is produced by the action of a dedicated enzyme, which is also stroma-localized. Upon synthesis it volatilizes and is immediately lost from the synthesizing leaf, with no known storage mechanisms. In emitting plants, as much as 20% of recently fixed carbon may be released back to the atmosphere as isoprene. The purpose of this wasteful metabolic flux is unclear and has been the focus of much study. The rate of isoprene emission is known to increase in response to high light and temperature stress, which has led to the hypothesis that it is a thermotolerance mechanism, and specifically a mechanism for the thermoprotection of photosynthesis. There are two competing hypotheses for how isoprene accomplishes this. The first and most widely accepted hypothesis is that isoprene, which is hydrophobic, intercalates into the thylakoid membrane and prevents the heat-induced modulation of membrane dynamics. The second hypothesis is that isoprene protects the thylakoid membrane lipids by scavenging reactive oxygen species. The work presented in this dissertation focused on several physiological consequences of isoprene emission from plants, both to resolve the membrane vs. antioxidant debate and to reveal novel functions. First, the effect of isoprene on gene expression in *Arabidopsis thaliana* was assessed through a microarray study. This study revealed that isoprene causes several gene expression changes that are similar to changes induced by abiotic stress. Isoprene was specifically found to induce the expression of

phenylpropanoid biosynthetic genes and a suite of stress-responsive transcription factors. These changes are inconsistent with the putative mechanisms of isoprene in reducing abiotic-stress, and suggests that isoprene is also a signaling molecule. It is hypothesized that isoprene alters gene expression by activating the biogenic volatile organic compound sensing machinery in plants. The nature of this sensing apparatus is unknown. To test the antioxidant hypothesis, the ability of isoprene to mitigate the toxicity of methyl vinyl ketone was tested. Methyl vinyl ketone is a product of the oxidative degradation of isoprene. Isoprene was found to prevent the induction of H_2O_2 and marker genes by methyl vinyl ketone, suggesting that it in fact does not act by conversion to methyl vinyl ketone. This result argues against the antioxidant hypothesis. The effect of isoprene on native and synthetic membranes was also tested using a variety of biophysical techniques. Two probes of membrane properties were used to assess the effect of isoprene on bilayer thickness and fluidity. Only the proteinaceous probe showed an effect of isoprene. The quantity of isoprene in bilayer membranes was measured and found to be much lower than previously thought. This suggests that isoprene does not work by modulating the dynamics of the bulk lipid phase of membranes and is the most compelling evidence to date against the lipid-acyl membrane mechanism of isoprene action. Rather, it is suggested that isoprene mediates thermoprotective effects by binding to and altering the dynamics of membrane-embedded proteins. This is similar to the mode of action of volatile anesthetics, and suggests a potentially much wider range of targets. This may also be the mechanism by which isoprene modulates gene expression changes.

ACKNOWLEDGEMENTS

I first want to thank my advisor, Dr. Thomas Sharkey, for his helpful criticism and support during the course of my degree. The lab environment that you have provided has been a wonderful place to explore my scientific ideas. I am grateful for the mistakes that you allowed me to make. Thank you for reigning me in when I was off course. Although it has been a painful process at times, I am better off because of it.

Thank you to my committee members Dr. David Weliky, Dr. Shelagh Ferguson-Miller, Dr. Gregg Howe, and Dr. Claire Vieille. You introduced me to foreign concepts and provided outside perceptions of my work that were tremendously useful in orienting my research within the broader body of human knowledge.

Thank you to all of the members of the Sharkey lab that have helped me over the years. Thank you in particular to Dr. Sean Weise, who has offered indispensable support to my studies and positive, humorous commentary at every available opportunity. Our gym sessions have been a highlight of my graduate school life. Your hilarious emails while I was in Germany kept my spirits up despite the pressure of conducting experiments while performing in a German rock band, being an international spy, and winning the Tour de France. Thanks also to Dr. Aparajita Banerjee and Dr. Ziru Li, who have been like siblings over the years. I really enjoyed our game nights and commiserating with you when things were not working. Thank you to Dr. Dilara Ally for teaching me much about R. Thank you to all of the other past and present members whose names are too numerous to list here.

Thank you to my friends and family for pushing me to complete my degree when the probability of a masters came up, and for keeping me grounded throughout this process.

TABLE OF CONTENTS

LIST OF TABLES

LIST OF FIGURES

KEY TO ABBREVIATIONS

ATP	adenosine triphosphate
BVOC	biogenic volatile organic carbon
CDP-ME	4-diphosphocytidyl-2-methylerythritol
CDP-MEP	4-diphosphocytidyl-2-methyerythritol-2-phosphate
CMK	4-diphosphocytidyl-2-methylerythritol kinase
CMS	4-diphosphocytidyl-2-methylerythritol synthase
DEG	differentially expressed gene
DMADP	dimethylallyldiphosphate
DMPC	dimyristoylphosphatidylcholine
DSPC	distearoylphosphatidylcholine
DNA	deoxyribonucleic acid
DXP	1-deoxyxylulose-5-phosphate
DXR	1-deoxyxylulose-5-phosphate reductoisomerase
DXS	1-deoxyxylulose-5-phosphate synthase
ERF	ethylene response factor
ES	enrichment score
FW	fresh weight
HDR	4-hydroxy-3-methylbut-2-enyldiphosphate reductase
HDS	4-hydroxy-3-methylbut-2-enyldiphosphate synthase
HMBDP	4-hydroxy-3-methylbut-2-enyldiphosphate

GAP	glyceraldehyde-2-phosphate
GC-FAME	gas chromatography fatty acid methyl ester analysis
GSEA	gene set enrichment analysis
H_2O_2	hydrogen peroxide
IDI	isopentenyldiphosphate isomerase
IDP	isopentenyldiphosphate
IE	isoprene-emitting
ISP	isoprene
IspS	isoprene synthase
K_{OW}	octanol-water partition coefficient
MEcDP	2-C-methyl-D-erythritol-2,4-cyclodiphosphate
MEP	2-C-methyl-D-erythritol
MVK	methyl vinyl ketone
NADPH	nicotinamide adenine dinucleotide
NE	non-emitting
PAL	phenylalanine ammonia lyase
PE	phosphatidylethanolamine
PCR	polymerase chain reaction
PSII	photosystem II
qRT-PCR	quantitative reverse transcription PCR
RNA	ribonucleic acid
RNAi	RNA interference

ROS	reactive oxygen species
SLPC	1-stearoyl-2-linoleoylphosphatidylcholine
SOPC	1-stearoyl-2-oleoylphosphatidylcholine
$^1O_2$	singlet oxygen
4CL	4-coumarate-CoA ligase

Chapter 1

Literature Review

Introduction

Isoprene (2-methyl-1,3-butadiene) is a simple terpene that is abundantly produced in plants. Upon its synthesis, it is immediately volatilized to the atmosphere, with no known storage mechanisms (Sanadze, 2010). Its high emission rate from certain plants was discovered in the middle of the twentieth century and has since been the subject of study in a wide variety of fields (Sanadze, 2004). The pathway for isoprene production has only been elucidated within the past few decades and its regulatory mechanisms are still under study (Cordoba et al., 2009; Banerjee and Sharkey, 2014). In contrast, the environmental regulation of isoprene emission is well understood, as are the effects of isoprene on atmospheric chemistry. Its physiological effects in plants are still being cataloged and its mode(s) of action, based on these physiological effects, are still being debated (Sharkey et al., 2008; Velikova et al., 2012).

Understanding the molecular mechanism of action and biological function of isoprene is important for several reasons. The study of isoprene regulation and function in plants grew out of a desire to better inform models of future emission rates, and that need is more urgent than ever. Isoprene is a significant contaminant in modern, high nitric and nitrous oxide (NO_x) atmospheres. Some future emission models incorporating the effect of land-use changes have predicted that deforestation will lead to future declines in global isoprene emission rates (Heald et al., 2008; Ganzeveld et al., 2010; Lathière et al., 2010). However, isoprene emission is more prevalent in hot, arid climates and it is possible that the composition of temperate forests will shift towards isoprene emitting species in the future. The characteristics of global climate change, including the alteration of CO_2, temperature, and ozone levels can have differing effects

on overall isoprene emission rate, and it is therefore unclear whether isoprene emission will increase or decrease in the future (Sharkey and Monson, 2014). Understanding the biological function of isoprene could lead to elucidation of previously neglected environmental variables that affect emission rates, as well as future changes in forest composition.

Isoprene is an industrial feedstock in the production of rubber and various chemicals. Therefore, efforts have been made to produce isoprene at large scales from microorganisms engineered to overexpress isoprene biosynthetic genes (Zurbriggen et al., 2012). Understanding the potential consequences of isoprene on the biology of microorganisms could be crucial for the viability of those systems. Finally, many crop species do not emit isoprene, and introduction of the capacity for emission could improve crop production in a warming climate. Understanding the function of isoprene would allow better prediction of which crops, under what conditions, are likely to benefit from isoprene emission.

Biological basis and regulation of isoprene emission

Precursor production

Terpenes and isoprene are derived from the precursor dimethylallyldiphosphate (DMADP), which exists in equilibrium with its isomeric form isopentenyldiphosphate (IDP) (Zhou et al., 2013). Plants possess two distinct and noninteracting pathways for DMADP production: the mevalonic acid pathway in the cytosol and the methyl erythritol phosphate (MEP) pathway in the plastid (Fig. 1.1). Isoprene synthase is located within chloroplasts, only DMADP from the MEP

pathway is available for isoprene production.

The existence of the MEP pathway was recognized in the early 1990s and fully elucidated by the early 2000s. Seven stromal enzymes convert photosynthetically derived glyceraldehyde-3-phosphate and pyruvate to DMADP using reducing and ATP equivalents derived from the photosynthetic electron transport chain. Given its recent discovery, regulatory mechanisms of the pathway are still being discovered. Recently, the pathway was discovered to be subject to feedback inhibition of the committed step by DMADP (Banerjee et al., 2013). Other enzymes in the pathway are likely regulated in the short term by phosphorylation and stromal redox status (Li and Sharkey, 2013; Banerjee and Sharkey, 2014). There is also evidence for transcriptional and translational control of pathway enzyme levels (Vranová et al., 2013).

Isoprene synthase

After production of DMADP by the MEP pathway, the final step in the biosynthesis of isoprene is cleavage of the pyrophosphate moiety by isoprene synthase to yield isoprene. The enzyme has a K_m in the low millimolar range as well as a low turnover number, which has led to the conclusion that it is inefficient relative to synthases of some higher isoprenoids (Silver and Fall, 1995; Sharkey et al., 2005). Both stromal and thylakoid anchored isoforms exist (Wildermuth and Fall, 1998; Schnitzler et al., 2005; Wiberley et al., 2005). Isoprene synthase protein levels are developmentally and environmentally regulated, but fine temporal control of isoprene emission rate appears to be controlled by changes in DMADP availability, rather than by abundance or activity of the synthase (Vickers et al., 2010).

Not all plants contain isoprene synthase, and the phylogenetic distribution of this enzyme has been intensely studied to determine past losses and gains. A consensus has yet to emerge, but it is likely that the capacity for isoprene emission has been gained and lost multiple times (Sharkey, 2013). The ease of gain of isoprene emission capacity has been attributed to the modest amino acid changes required to convert monoterpene synthases into functioning isoprene synthases (Gray et al., 2011; Monson et al., 2013). Rapid transition is consistent with the view that isoprene emission is adaptive only within a narrow range of phenotypes and environmental conditions.

Environmental regulation of isoprene emission rate

While our understanding of the regulatory mechanisms of the MEP pathway, and to a lesser extent of isoprene synthase, is incomplete, the effect of environmental factors on the overall emission rate is thoroughly understood. For example, isoprene emission has been recognized as light-dependent since the phenomenon was first observed (Sanadze, 2004). While light may alter the levels of isoprene synthase protein over long periods of time, in the short term this regulation is exerted through the availability of DMADP (Sasaki et al., 2005). Without light, flux through the MEP pathway ceases, as the pathway uses carbon skeletons, reducing power, and ATP equivalents from the photosynthetic electron transport chain and Calvin cycle (Rasulov et al., 2009). Post-translational redox regulation of MEP pathway enzymes may also contribute to fine tuning of the pathway flux.

Temperature also affects the rate of isoprene emission, with maximal isoprene emission

rates occurring anywhere from 38-45 °C. Interestingly, this effect cannot be explained by increasing availability of reducing power for the MEP pathway, as the stroma becomes oxidized at high temperatures (Schrader et al., 2007). An MEP pathway metabolite profiling study that was previously conducted in the lab suggests that the rapid increase is due rather to increases in the rate of isoprene synthase (Li et al., 2011). This is in agreement with kinetic studies of isoprene synthase that have placed its temperature optimum at 45-50 °C (Monson et al., 1992; Lehning et al., 1999). Therefore increases in isoprene synthase activity are believed to be responsible for rapid temperature-induced changes in isoprene emission rates. Over extended periods of heat stress damage to the photosynthetic apparatus accumulates, thus reducing the rate of photosynthesis, DMADP synthesis, and isoprene emission.

Effects and modes of action of isoprene emission

Atmospheric chemistry of isoprene

The global annual production of isoprene has been estimated at ~500 Tg (Guenther et al., 1995; Guenther et al., 2012), or slightly less than a cubic kilometer in the liquid phase. This is a significant contribution to the atmosphere and has been the impetus for much study of the gas phase chemistry of isoprene. Isoprene primarily undergoes UV-catalyzed reaction with hydroxyl radicals and ozone. Various intermediate peroxides are formed whose ultimate breakdown is affected by the concentration of NO_x (Fehsenfeld et al., 1992; Harley et al., 1999). At low NO_x concentrations isoprene effectively reduces atmospheric ozone, while at high concentrations

(such as those found in urban areas) it catalyzes ozone formation and can be considered a pollutant. Isoprene also reacts with NO_x to generate organic nitrates, which affects nitrate deposition rates (Horowitz et al., 1998; Zhang et al., 2012).

Physiological effects of isoprene emission

Under the correct conditions, native emitters can emit a quarter to one half of their recently fixed carbon as isoprene (Sharkey and Loreto, 1993; Way et al., 2011). This represents a significant loss of energy to those plants, and therefore likely provides some benefit in return. One process that could provide a large enough return on investment is photosynthesis. This view is supported by the fact that isoprene emission is maximal at 38-45 °C, temperatures at which photosynthesis is damaged. These correlations led to the discovery of isoprene-induced thermotolerance of photosynthesis by this lab in the mid 1990s (Sharkey and Singsaas, 1995; Singsaas et al., 1997). This work was performed in kudzu and suppressed native isoprene emission by incubating leaves in darkness and pure nitrogen during the course of measurements (Fig. 1.2).

This finding has been subsequently verified by other labs using a variety of techniques. The protective effect of isoprene on photosynthesis has been shown in nonemitters by fumigation as well as by transformation with isoprene synthase (Loivamäki et al., 2007; Sasaki et al., 2007; Ryan et al., 2014). In native emitters, studies have prevented endogenous production through the use of RNAi knockdown of isoprene synthase and through the use of MEP pathway inhibitors, to similar effect (Sharkey et al., 2001; Behnke et al., 2007; Behnke et al., 2010). Focus has generally been directed at the thylakoid membrane, and several studies have reported effects on

the light harvesting arrays of photosystem II (Velikova et al., 2011; Pollastri et al., 2014). However, some studies have failed to see protection (Logan et al., 1999; Logan and Monson, 1999), suggesting it is subtle and subject to factors that are not understood.

Isoprene is also known to prevent damage caused by reactive oxygen species, specifically ozone (Loreto et al., 2001; Loreto and Velikova, 2001) and singlet oxygen (Affek and Yakir, 2002). This observation may be explained by the known chemistry of isoprene in the atmosphere, and studies from many different labs have confirmed this phenomenon (Loreto et al., 2001; Loreto and Velikova, 2001; Vickers et al., 2009b). This has led some researchers to propose that ROS quenching is the basis of all of the abiotic stress mitigating properties of isoprene, including the enhanced thermoprotection of photosynthesis (Vickers et al., 2009a).

Determining how isoprene enhances photosynthetic thermotolerance

Many molecular effects of isoprene have been proposed. Linking these molecular effects to effects on whole leaf and photosynthetic physiology is difficult. As an explanation for the mitigation of myriad stresses by isoprene, the two most discussed and accepted mechanisms are ROS quenching and membrane modification. Their relative contribution to the enhancement of the photosynthetic thermotolerance by isoprene is a matter of debate. There is a causal dilemma that has made resolution of this debate difficult. The thylakoid membrane is poised for the generation of ROS in response to abiotic and biotic stress, and photosynthesis is actually a requirement for the induction of some defense responses (Chandra-Shekara et al., 2006; Göhre et al., 2012). Therefore, while the thylakoid membrane may be oxidized by ROS, a damaged

thylakoid membrane presumably generates more ROS. This represents a positive feedback loop. With such a system in mind, many of the effects of isoprene that have previously been attributed to ROS quenching or membrane stabilization may be attributed to either mechanism. Given this coupling in living systems, delineation of an exact mechanism requires quantitative analysis of the chemical and biophysical aspects of both isoprene-mediated ROS quenching and membrane perturbation.

If compounds similar to isoprene but without ROS quenching capacity (alkanes, for instance) enhanced photosynthetic thermotolerance one could eliminate ROS quenching as a likely mechanism. The ability of several small hydrophobic compounds to promote the recovery of CO_2 assimilation following a short heat stress episode was tested in *Phaseolus vulgaris* (Sharkey et al., 2001). In this study, only compounds with double bonds were beneficial. Double bonds may be necessary for the physical interaction of small molecules and the thylakoid membrane. Therefore, this approach does not resolve the two mechanisms.

Two studies have characterized the biophysical effects of isoprene on thylakoid and synthetic membranes (Velikova et al., 2011; Pollastri et al., 2014). The magnitude of the psi-type band of the circular dichroism spectrum of leaves is believed to reflect long range ordering of chiral domains, specifically light harvesting complex arrays (Dobrikova et al., 2003). Using this technique, Velikova et al. demonstrated increased thermal stability of light harvesting arrays in the presence of isoprene. Isoprene also decreased the rate of ion leakage across the thylakoid membrane and increased the thermal stability of photosystem II, as measured by the electrochromic shift and thermoluminescence, respectively. Following up on these findings, Pollastri et al. demonstrated that, under moderate heat stress conditions, isoprene increases the

proportion of captured light that is used for productive photosynthesis. Light harvesting complexes are responsible for the so called nonphotochemical quenching of fluorescence. This process is used by plants to harmlessly dissipate excess light energy as heat, and is affected by the organization of light harvesting arrays (Horton et al., 2005). It seems likely that the increased thermal stability of arrays reported by Velikova et al. is responsible for the increased photosynthetic productivity reported by Pollastri et al.

While the work of Velikova et al. and Pollastri et al. is a step towards linking the physiological and molecular effects of isoprene, these studies were performed in vivo and are still subject to the causality dilemma. Two studies of the effects of isoprene on highly controlled systems are not subject to this dilemma (Logan et al., 1999; Siwko et al., 2007). Logan et al. tested isoprene for the ability to alter the physical properties of phosphatidylcholine vesicles and isolated thylakoids and for the ability to protect these membranes from hydroxyl radical-mediated peroxidation. The rate of carboxyfluorescein leakage from vesicles, as well as the rate of proton efflux from dark-adapted thylakoids, were unaffected by isoprene. Differential scanning calorimetry of the thylakoid membrane similarly revealed no alteration in the temperature-dependent breakdown of membrane-embedded proteins and domains. The authors used a Fenton reaction to generate hydroxyl radicals in the liposome preparations, and isoprene failed to protect lipids from oxidative stress. In contrast, Siwko et al. used an in silico approach to study the effect of isoprene on the physical properties of membranes composed of dimyristoylphosphatidylcholine. Dimyristoylphosphatidylcholine is a simple lipid containing two fully saturated acyl chains that are 14 carbons in length. At 70 °C the authors predicted that isoprene would cause an increase in the lipid order parameter of the acyl chains equivalent to a

decrease in membrane temperature of 10 °C (Fig. 1.3).

More work is needed to reconcile these studies to each other and to link the molecular and physiological effects of isoprene. Only when the ROS quenching and membrane stabilization hypotheses have been refined, tested, and finally linked to the various observed physiological effects of isoprene, will one be able to consider the mechanism of action of isoprene as being solved. Until that occurs, it is prudent to continue cataloging the effects of isoprene on plants. In this thesis, I investigate the effects of isoprene on plants at the cellular and molecular level. In chapter two I report results of a microarray-based study of the gene expression changes that occur in the nonemitting plant *Arabidopsis thaliana* in response to exogenous isoprene. I observed widespread reprogramming and suggest that isoprene may have a previously unrecognized role as signaling molecule. In chapter three I use a mix of biophysical techniques and molecular biology to test aspects of both the ROS quenching and membrane hypotheses. In chapter four I determine that the concentration of isoprene in the thylakoid membrane is much lower than previously predicted. The concentrations are likely too low to alter the dynamics of the thylakoid membrane lipid chains. In chapter five I discuss the future directions that the field will need to take and the questions that will need to be answered in order to determine the mechanism of action of isoprene.

APPENDIX

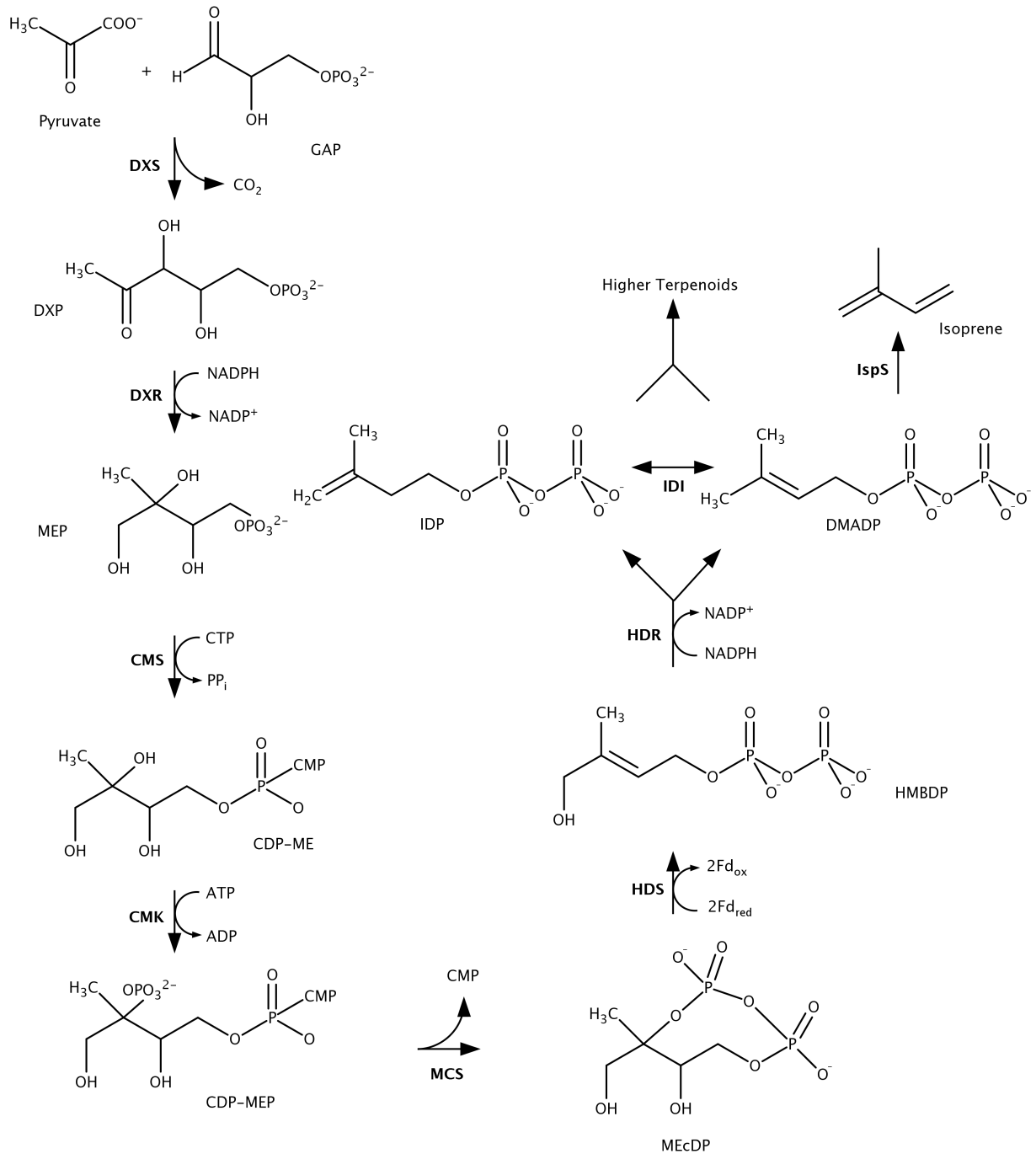

Figure 1.1 The methyl erythritol phosphate (MEP) pathway. Abbreviated enzyme names are displayed in bold lettering adjacent to their corresponding reaction arrows. Abbreviated metabolite names are displayed in normal lettering adjacent to their corresponding structures. For the full names of the enzymes and metabolites, the reader is referred to the list of abbreviations at the beginning of this thesis.

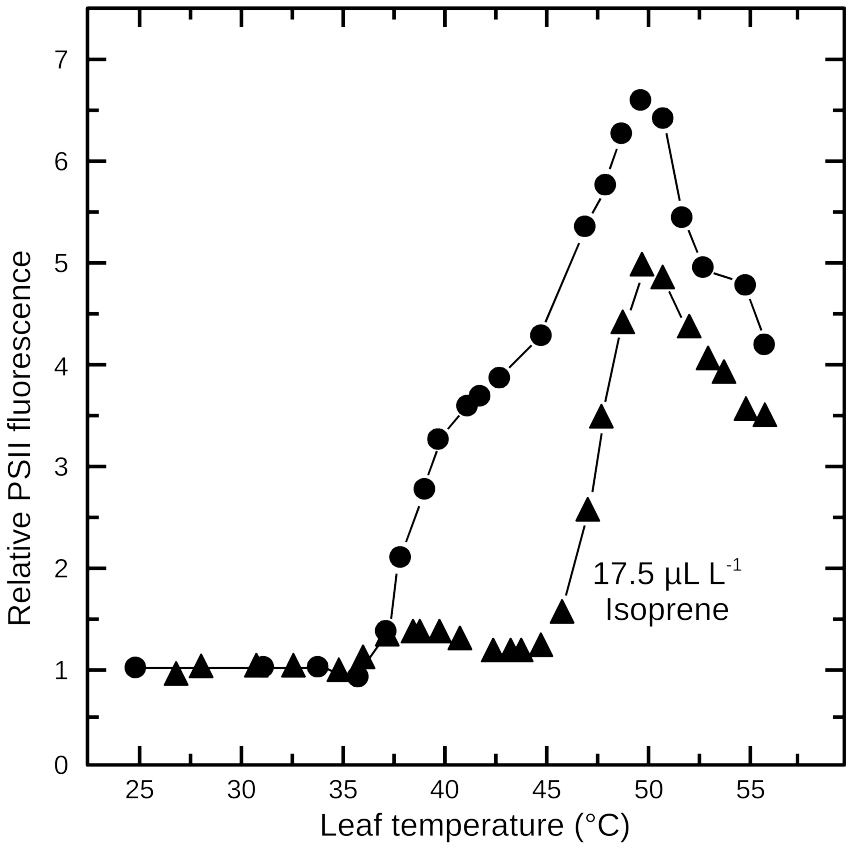

Figure 1.2 Isoprene increases the temperature of induction of photosystem II fluorescence in kudzu. Circles represent fluorescence in the absence of isoprene, triangles represent fluorescence in the presence of exogenously added isoprene. Kudzu is a native emitter, and isoprene production was inhibited by subjecting the plants to an atmosphere of pure nitrogen. Adapted from Sharkey and Singsaas, 1995.

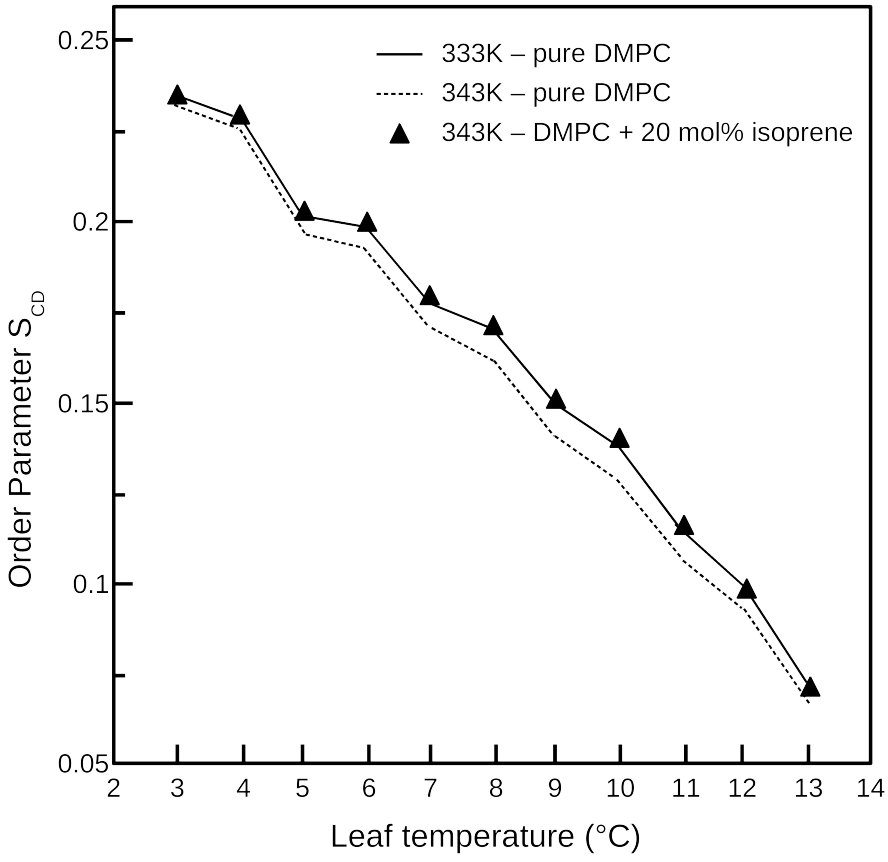

Figure 1.3 Isoprene-induced stabilization of lipid acyl chains. A larger order parameter indicates a straighter lipid chain. DMPC = dimyristoylphosphatidylcholine. Figure adapted from Siwko et al., 2007.

REFERENCES

REFERENCES

Affek HP, Yakir D (2002) Protection by isoprene against singlet oxygen in leaves. Plant Physiology **129**: 269–277

Banerjee A, Sharkey TD (2014) Methylerythritol 4-phosphate (MEP) pathway metabolic regulation. Natural Product Reports **31**: 1043–1055

Banerjee A, Wu Y, Banerjee R, Li Y, Yan H, Sharkey TD (2013) Feedback inhibition of deoxy-d-xylulose-5-phosphate synthase regulates the methylerythritol 4-phosphate pathway. Journal of Biological Chemistry **288**: 16926–16936

Behnke K, Ehlting B, Teuber M, Bauerfeind M, Louis S, Hänsch R, Polle A, Bohlmann J, Schnitzler J-P (2007) Transgenic, non-isoprene emitting poplars don't like it hot: Thermotolerance in isoprene emission knock-down mutants of poplar. The Plant Journal **51**: 485–499

Behnke K, Loivamäki M, Zimmer I, Rennenberg H, Schnitzler J-P, Louis S (2010) Isoprene emission protects photosynthesis in sunfleck exposed Grey Poplar. Photosynthesis Research **104**: 5–17

Chandra-Shekara AC, Gupte M, Navarre D, Raina S, Raina R, Klessig D, Kachroo P (2006) Light-dependent hypersensitive response and resistance signaling against Turnip Crinkle Virus in *Arabidopsis*. The Plant Journal **45**: 320–334

Cordoba E, Salmi M, León P (2009) Unravelling the regulatory mechanisms that modulate the MEP pathway in higher plants. Journal of Experimental Botany **60**: 2933–2943

Dobrikova AG, Várkonyi Z, Krumova SB, Kovács L, Kostov GK, Todinova SJ, Busheva MC, Taneva SG, Garab G (2003) Structural rearrangements in chloroplast thylakoid membranes revealed by differential scanning calorimetry and circular dichroism spectroscopy. Thermo-optic effect. Biochemistry **42**: 11272–11280

Fehsenfeld F, Calvert J, Fall R, Goldan P, Guenther AB, Hewitt CN, Lamb B, Liu S, Trainer M, Westberg H, et al (1992) Emissions of volatile organic compounds from vegetation and the implications for atmospheric chemistry. Global Biogeochemical Cycles **6**: 389–430

Ganzeveld L, Bouwman L, Stehfest E, van Vuuren DP, Eickhout B, Lelieveld J (2010) Impact of future land use and land cover changes on atmospheric chemistry-climate interactions. Journal of Geophysical Research: Atmospheres **115**: D23301

Göhre V, Jones AM, Sklenár J, Robatzek S, Weber AP (2012) Molecular crosstalk between PAMP-triggered immunity and photosynthesis. Molecular Plant-Microbe Interactions **25**: 1083–1092

Gray DW, Breneman SR, Topper LA, Sharkey TD (2011) Biochemical characterization and homology modeling of methylbutenol synthase and implications for understanding hemiterpene synthase evolution in plants. Journal of Biological Chemistry **286**: 20582–20590

Guenther AB, Hewitt CN, Erickson D, Fall R, Geron C, Graedel T, Harley P, Klinger L, Lerdau M, Mckay WA, et al (1995) A global model of natural volatile organic compound emissions. Journal of Geophysical Research: Atmospheres **100**: 8873–8892

Guenther AB, Jiang X, Heald CL, Sakulyanontvittaya T, Duhl T, Emmons LK, Wang X (2012) The Model of Emissions of Gases and Aerosols from Nature version 2.1 (MEGAN2.1): an extended and updated framework for modeling biogenic emissions. Geoscientific Model Development **5**: 1503–1560

Harley PC, Monson RK, Lerdau MT (1999) Ecological and evolutionary aspects of isoprene emission from plants. Oecologia **118**: 109–123

Heald CL, Henze DK, Horowitz LW, Feddema J, Lamarque J-F, Guenther A, Hess PG, Vitt F, Seinfeld JH, Goldstein AH, et al (2008) Predicted change in global secondary organic aerosol concentrations in response to future climate, emissions, and land use change. Journal of Geophysical Research: Atmospheres **113**: D05211

Horowitz LW, Liang J, Gardner GM, Jacob DJ (1998) Export of reactive nitrogen from North America during summertime: Sensitivity to hydrocarbon chemistry. Journal of Geophysical Research: Atmospheres **103**: 13451–13476

Horton P, Wentworth M, Ruban A (2005) Control of the light harvesting function of chloroplast membranes: The LHCII-aggregation model for non-photochemical quenching. FEBS Letters **579**: 4201–4206

Lathière J, Hewitt CN, Beerling DJ (2010) Sensitivity of isoprene emissions from the terrestrial biosphere to 20th century changes in atmospheric CO2 concentration, climate, and land use. Global Biogeochemical Cycles **24**: GB1004

Lehning A, Zimmer I, Steinbrecher R, Brüggemann N, Schnitzler J-P (1999) Isoprene synthase activity and its relation to isoprene emission in *Quercus robur* L-leaves. Plant, Cell & Environment **22**: 495–504

Li Z, Ratliff EA, Sharkey TD (2011) Effect of temperature on postillumination isoprene emission in oak and poplar. Plant Physiology **155**: 1037–1046

Li Z, Sharkey TD (2013) Metabolic profiling of the methylerythritol phosphate pathway reveals the source of post-illumination isoprene burst from leaves: MEcDP supports dark isoprene emission. Plant, Cell & Environment **36**: 429–437

Logan BA, Anchordoquy TJ, Monson RK, Pan RS (1999) The effect of isoprene on the properties of spinach thylakoids and phosphatidylcholine liposomes. Plant Biology **1**: 602–606

Logan B, Monson R (1999) Thermotolerance of leaf discs from four isoprene-emitting species is not enhanced by exposure to exogenous isoprene. Plant Physiology **120**: 821–825

Loivamäki M, Gilmer F, Fischbach RJ, Sorgel C, Bachl A, Walter A, Schnitzler J-P (2007) *Arabidopsis*, a model to study biological functions of isoprene emission? Plant Physiology **144**: 1066–1078

Loreto F, Mannozzi M, Maris C, Nascetti P, Ferranti F, Pasqualini S (2001) Ozone quenching properties of isoprene and its antioxidant role in leaves. Plant Physiology **126**: 993–1000

Loreto F, Velikova V (2001) Isoprene produced by leaves protects the photosynthetic apparatus against ozone damage, quenches ozone products, and reduces lipid peroxidation of cellular membranes. Plant Physiology **127**: 1781–1787

Monson RK, Jaeger CH, Adams WW, Driggers EM, Silver GM, Fall R (1992) Relationships among isoprene emission rate, photosynthesis, and isoprene synthase activity as influenced by temperature. Plant Physiology **98**: 1175–1180

Monson RK, Jones RT, Rosenstiel TN, Schnitzler J-P (2013) Why only some plants emit isoprene. Plant, Cell & Environment **36**: 503–516

Pollastri S, Tsonev T, Loreto F (2014) Isoprene improves photochemical efficiency and enhances heat dissipation in plants at physiological temperatures. Journal of Experimental Botany **65**: 1565–1570

Rasulov B, Huve K, Valbe M, Laisk A, Niinemets Ü (2009) Evidence that light, carbon dioxide, and oxygen dependencies of leaf isoprene emission are driven by energy status in hybrid aspen. Plant Physiology **151**: 448–460

Ryan AC, Hewitt CN, Possell M, Vickers CE, Purnell A, Mullineaux PM, Davies WJ, Dodd IC (2014) Isoprene emission protects photosynthesis but reduces plant productivity during drought in transgenic tobacco (*Nicotiana tabacum*) plants. New Phytologist **201**: 205–216

Sanadze GA (2010) Photobiosynthesis of isoprene as an example of leaf excretory function in the light of contemporary thermodynamics. Russian Journal of Plant Physiology **57**: 1–6

Sanadze GA (2004) Biogenic isoprene (a review). Russian Journal of Plant Physiology **51**: 729–741

Sasaki K, Ohara K, Yazaki K (2005) Gene expression and characterization of isoprene synthase from *Populus alba*. FEBS Letters **579**: 2514–2518

Sasaki K, Saito T, Lämsä M, Oksman-Caldentey K-M, Suzuki M, Ohyama K, Muranaka T, Ohara K, Yazaki K (2007) Plants utilize isoprene emission as a thermotolerance mechanism. Plant and Cell Physiology **48**: 1254–1262

Schnitzler J-P, Zimmer I, Bachl A, Arend M, Fromm J, Fischbach RJ (2005) Biochemical properties of isoprene synthase in poplar (*Populus* × *canescens*). Planta **222**: 777–786

Schrader SM, Kleinbeck KR, Sharkey TD (2007) Rapid heating of intact leaves reveals initial effects of stromal oxidation on photosynthesis. Plant, Cell & Environment **30**: 671–678

Sharkey TD (2013) Is it useful to ask why plants emit isoprene?: Isoprene synthase evolution. Plant, Cell & Environment **36**: 517–520

Sharkey TD, Chen X, Yeh S (2001) Isoprene increases thermotolerance of fosmidomycin-fed leaves. Plant Physiology **125**: 2001–2006

Sharkey TD, Loreto F (1993) Water stress, temperature, and light effects on the capacity for isoprene emission and photosynthesis of kudzu leaves. Oecologia **95**: 328–333

Sharkey TD, Monson RK (2014) The future of isoprene emission from leaves, canopies and landscapes. Plant, Cell & Environment **37**: 1727–1740

Sharkey TD, Singsaas E (1995) Why plants emit isoprene. Nature **374**: 769–769

Sharkey TD, Wiberley AE, Donohue AR (2008) Isoprene emission from plants: why and how. Annals of Botany **101**: 5–18

Sharkey TD, Yeh S, Wiberley AE, Falbel TG, Gong D, Fernandez DE (2005) Evolution of the isoprene biosynthetic pathway in kudzu. Plant Physiology **137**: 700–712

Silver G, Fall R (1995) Characterization of aspen isoprene synthase, an enzyme responsible for leaf isoprene emission to the atmosphere. Journal of Biological Chemistry **270**: 13010–13016

Singsaas EL, Lerdau M, Winter K, Sharkey TD (1997) Isoprene increases thermotolerance of isoprene-emitting species. Plant Physiology **115**: 1413–1420

Siwko ME, Marrink SJ, de Vries AH, Kozubek A, Schoot Uiterkamp AJM, Mark AE (2007) Does isoprene protect plant membranes from thermal shock? A molecular dynamics study. Biochimica et Biophysica Acta - Biomembranes **1768**: 198–206

Velikova V, Sharkey TD, Loreto F (2012) Stabilization of thylakoid membranes in isoprene-emitting plants reduces formation of reactive oxygen species. Plant Signaling & Behavior **7**: 139–41

Velikova V, Várkonyi Z, Szabó M, Maslenkova L, Nogues I, Kovács L, Peeva V, Busheva M, Garab G, Sharkey TD, et al (2011) Increased thermostability of thylakoid membranes in isoprene-emitting leaves probed with three biophysical techniques. Plant Physiology **157**: 905–916

Vickers CE, Gershenzon J, Lerdau MT, Loreto F (2009a) A unified mechanism of action for volatile isoprenoids in plant abiotic stress. Nature Chemical Biology **5**: 283–291

Vickers CE, Possell M, Cojocariu CI, Velikova VB, Laothawornkitkul J, Ryan A, Mullineaux PM, Nicholas Hewitt C (2009b) Isoprene synthesis protects transgenic tobacco plants from oxidative stress. Plant, Cell & Environment **32**: 520–531

Vickers CE, Possell M, Hewitt CN, Mullineaux PM (2010) Genetic structure and regulation of isoprene synthase in Poplar (*Populus* spp.). Plant Molecular Biology **73**: 547–558

Vranová E, Coman D, Gruissem W (2013) Network analysis of the MVA and MEP pathways for isoprenoid synthesis. Annual Review of Plant Biology **64**: 665–700

Way DA, Schnitzler J-P, Monson RK, Jackson RB (2011) Enhanced isoprene-related tolerance of heat- and light-stressed photosynthesis at low, but not high, CO_2 concentrations. Oecologia **166**: 273–282

Wiberley AE, Linskey AR, Falbel TG, Sharkey TD (2005) Development of the capacity for isoprene emission in kudzu. Plant, Cell & Environment **28**: 898–905

Wildermuth MC, Fall R (1998) Biochemical characterization of stromal and thylakoid-bound isoforms of isoprene synthase in willow leaves. Plant Physiology **116**: 1111–1123

Zhang L, Jacob DJ, Knipping EM, Kumar N, Munger JW, Carouge CC, van Donkelaar A, Wang YX, Chen D (2012) Nitrogen deposition to the United States: distribution, sources, and processes. Atmospheric Chemistry and Physics **12**: 4539–4554

Zhou C, Li Z, Wiberley-Bradford AE, Weise SE, Sharkey TD (2013) Isopentenyl diphosphate and dimethylallyl diphosphate/isopentenyl diphosphate ratio measured with recombinant isopentenyl diphosphate isomerase and isoprene synthase. Analytical Biochemistry **440**: 130–136

Zurbriggen A, Kirst H, Melis A (2012) Isoprene production via the mevalonic acid pathway in *Escherichia coli* (bacteria). Bioenergy Research **5**: 814–828

Chapter 2

Microarray Profiling of Isoprene-Induced Transcriptional Changes in *Arabidopsis thaliana*

Abstract

Isoprene is a well-studied volatile hemiterpene that protects plants from abiotic stress through mechanisms that are not fully understood. The antioxidant and membrane stabilizing potential of isoprene are the two most commonly invoked mechanisms. However, isoprene also affects phenylpropanoid metabolism, suggesting an additional role as a signaling molecule. In this study, microarray based gene expression profiling reveals widespread transcriptional reprogramming of *Arabidopsis thaliana* plants fumigated for 24 hrs with a physiologically relevant concentration of isoprene. Functional enrichment analysis of fumigated plants revealed enhanced heat- and light-stress-responsive processes in response to isoprene. Isoprene induced a network enriched in ERF and WRKY transcription factors, which may play a role in stress tolerance. The isoprene-induced upregulation of phenylpropanoid biosynthetic genes was specifically confirmed using quantitative reverse transcription polymerase chain reaction. These results support a role for isoprene as an endogenous signaling molecule, in addition to its possible roles as an antioxidant and membrane thermoprotectant.

Introduction

Isoprene is a volatile hydrocarbon emitted from some plants. It is synthesized in the chloroplast stroma from dimethylallyldiphosphate (DMADP) by isoprene synthase, a species-specific enzyme closely related to monoterpene synthases (Silver and Fall, 1995; Miller et al., 2001; Sharkey et al., 2013). DMADP is synthesized from the primary products of photosynthesis by the chloroplast-localized methylerythritol 4-phosphate (MEP) pathway (Lichtenthaler et al., 1997; Banerjee and Sharkey, 2014). The rate of isoprene synthesis is therefore dependent on light, but is also highly temperature sensitive (Monson and Fall, 1989; Sanadze, 2004).

The global annual production of isoprene from plants has been estimated to exceed 500 Tg (Guenther et al., 1995; Arneth et al., 2008; Guenther et al., 2012). It is the single most abundant plant-derived biogenic volatile organic compound (BVOC), and contributes significantly to the formation of ozone and smog in high NO_X atmospheres (Fehsenfeld et al., 1992). Native emitters typically commit 2% of their recently fixed carbon to isoprene (Schnitzler et al., 2010; Way et al., 2011). However, the rate of isoprene emission is affected by many factors including an endogenous circadian rhythm (Loivamäki et al., 2006; Wilkinson et al., 2006), salt and drought stress (Loreto and Delfine, 2000; Fortunati et al., 2008), CO_2 (Rosenstiel et al., 2003), light, and temperature. Oak trees at 40 °C leaf temperature release 14% of photosynthesized carbon as isoprene (Way et al., 2013) and kudzu may emit 64% of its carbon under conditions that can occur naturally (Sharkey and Loreto, 1993). Poplar emits 25% of its recently fixed carbon as isoprene at 42 °C (Way et al., 2011). Given the large amount of energy and carbon required to synthesize isoprene, it is assumed it provides some benefit to the

synthesizing organism.

Isoprene protects plants from abiotic stress, especially stress of a stochastic nature. The mechanism by which it does so is still a matter of debate, though several hypotheses have been advanced. The two most widely accepted hypotheses are that isoprene stabilizes the thylakoid membrane against heat-induced denaturation (Sharkey and Singsaas, 1995; Velikova et al., 2011) and that isoprene reacts with and quenches reactive oxygen species (ROS) (Loreto et al., 2001; Loreto and Velikova, 2001; Vickers et al., 2009a; Vickers et al., 2009b; Jardine et al., 2012). Additional mechanisms are possible. For example, the over-accumulation of phosphorylated MEP pathway metabolites is postulated to be a harmful consequence of impaired MEP pathway flux which could potentially sequester phosphate from the thylakoid ATP synthase and inhibit the chloroplast electron transport chain. It has therefore been postulated that isoprene could act as a release mechanism for carbon inadvertently diverted to the methylerythritol pathway (Rosenstiel et al., 2004).

Research within the field has focused on the ROS quenching and membrane stabilizing mechanisms, and there is ongoing debate about which represents the true universal mechanism of isoprene action. In this dichotomous view of isoprene function, the possibility for isoprene as a volatile intra- or inter- plant signaling compound has been largely overlooked, despite several studies suggesting that such plant (Terry et al., 1995) or plant-animal (Laothawornkitkul et al., 2008; Loivamäki et al., 2008) signaling occurs. This is in part due to the volatility of isoprene and the brevity with which it is retained in plant tissues following synthesis (Li et al., 2011).

Previous studies have characterized the physiological, transcriptional, metabolic, and proteinaceous changes that occur in Grey Poplar engineered to reduced the amount of isoprene

synthase (Behnke et al., 2007; Behnke et al., 2009; Behnke et al., 2010a; Behnke et al., 2010b; Ghirardo et al., 2014; Velikova et al., 2014). These studies were initially focused on characterizing the heat-stress ameliorating effects of isoprene, specifically on photosynthesis. Non-emitting (NE) poplar exhibited lower electron transport and CO_2 assimilation rates in response to heat stress than did isoprene-emitting (IE) poplar, and also accumulated more zeaxanthin under non-stress conditions (Behnke et al., 2007). Photosynthesis in NE poplar was also shown to be more susceptible to oxidative stress (Behnke et al., 2009), and transient high light stress (Behnke et al., 2010b). Subsequent studies focused on the transcriptional and proteomic changes induced by isoprene emission. Over an extended period of high light and heat stress, accumulation of H_2O_2 was observed in NE leaves and correlated to the repression of anthocyanin biosynthetic genes (Behnke et al., 2010a). Reduced expression of phenylpropanoid biosynthetic genes was also observed in NE poplar. These studies represent a valuable resource for elucidating potential isoprene-responsive pathways and signaling mechanisms in native emitters. The publicly available whole-transcriptome data from two studies is particularly valuable (Behnke et al., 2010a; Behnke et al., 2010b).

To determine the mechanism(s) by which isoprene may alter gene expression in plants, it is useful to remove or mitigate as many confounding factors as possible. Two confounding factors in the study of this phenomenon in native emitters are signaling due to high-light and heat stress, and signaling due to reduced MEP pathway metabolite levels in NE lines. 2-C-methylerythritol-2,4-cyclodiphosphate (MEcDP), an MEP pathway intermediate, has been suggested as a retrograde signaling molecule of stress (Xiao et al., 2012). This has been recently corroborated by discovery of MEcDP conversion to hemiterpene glycosides (González-

Cabanelas et al., 2015). The level of MEcDP correlates with isoprene emission rate in IE poplar, but is uncoupled and heavily reduced in NE lines (Ghirardo et al., 2014). This is likely due to feedback inhibition of the committed step of the MEP pathway by DMADP (Banerjee et al., 2013). It is possible that reduction of MEcDP in NE poplar lines causes confounding alterations in signaling that could be attributed to isoprene.

In this study, isoprene-induced transcriptional changes were profiled in the non-emitting plant *Arabidopsis thaliana* under non-stressful conditions. Widespread reprogramming was observed. This included the induction of chloroplast and phenylpropanoid biosynthetic genes and the translation machinery. Fumigation of a non-emitter precludes that these changes stem from alteration of MEcDP levels, while the use of non-stressful conditions reduces the potential for confounding ROS-based signaling. Several of these transcriptional changes were present in the dataset of (Behnke et al., 2010a), suggesting a conserved signaling function for isoprene. The mechanism(s) by which isoprene is perceived and translated into transcriptional changes is unclear.

Methods and materials

Plant material

Arabidopsis thaliana (Columbia ecotype Col-0) plants were grown to maturity (5-6 weeks) under a 12 hr photoperiod in 120 µmol m^{-2} s^{-1} fluorescent lighting, 60% relative humidity, and a 23/20 °C day-night temperature. Plants were grown in UV-stabilized 4.75 inch (RLC3) Ray Leach

Cone-tainers (Hummert International, Earth City, MO, USA) in an equal mix of potting soil, perlite, and medium vermiculite. To minimize soil-atmosphere gas exchange, the top of each tube was plugged with sculpting clay and plants grew through an 8 mm diameter aperture. Plants were bottom watered twice a week with half-strength Hoagland solution. A wire mesh was placed in the bottom of each Cone-tainer to prevent soil loss. During treatments, plants were fumigated for 24 hrs in a custom-built gas exchange chamber under a 12 hr photoperiod. Lighting (120 μmol m^{-2} s^{-1}) was provided by a white LED lamp. A water bath connected to a water jacket in the base of the gas-exchange chamber maintained the temperature at 23 °C. Gases were mixed from cylinders to ratios of 80% N_2 and 20% O_2. This mix was humidified to approximately 60% relative humidity, and 400 μL L^{-1} CO_2 was added using Mass-Flo® controllers (model #1479A, MKS Instruments, Andover, MA, USA). Isoprene was added to a final concentration of 20 μL L^{-1} in the treatments where it was present (Singsaas et al., 1997). Three fumigations were performed in both the presence and absence of isoprene. Gas exchange was monitored using a LICOR 6400 photosynthesis system (LI-COR, Lincoln, NE, USA). Following treatment leaf samples were flash frozen in liquid nitrogen and stored at -80 °C until use. Upon use, frozen tissue samples were ground using a Retsch mill.

Microarray hybridization

For both conditions, total RNA was isolated from single leaves from three different plants, using an RNeasy Plant Mini Kit (Qiagen, Venlo, The Netherlands). An Agilent Bioanalyzer (Agilent, Santa Clara, CA, USA) was used to check RNA quality. Nucleic acid labeling was performed

according to Agilent recommended procedures for single-color arrays at the Michigan State University Research Technology Support Facility. Labeled RNA was hybridized to Agilent 4x44K *Arabidopsis* Gene Expression (V4) Microarrays (Agilent G2519F-021169). Arrays were scanned with an Agilent G2565B Array Scanner, and images were analyzed using the Feature Extractor v9.5 default protocol GE1-v5_95_Feb07.

Microarray data analysis

Quantile normalization was performed on all probes using the "gProcessedSignal" column of the Feature Extractor files (Bolstad et al., 2003). Probe annotations were downloaded from the Agilent E-array website (021169_D_AA_20140929.txt). Ensembl Plants Biomart was used to convert common names to TAIR locus and RefSeq mRNA IDs (Kinsella et al., 2011). A two tailed Student's *t*-test with equal variances was performed on the (log base two) expression values. Genes were considered differentially expressed at $p < 0.05$ and a fold change of two or greater. Functional annotation of the differentially expressed gene (DEG) lists was performed using the DAVID Functional Annotation Clustering Tool (Huang et al., 2007). Whole-array gene ontology and KEGG pathway enrichment analysis was performed using Gene Set Enrichment Analysis (GSEA) (Subramanian et al., 2005). Unlogged expression values of individual arrays were used in GSEA. Gene set files were downloaded from Arapath (Lai et al., 2012). Combined KEGG pathway and gene ontology gene sets were used in a single analysis. Results were identical when analyses were separate. Gene set permutations of the collapsed probesets were used due to the number of replicates. Results were visualized using the Enrichment Map app for

Cytoscape (Merico et al., 2010). Coexpression analysis was performed using the STRING database (Franceschini et al., 2013). Nodes with at least 2 edges to other nodes in the network were retained for further analysis. Additional nodes were retrieved using the GeneMANIA prediction server (Warde-Farley et al., 2010), and edge confidence scores for the expanded network were retrieved from STRING. Network visualization was performed using Cytoscape.

Quantitative reverse transcription polymerase chain reaction (qRT-PCR)

For each condition, the plant material consisted of single leaves from three plants, grown and treated identically to those used for the microarray. The methods for qRT-PCR are similar to those previously described (Weise et al., 2012). Briefly, RNA was extracted using a Qiagen RNeasy Plant Mini Kit according to the manufacturers directions. DNA was degraded with on-column DNAse treatment. The quality and yield of mRNA were estimated from sample absorbance at 260 nm and 280 nm. cDNA was synthesized from 1 µg of mRNA using Superscript II Reverse Transcriptase (Thermo Fisher Scientific, Waltham, MA, USA) and oligo dT primer. To generate a standard curve, slightly larger templates for each gene of interest were generated using polymerase chain reaction (PCR). The size of each template was confirmed using gel electrophoresis. Template-generating PCR reactions were cleaned using a Wizard SV Gel and PCR Clean-Up System kit (Promega, Madison, WI, USA), and template concentration was estimated from sample absorbance at 260 nm and 280 nm. Dilutions of these templates were used to generate standard curves. Actin2 was used as the housekeeping gene for sample normalization. Primers used in the qRT-PCR analysis and for the production of templates were

designed using Primer-BLAST (Ye et al., 2012)(sequences not shown).

Results

Functional annotation of isoprene responsive genes

The microarray analysis identified 167 differentially expressed genes that were responsive to isoprene. Of these, 95 were upregulated and 72 were downregulated (Table 2.1). Functional enrichment of the DEG lists were determined using the DAVID Functional Annotation Clustering Tool. Among the 95 upregulated genes, 93 were mapped to the DAVID database using RefSeq mRNA identifiers. Among the mapped genes, 12 clusters were detected (Table 2.2). The most significant of these corresponded to 19 metal and ion binding proteins. These included the chloroplast-localized calmodulin-like 37, ferritin-4, and ENH1, along with 4 zinc finger proteins and 3 copper transport proteins. Cluster 2 corresponded to a set of 10 genes responsive to organic substances and hormones. Cluster 3 indicated an overabundance of transcription factors. Thus, there is a general increase in the expression of signal sensing, signal transduction, and transcriptional activation machinery in response to isoprene fumigation. Several other notable clusters were observed. Among these were a six-gene cluster involved in floral development, including the chloroplast-localized SEPALLATA 2. A membrane- and chloroplast- centric cluster were also observed.

Among the 72 downregulated genes, seven functionally enhanced clusters were observed (Table 2.3). The most significant of these were a group of 13 genes involved in light-sensing.

Genes in this group included PIF6, ELF4, a phototropic responsive NPH3 family protein, DIN10, and PRR7. The floral timing gene AGL68 was also repressed. The second cluster found among genes with reduced expression consisted of sugar transport genes, and contained the putative sucrose transporter ERD6. Sugar transport has been suggested as a mechanism for energy sensing within cells, and in particular as a mechanism for chloroplast-localized light sensing. These clusters indicate that the cellular light-sensing and sugar-cycling machinery were repressed in the presence of isoprene.

Coexpression network analysis

Differentially expressed gene lists are useful for identifying the most highly altered genes. Coexpression based network analysis of the DEG list was performed to identify modules responsible for driving the changes observed in the GSEA analysis, as well as additional genes of interest. Gene lists were submitted to the STRING database using a medium confidence threshold. Among upregulated genes, 4 groups with linkage evidence were observed, with 2, 2, 5, and 11 members each. Among downregulated genes there were 4 coexpressed groups with 2, 2, 3, and 3 members each. Within the 11-member network of upregulated genes 8 nodes had 2 or more edges to other nodes, and were retained for further analysis. Twenty additional genes in this network were retrieved from the GeneMania web server, of which 17 were mapped to probes. All 17 trended up in the presence of isoprene. Genes that were upregulated by less than a factor of 2 and/or had *p*-values greater than 0.5 were excluded from the expanded network, yielding a 22-node network upregulated by isoprene by at least two fold (Fig. 2.1 & Table 2.4). Functional

annotation using DAVID revealed the overabundance of stress and hormone responsive genes, and transcription factors (Table 2.5). Ten of the 22 genes were transcription factors. These included three WRKY and three ERF transcription factors. Five genes were annotated as ethylene responsive by The Arabidopsis Information Resource. To test whether isoprene may have been activating the ethylene receptor family, DEG lists from two ethylene microarray studies using *Arabidopsis* were compared to the current dataset (Zhong and Burns, 2003; De Paepe et al., 2004). Neither study showed trends similar to those induced by isoprene, suggesting that isoprene does not target ethylene receptors.

Gene set enrichment and leading edge analysis

Gene sets (1134) corresponding to both gene ontology terms and KEGG pathways were submitted to the GSEA program. Of these, 465 were retained after restricting to sets containing between 15 and 500 genes. Of the 465 gene sets tested for significance, 59 and 25 were upregulated and downregulated, respectively, at a nominal p-value < 0.05 and a false-discovery rate < 0.25. Only two KEGG-derived gene sets, ribosome and aminoacyl tRNA biosynthesis, were enriched, both upregulated. No additional KEGG pathways were discovered despite reducing the minimum set size to three. Many of the upregulated ontologies appeared functionally redundant and indeed contained partially overlapping gene sets. The KEGG-derived gene sets were largely overlapping with those from the gene ontology. Gene set overlap was visualized with the Enrichment Map app for Cytoscape (Fig. 2.2), using an overlap coefficient threshold of 0.3 for edge retention. Further manual clustering of gene sets highlighted several

expression motifs.

Many of these ontologies and ontology clusters were consistent with the results of the DEG functional annotation. These included the increased expression of metal ion binding and chloroplast and membrane centric gene ontologies, as well as the repression of light signaling pathways and sugar transporters, in the presence of isoprene. Metal ion binding was the least strongly upregulated gene set to still be deemed significant, despite being the most significant cluster in the DEG functional annotation. The enrichment score was driven by 16 genes, only 3 of which also drove the DEG enrichment: ENH1, AT4G05030, and AT5G52760. A large cluster of overlapping cellular component ontologies centered on the chloroplast. The chloroplast stroma, chloroplast envelope, and chloroplast thylakoid membrane ontology enrichments were driven by 206, 211, and 136 genes, respectively. Among leading edge genes, 32, 41, and 78 overlapped between the thylakoid membrane and stroma, thylakoid membrane and envelope, and stroma and envelope gene sets, respectively. Fifteen leading edge genes were common to all 3. A mix of biological process and cellular component ontologies focused on mitochondrial and plasma membranes were also upregulated by isoprene. The mitochondrial inner membrane, photorespiration, and anchored to membrane ontologies contained 7, 14, and 113 leading edge genes, respectively. No leading edge overlap existed between these gene sets. Among downregulated gene sets there were both light-signaling and sugar transporter ontologies, in full agreement with the DEG enrichment. The gene set enrichment analysis also highlighted several novel patterns. Among these were an upregulation of cell wall biosynthesis, an upregulation of the transcriptional and translational machinery, and an upregulation of cell cycle and DNA replication related ontologies. Several stress responses were downregulated. Finally, despite an

upregulation of floral development genes in the DEG annotation, this motif was downregulated in the gene set enrichment analysis.

Comparison to Populus x canescens

MapMan was used for visual comparison of the isoprene induced transcriptional changes in *Arabidopsis* (Fig. 2.3a) to the transcriptional changes in isoprene synthase inhibited *Populus* x *canescens* (Fig. 2.3). In both sets of data, lipid related gene expression was modulated, but without a clear trend. Cell wall metabolism also changed greatly, with three groups being coherently upregulated. These groups included cell expansins, (fasciclin-like) arabinogalactan proteins, and cellulose synthases. At a fold change of two or greater, 17 expansins were up, while only 4 were down. Ten and one arabinogalactan proteins were up and down, respectively. Six cellulose synthases were up by two-fold or more, with none down.

Storage sugar metabolism was shifted away from starch and toward sucrose. Starch synthesis and degradation processes both decreased. Among degradative proteins this effect was pronounced, with 2 and 8 proteins being up and down, respectively, by a factor of two or more. Among the repressed genes were glucan phosphorylase 2, disproportionating enzyme 1 & 2, alpha amylase, and glucan water dikinase 1-3. The effect was less pronounced among starch synthesis: only a single isoform of branching enzyme was down by a factor of two or more. Sucrose degradation was not strongly affected, but sucrose-phosphate synthase 3F was upregulated in response to isoprene. This trend suggests that, in *Arabidopsis*, relatively more sugar was exported from the chloroplast during the day in response to isoprene fumigation.

Repression of starch related genes was not observed in *Populus* x *canescens*. In this dataset, SEX1, a glucan water dikinase, was actually increased by isoprene. Also in this dataset, the sucrose-phosphate synthase 1F isoform was decreased. The trend is therefore opposite to that seen in *Arabidopsis*, and suggests that, in response to isoprene, less sugar was exported from the chloroplast.

Light reaction machinery, although not strongly affected, trended down in *Populus* but up in *Arabidopsis*. Behnke reported a decrease in central carbon metabolism pathway genes in isoprene emitting poplar; this change was not evident in *Arabidopsis*. Downregulation of central carbon metabolism in the Behnke poplar RNAi lines may be a consequence of diminished MEP pathway flux. In *Arabidopsis*, carbonic anhydrases were upregulated and three were greater than two-fold increased. No change occurred in *Populus*. No coherent changes occurred in nucleotide metabolism in either dataset. Synthesis and degradation of the oxaloacetate/aspartate family of amino acids increased only in *Arabidopsis*. Aromatic amino acid biosynthesis was upregulated in both data sets.

In secondary metabolism, both flavonoid and phenylpropanoid biosynthetic genes were upregulated in response to isoprene. Among flavonoids, using a two-fold cutoff, 14 genes were up while only six were down. The upregulated genes included UDP-glucosyltransferase 73C6, UDP-glucosyltransferase 78D2, chalcone synthase, and chalcone isomerase. Ten and two genes involved in the biosynthesis of phenylpropanoids and phenolics were up and down regulated, respectively. Laccases also trended upwards, though only weakly. Laccase 5 and laccase 8 increased by more than two-fold.

The increase of phenylpropanoids is interesting. Behnke reported an accumulation of

phenolics, as well as upregulation of several phenylpropanoid biosynthetic genes, in wild type poplar, a result that was also observed in fumigated *Arabidopsis* (Fig. 2.4). The genes most responsible for controlling metabolic flux to phenylpropanoids, phenylalanine ammonia lyase, and 4-coumarate-CoA ligase, were increased in both datasets. Additional fumigations were performed to validate the upregulation of phenylalanine ammonia lyase 1 (PAL1) and 4-coumarate-CoA ligase 1 (4CL) using qRT-PCR (Fig. 2.5). PAL1 was two-fold upregulated, while 4CL was up by 25%, and both increases were statistically significant.

Behnke et al. attributed the increase of phenylpropanoids and PAL in the presence of isoprene in poplar to a decrease in H_2O_2 levels due to ROS quenching. They cited an H_2O_2 repressed cluster of 89 genes that contained many of the phenylpropanoid biosynthetic genes. Due to the complex nature of plant signal transduction networks, this gene network may not be repressed by H_2O_2 under all environmental conditions. The 89 genes in the H_2O_2 repressed network were surveyed in the *Arabidopsis* data. Using a fold change of two or greater as the cutoff criterion, 10 of the loci were increased by the presence of isoprene, while 32 were decreased. This suggests that in the non-stressful conditions used in this study, PAL1 and 4CL were not de-repressed by the H_2O_2 quenching capacity of isoprene.

Discussion

This study implicates isoprene as a volatile signaling molecule of environmental stress. To eliminate confounding MEcDP or ROS based signaling, gene expression of the non-emitting plant *A. thaliana* was monitored in response to isoprene under non-stressful conditions.

Functional annotations and enrichment analyses revealed upregulation of transcription factors, chloroplast components, signal transduction and signal sensing machinery in response to isoprene. Upregulation of a gene network enriched in ERF and WRKY transcription factors was also observed. Finally, isoprene induced key genes involved in the biosynthesis of phenylpropanoids. Genes associated with lignin and anthocyanin biosynthesis, the two major downstream sinks for phenylpropanoids, were also induced. Taken together, these processes point to a concerted reprogramming of gene expression.

Environmental and stress stimuli are translated to gene expression changes in plants by a complex network of transcription factor and signal transduction elements. Focus was placed on the abundance of ERF/AP2 and WRKY transcription factors that were upregulated in the presence of isoprene (Fig. 2.1). Both transcription factor families are enriched in the plant kingdom relative to other eukaryotes. ERFs are almost exclusive to plants, but also occur in bacteria (Wessler, 2005). Also, the majority of ERFs lack introns (Magnani et al., 2004). This has led to the belief that this family of genes is bacterial in origin, and was recruited to the early endosymbiont precursors of modern plants in order to mediate plastid:nucleus signaling (Tanaka and Hanaoka, 2013). It is believed that following their acquisition, the sessile nature of plants and the need to integrate and respond to complex and interconnected environmental stimuli led to the expansion of these gene families in plants (Vogel et al., 2012). In *Arabidopsis*, 147 ERF/AP2 and 72 WRKY transcription factors are now widely implicated in responses to abiotic stress (Zhang and Wang, 2005; Nakano et al., 2006; Mizoi et al., 2012).

The ERF family is subdivided into 12 phylogenetic groups (Nakano et al., 2006). The isoprene induced coexpression network contained three ERF family members. Two of these

genes, ERF13 and ERF105, map to group IX, while RRTF1 is a member of group X. ERF13 and ERF105 have not been critically linked to any stress responses or gene clusters. RRTF1, on the other hand, has previously been identified as a central component of a high light and redox sensitive cluster of 30 genes (Khandelwal et al., 2008). The transcription of a majority of these genes were dependent upon RRTF1 following light stress, and T-DNA insertion mutants were significantly more sensitive to high light stress than wild type. The gene cluster in question was repressed under high light and 3-(3,4-dichlorophenyl)-1,1-dimethylurea treatment, leading the authors to conclude that it is likely repressed by H_2O_2 accumulation. The upregulation of RRTF1 in response to isoprene may be due to an alternative signaling pathway to that described by Khandelwal et al. Three members of the WRKY transcription factor family were also present. WRKY18 and WRKY40 are members of WRKY subgroup IIa, while WRKY46 belongs to group III (Eulgem et al., 2000). WRKY18 and WRKY40 have been implicated in abscisic acid signaling (Shang et al., 2010), and their double mutants display altered pathogen susceptibility (Wang et al., 2006).

The purpose of enrichment and coexpression analyses is to identify biologically relevant trends. The coexpression network further highlights those genes that are likely to be meaningful, and was enriched in ERF and WRKY transcription factors. However, transcription factor networks are complex and highly interconnected, and individual transcription factors are often involved in seemingly disparate processes. It is therefore difficult to determine a function of a cluster of genes from the function of one or even a few transcription factors. Relevant trends are much more likely to be found by comparison of suites of transcription factors. To this end, an attempt was made to identify studies with similar gene WRKY and ERF transcription factor

profiles. Eight of the 22 genes identified by coexpression analysis, including all of the WRKY and ERF transcription factors as well as MYB15 and CML37, were among those significantly upregulated in response to constitutive overexpression of Multiprotein Bridging Factor 1 (Suzuki et al., 2005). Plants overexpressing this protein were resistant to osmotic and heat stress. This suggests that one function of this gene network may be to promote resistance to heat stress.

Upregulation of phenylalanine ammonia lyase and 4-coumarate-CoA ligase also suggests upregulation of abiotic stress defense pathways in response to isoprene. Phenylpropanoid biosynthesis is a general response to stress, as are lignins and anthocyanins. Lignin, a structural component of the cell wall and xylem, along with anthocyanins, constitute the major sinks for phenylpropanoids. Both are believed to play a role in photoprotection, especially against ultraviolet radiation, as both contain ultraviolet absorbing moieties (Steyn et al., 2002; Nanbu et al., 2013; Yong Qian, 2014). Lignin deposition is known to increase in response to high light stress (Moura et al., 2010). Anthocyanins accumulate under both cold stress and high light stress (Christie et al., 1994; Bilger et al., 2007; Thwe et al., 2014). The upregulation of cell wall modifying genes in response to isoprene (Fig. 2.2), notably laccases, suggests that lignin biosynthesis was also upregulated. Laccases perform one-electron oxidations of phenylpropanoid derived monolignols, the final step in lignin biosynthesis. Also, glycosyltransferases were upregulated in response to isoprene. Glycosylation is the most common stabilizing modification of anthocyanins (Springob et al., 2003; Yonekura-Sakakibara et al., 2008). Taken together, these data point towards an upregulation of lignin and anthocyanin biosynthesis in response to isoprene fumigation.

It is difficult to explain these trends in terms of the purported antioxidant properties of

isoprene. PAL is considered to be a stress responsive gene, as its expression is induced by high light and cold stress (Leyva et al., 1995; Hemm et al., 2004). Ozone and drought stress also increase PAL expression (Pääkkönen et al., 1998). ROS accumulation is an almost ubiquitous feature of stress in plants, including cold, drought, and salt stress (Xiong et al., 2002) and would be expected to increase phenylpropanoid biosynthesis in most environmental contexts. In this view, isoprene, as an adaptation to abiotic stress and an antioxidant, should decrease the expression of phenylpropanoid biosynthesis genes. The increase of phenylpropanoids and PAL in the presence of isoprene in poplar had previously been attributed to a decrease in H_2O_2 levels due to ROS quenching (Behnke et al., 2010a). This was based on a study of catalase deficient *Arabidopsis* mutants where a group of H_2O_2 repressed genes containing the phenylpropanoid biosynthetic genes was identified (Vanderauwera et al., 2005). This set of genes was identified by comparative analysis of wild type and mutant plants that had been stressed by high light. The fact that most genes in this cluster were repressed in response to isoprene suggests that this gene cluster was not under the control of H_2O_2 in the conditions used in this study. If the induction of PAL were due to quenching of H_2O_2 by isoprene, one would expect at least a subtle upregulation of these genes. Instead, gene expression changes in response to isoprene appear similar to changes caused by H_2O_2. The results of this study shows that isoprene can activate the same genes that are activated by abiotic stress.

"Priming", as this phenomenon may be referred to, is a common theme in BVOC mediated plant-plant communication. For example, methyl salicylate, the volatile form of salicylic acid, is produced in response to pathogen attack. Following interplant transit, it is converted to its active form in the tissue of sink plants and mediates increased pathogen

resistance (Shulaev et al., 1997). Similarly, methyl jasmonate is a volatile form of jasmonate that is capable of mediating plant crosstalk (Farmer and Ryan, 1990). The hormone is sequestered in the sink tissue by demethylation and conversion to jasmonoyl-isoleucine, after which it acts as a molecular glue to promote the association of its receptor to target proteins (Campos et al., 2014). Besides these well known hormones, many other poorly defined volatile mixtures induced by insect feeding or environmental cues enhance the basal resistance of adjacent plants to abiotic and biotic stresses (Conrath et al., 2006; Aranega-Bou et al., 2014). The majority of these are terpenes, though C6 aldehydes and alcohols (green leaf volatiles), and short chain oxygenated compounds (methanol and acetaldehyde), are also emitted. In total, over 1500 plant derived BVOCs are known (Loreto and Schnitzler, 2010).

Given the diversity of compounds, it is likely that several different mechanisms exist for their perception by plants (Heil, 2014). These mechanisms may be general to lipophilic compounds. The stereochemistry of six carbon green leaf volatiles does not affect the induction of defense responses in lima bean (Heil et al., 2008), indicating that protein receptors are not likely involved. Green leaf volatiles cause membrane depolarization and cytosolic calcium influx (Zebelo et al., 2012). Epigenetic changes occur in response to jasmonic acid signaling and are responsible for propagation of priming across generations. This has also been suggested as a consequence of BVOC signaling (Heil, 2014). It is possible that isoprene is sensed by the BVOC sensing machinery and thus causes similar signaling changes.

It is unlikely that non-emitters such as *Arabidopsis* are exposed to the levels of isoprene used in this study, however, this concentration is perfectly plausible for a highly emitting plant. The mechanisms for perception of BVOCs, including isoprene, are likely conserved and non-

specific within the plant kingdom, so endogenous isoprene signaling by native emitters is likely. Furthermore, repeated or prolonged exposure to low levels of green leaf volatiles produces additive effects (Girón-Calva et al., 2012; Shiojiri et al., 2012), and effects may be propagated across generations (Rasmann et al., 2012). Therefore, chronic exposure of non-emitters to trace levels of isoprene may still cause physiologically relevant transcriptional reprogramming. Further time and dosage response studies, in both emitting and non-emitting plants, are needed to resolve these questions, but are beyond the scope of the current study.

In conclusion, I have catalogued the gene expression changes induced by isoprene in the non-emitting plant *Arabidopsis*. Non-stressful conditions were used to mitigate the possibility for confounding signaling due to ROS quenching. Upregulation of several stress responsive motifs was still observed. This included, notably, the induction of phenylpropanoid biosynthesis. This pattern has been observed previously in *Populus* inhibited in isoprene biosynthesis (Behnke et al., 2010a). However, the changes that were observed by Behnke may have been due to the presence of isoprene in emitting lines or the absence of MEcDP in non-emitting lines. The results of the current study suggest that at least some of these changes were due to a previously unrecognized signaling capacity of isoprene.

Acknowledgements

This material is based upon work supported by the National Science Foundation under Grant No. 0950574. I thank Drs. Jin Chen and Kevin Childs for helpful discussions.

APPENDIX

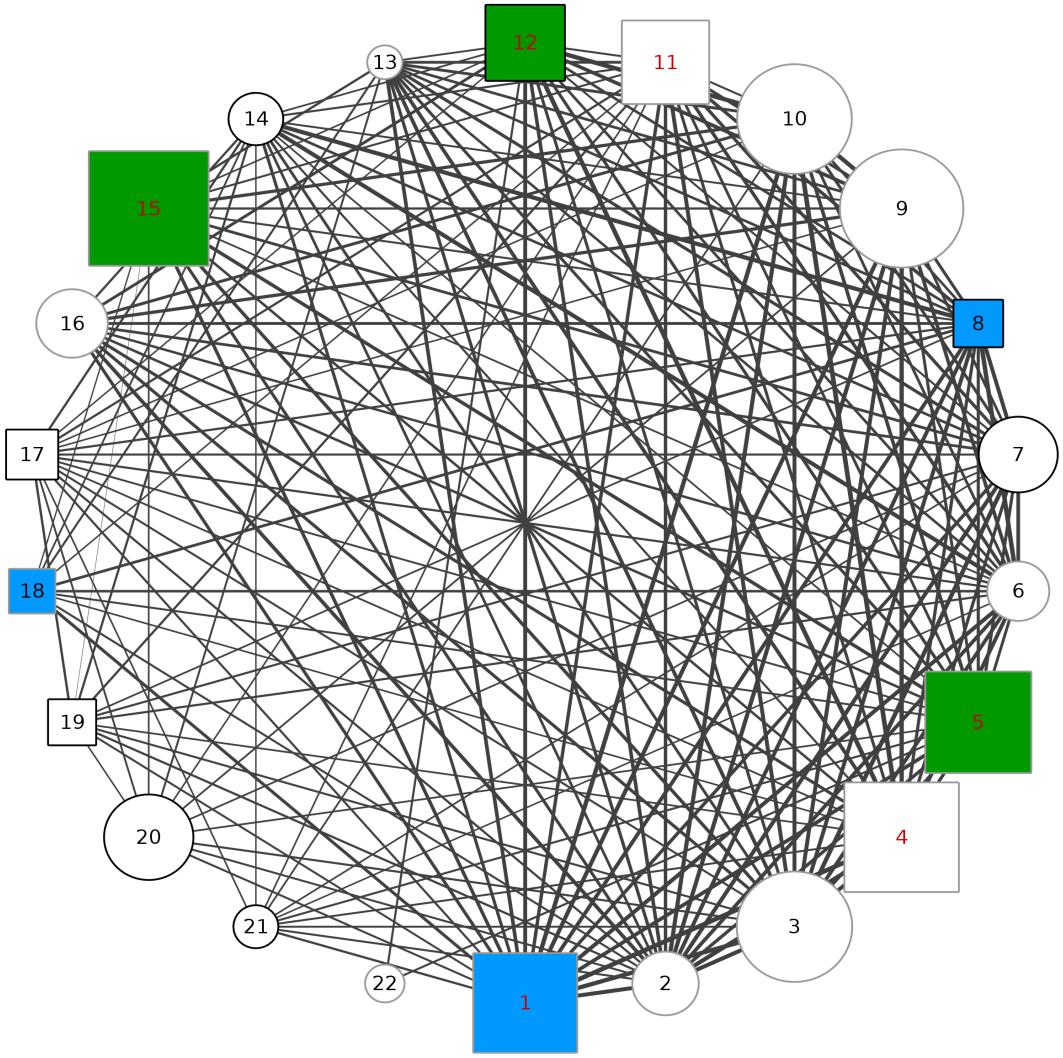

Figure 2.1 An isoprene-upregulated gene network enriched in transcription factors and carbohydrate response elements. Transcription factors are denoted by squares. Nodes representing ERF and WRKY transcription factors are denoted by green and blue fill, respectively. Red font indicates ethylene responsive genes. Size of the node is proportion to fold change (log 2) caused by the presence of isoprene. Edge weight indicates the STRING coexpression score. Black borders indicate the core nodes used to retrieve peripheral nodes, which are bordered in gray. Nodes were ranked according to the closeness centrality in the CytoNCA app for cytoscape (Tang et al., 2015).

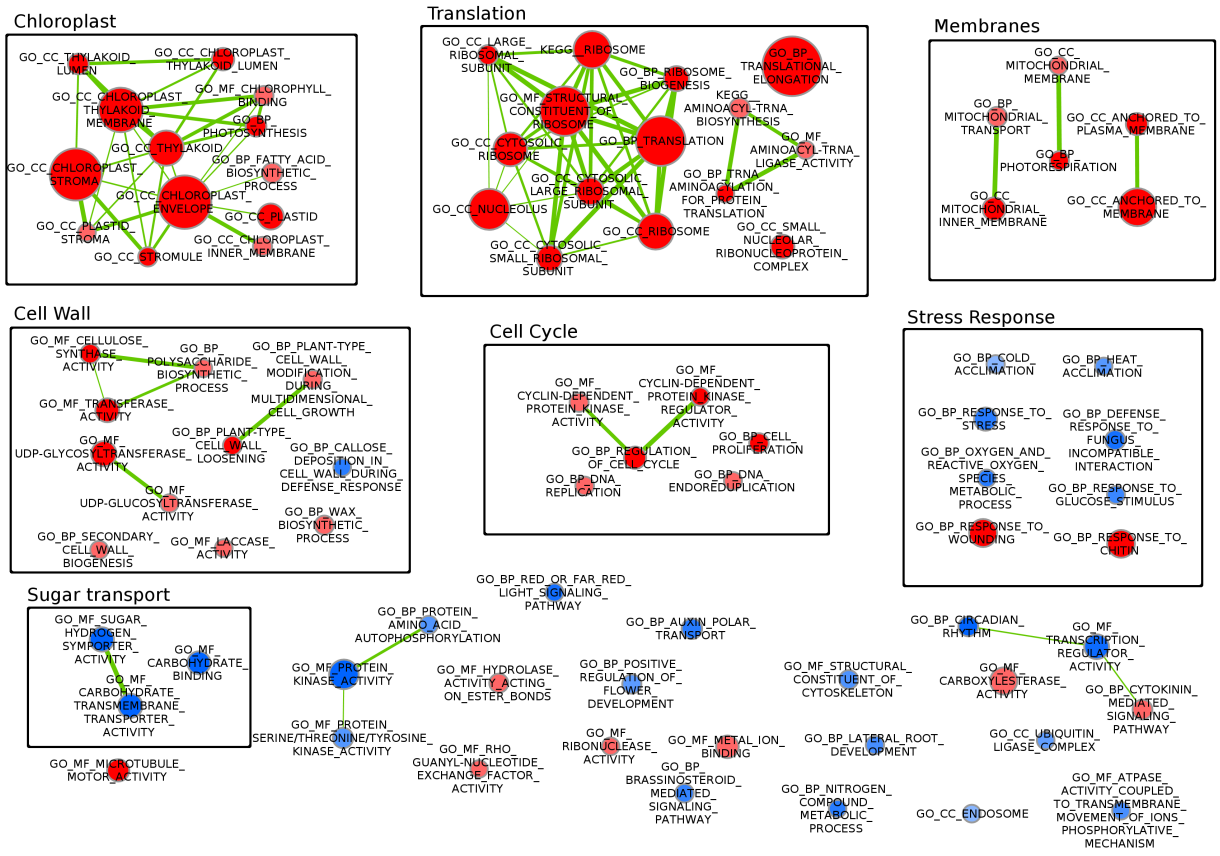

Figure 2.2 Network visualization of Gene Set Enrichment Analysis. Node size indicates the number of genes in the gene set. Node colors indicates the normalized enrichment score. Red nodes are upregulated in response to isoprene, blue nodes are downregulated. Edge thickness represents the degree of gene overlap between ontology terms.

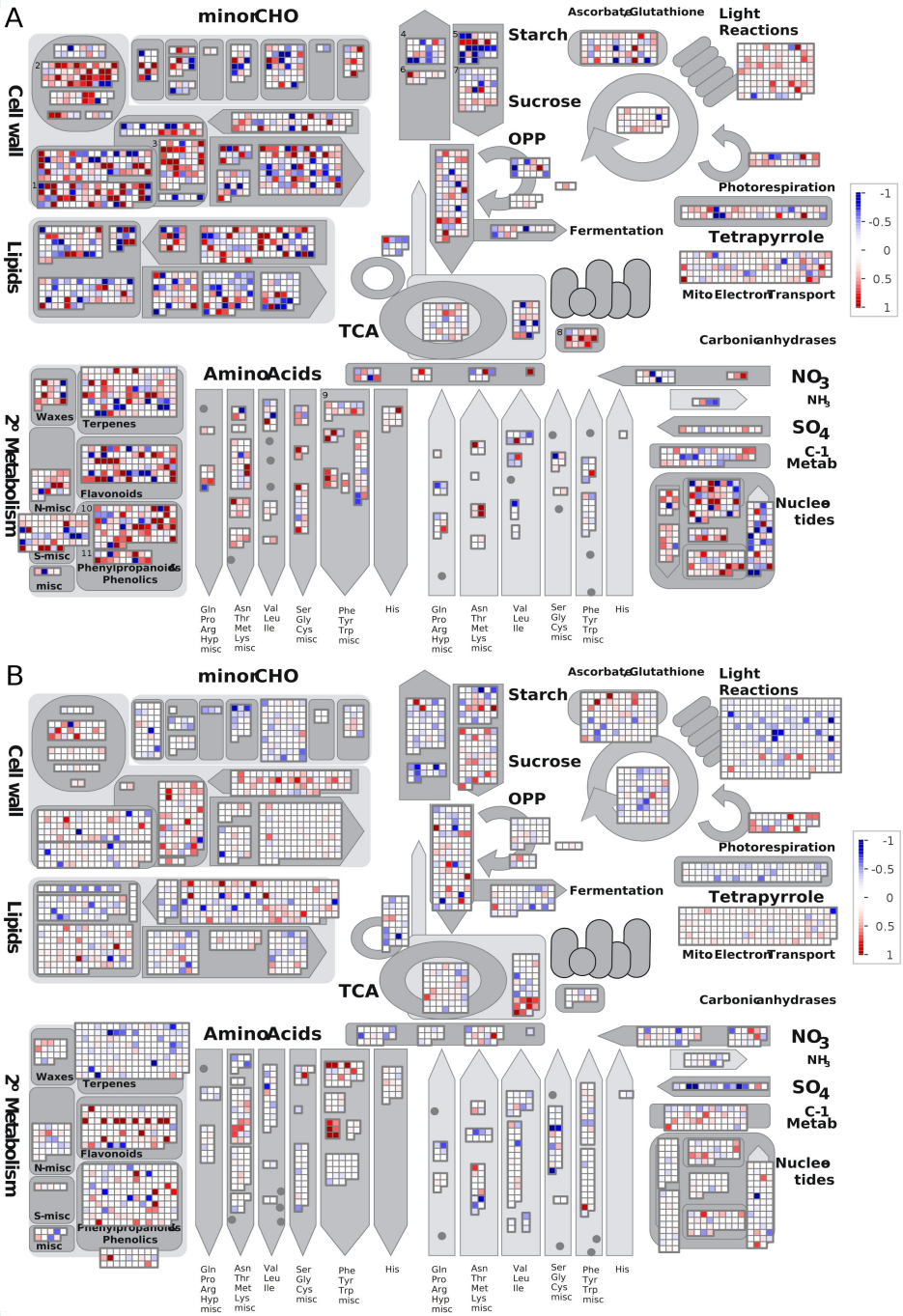

Figure 2.3 MapMan metabolic overview. Microarray data from (a) isoprene fumigated *Arabidopsis thaliana* and (b) *Populus canescens* RNAi lines. Data are in log base 2. Red indicates gene upregulation in the condition or genotype in which isoprene is present or produced. Numerals indicate gene clusters of interest: 1, expansins; 2, (fasciclin-like) arabinogalactan proteins; 3, cellulose synthases; 4, starch synthesis; 5, starch degradation; 6, sucrose synthesis; 7, sucrose degradation; 8, carbonic anhydrases; 9, aromatic amino acid biosynthesis; 10, phenylpropanoid biosynthesis and transferases; 11, laccases.

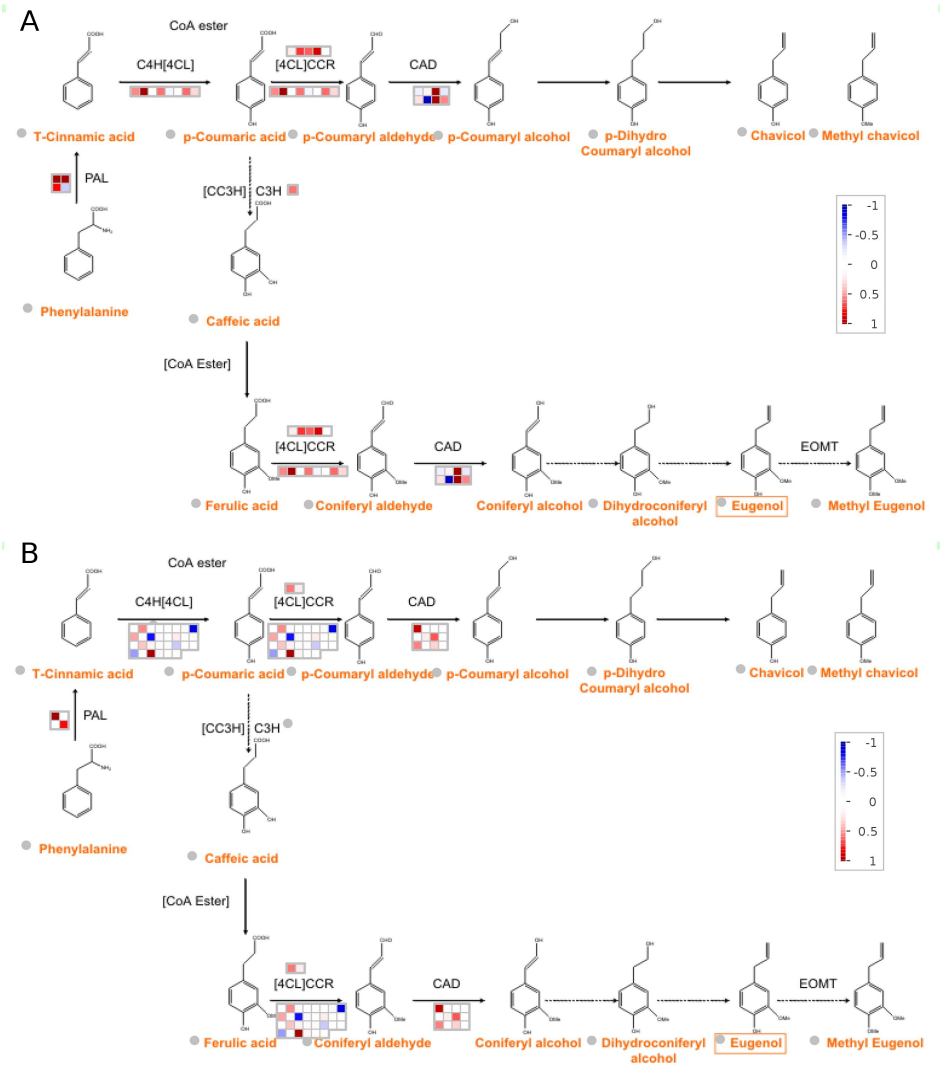

Figure 2.4 MapMan phenylpropanoid view. Microarray data from (a) isoprene fumigated *Arabidopsis thaliana* and (b) *Populus canescens* RNAi lines. Data are in log base 2. Red indicates gene upregulation in the condition or genotype in which isoprene is present or produced.

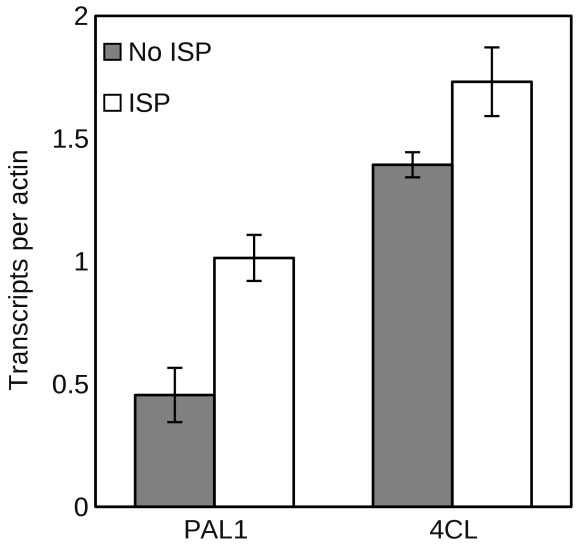

Figure 2.5 qRT-PCR verification of isoprene induced phenylpropanoid biosynthesis. Error bars are the standard error of three biological replicates. The isoprene induced increase in phenylalanine ammonia lyase 1 (PAL1) and 4-coumarate-coA ligase 1 (4CL) transcripts was significant at *p*-values of 0.009 and 0.043, respectively, using a one tailed, unpaired Student's *t*-test with equal variance.

Table 2.1 Differentially expressed genes.

Feature #	Gene Symbol	Description	Fold Change
22542	AT3G25750	putative F-box protein	3.368
22898	AT2G37730	folylpolyglutamate synthase	2.792
25481	AT2G04515	uncharacterized protein	2.647
21053	AT3G28600	AAA-type ATPase family protein	3.445
14200	AT1G54000	GDSL esterase/lipase	3.259
38196	AT3G47660	Regulator of chromosome condensation (RCC1) family protein	2.058
19718	CML37	calcium-binding protein CML37	6.176
38744	ZAT7	zinc finger protein ZAT7	3.172
37476	AT5G52760	copper transport family protein	3.389
1119	AT3G48640	uncharacterized protein	2.085
13057	AT1G02816	uncharacterized protein	2.131
23722	AT3G15670	armadillo/beta-catenin-like repeat-containing protein	3.195
18656	AT3G46080	protein LIGHT SENSITIVE HYPOCOTYLS 6	2.873
21506	SDH1-1	succinate dehydrogenase [ubiquinone] flavoprotein subunit 1	3.557
17257	TPS13	(Z)-gamma-bisabolene synthase 2	2.503
34624	AT5G47920	uncharacterized protein	2.976
19351	AT4G39675	uncharacterized protein	2.030
26717	AT3G20270	equilibrative nucleotide transporter 1	2.044
20141	ORP4B	OSBP(oxysterol binding protein)-related protein 4B	2.981
8198	ENH1	protein ENHANCER OF SOS3-1	3.796
33013	AT1G48100	AAA-type ATPase family protein	5.818
19955	AT5G55570	uncharacterized protein	2.865
8211	EDL3	EID1-like F-box protein 3	2.985
20955	AT4G15050	uncharacterized protein	2.538
6811	WRKY46	putative WRKY transcription factor 46	2.986
22684	CHR17	chromatin remodeling factor17	2.495
22197	AT5G43040	protein RER1D	2.125
22738	ASL9	ASYMMETRIC LEAVES 2-like 9	2.113
38600	AT4G20650	receptor-like protein kinase-related protein	2.221
19080	NAMT1	methyltransferase family protein NAMT1	2.250
22043	AT1G68650	uncharacterized protein	2.065
8467	AT3G18950	WD40 domain-containing protein	3.545
22377	AT5G10990	cytochrome P450 710A4	8.448
18235	AT1G24420	HXXXD-type acyl-transferase-like protein	2.907

Table 2.1 (cont'd)

Feature #	Gene Symbol	Description	Fold Change
23947	RAB28	S-adenosyl-L-methionine-dependent methyltransferases superfamily protein	3.417
44464	FER4	ferritin 4	5.292
13340	SEP2	developmental protein SEPALLATA 2	2.189
30610	AT3G27025	uncharacterized protein	3.923
23661	AT3G26770	NAD(P)-binding Rossmann-fold superfamily protein	5.163
44299	AT5G45630	uncharacterized protein	7.959
11620	AT3G19030	uncharacterized protein	4.879
34739	SIP1	putative galactinol--sucrose galactosyltransferase 5	2.228
23383	chr40	chromatin remodeling 40	2.555
17603	LCR53	low-molecular-weight cysteine-rich 53	3.335
2354	LEA4-5	late embryogenesis abundant protein 4-5	3.420
23082	AT1G50750	plant mobile domain family protein	2.169
29941	PDF1	protodermal factor 1	2.538
35448	HVA22B	endonuclease 5	2.296
38859	UPS4	cadmium resistance protein 1	2.394
25826	AT3G24460	Serinc-domain containing serine and sphingolipid biosynthesis protein	6.401
10346	AT3G62990	uncharacterized protein	4.194
14048	AT1G33480	RING-H2 finger protein ATL58	2.237
6838	AT4G05030	putative copper transport protein	5.580
11337	AT5G19230	GPI-anchored glycoprotein membrane precursor	2.662
20010	MYB9	myb domain protein 9	2.248
39427	DOGT1	UDP-glycosyltransferase 73C5	2.684
9617	AT2G41040	uncharacterized methyltransferase	2.266
29723	PIP2;5	putative aquaporin PIP2-5	4.458
32284	AT5G51190	ethylene-responsive transcription factor ERF105	6.239
12127	MLO5	protein trichome birefringence-like 23	2.224
14231	ENODL13	early nodulin-like protein 13	2.360
12983	RIP2	ROP interactive partner 4	2.067
39707	HSFC1	heat stress transcription factor C-1	4.750
863	MES16	40S ribosomal protein S15a-4	3.548
1299	AT2G47130	short-chain dehydrogenase	2.072
32577	AT2G28570	uncharacterized protein	2.518
43536	AT5G46115	uncharacterized protein	3.166
21198	AT1G58037	Cysteine/Histidine-rich C1 domain family protein	13.120
16006	AT5G22390	uncharacterized protein	2.502

Table 2.1 (cont'd)

Feature #	Gene Symbol	Description	Fold Change
25909	AT2G28690	uncharacterized protein	2.309
9672	AT5G66740	uncharacterized protein	3.625
11340	ENODL15	early nodulin-like protein 15	2.249
6888	AT1G76620	uncharacterized protein	2.325
15408	AT3G06520	agenet domain-containing protein	2.099
20965	AT1G61920	uncharacterized protein	2.495
33951	PUB18	U-box domain-containing protein 18	2.376
8088	AT4G24973	self-incompatibility S1 family protein	2.040
24238	AT3G06890	uncharacterized protein	2.003
43107	PRA1.B5	prenylated RAB acceptor 1.B5	2.043
22511	AT1G67855	uncharacterized protein	2.567
15875	SDC	F-box domain containing protein	2.581
3201	F3H	flavanone 3-hydroxylase	3.903
26747	AT2G26690	nitrate transporter 1.4	2.223
20031	PPa2	soluble inorganic pyrophosphatase 2	3.181
8556	RXF26	anther-specific proline-rich protein RXF26	2.197
21849	AT5G28615	RNA-directed DNA polymerase-related family protein	2.557
44610	AT1G07450	NAD(P)-binding Rossmann-fold superfamily protein	2.201
26365	DOF1	DOF zinc finger protein 1	2.238
33911	AT2G24030	zinc ion binding / nucleic acid binding protein	3.702
5615	AT1G54530	uncharacterized protein	2.040
41361	AT3G46650	UDP-glycosyltransferase-like protein	3.868
38118	TAR2	cysteine/histidine-rich C1 domain-containing protein	2.039
4416	AT3G53380	uncharacterized protein	2.469
4955	AT5G19850	hydrolase, alpha/beta fold family protein	2.196
21425	RALFL15	protein RALF-like 15	4.039
30201	AT3G29410	non-specific phospholipase C3	0.494
31667	HSD1	Hydroxysteroid dehydrogenase 1	0.477
4762	DIN10	putative galactinol--sucrose galactosyltransferase 6	0.320
23732	WAG1	UDP-glucosyl transferase 89B1	0.398
19240	NSP1	Nitrile-specifier protein 1	0.374
44924	ELF4	Early flowering 4	0.208
17658	ASN1	asparagine synthetase [glutamine-hydrolyzing]	0.249
39564	AT4G38380	MATE efflux family protein 3	0.337
15248	AT3G08670	uncharacterized protein	0.464
33581	AT4G33980	uncharacterized protein	0.183
4881	AT3G44170	uncharacterized protein	0.439

Table 2.1 (cont'd)

Feature #	Gene Symbol	Description	Fold Change
28903	AT2G22820	uncharacterized protein	0.471
36887	CYP78A7	cytochrome P450, family 78, subfamily A, polypeptide 7	0.483
24885	AT5G16230	Plant stearoyl-acyl-carrier-protein desaturase family protein	0.319
28074	AT3G19850	phototropic-responsive NPH3 family protein	0.490
10713	PIL2	transcription factor PIF6	0.140
3186	AT5G39020	putative receptor-like protein kinase	0.399
42147	NAC047	NAC domain containing protein 47	0.250
22077	MAF5	protein MADS AFFECTING FLOWERING 5	0.069
44635	PLS	POLARIS protein	0.218
19579	AT1G29110	cysteine proteinases superfamily protein	0.358
40178	AT2G36470	uncharacterized protein	0.375
6263	EBF2	rhomboid protein-like protein	0.392
38539	AT1G75140	uncharacterized protein	0.370
72	AT4G28040	nodulin MtN21-like transporter family protein	0.315
27164	AT3G11850	uncharacterized protein	0.432
33839	RALFL29	protein RALF-like 29	0.476
13433	AT5G01950	leucine-rich repeat protein kinase-like protein	0.313
44155	ERD6	transcription factor bHLH25	0.402
40478	AT4G29103	uncharacterized protein	0.450
43772	AT5G37740	calcium-dependent lipid-binding domain-containing protein	0.424
6595	SD1-29	plant invertase/pectin methylesterase inhibitor domain-containing protein	0.448
34263	ST2A	Adenine nucleotide alpha hydrolases-like superfamily protein	0.142
3862	KTI1	acyltransferase-like protein	0.397
39344	NAC019	polynucleotidyl transferase, ribonuclease H-like superfamily protein	0.428
39102	AT1G07280	tetratricopeptide repeat-containing protein-like protein	0.373
4434	AT5G05320	FAD/NAD(P)-binding oxidoreductase family protein	0.350
5646	AT5G57340	uncharacterized protein	0.284
29191	AT4G39270	leucine-rich repeat protein kinase-like protein	0.323
5603	AT5G26220	ChaC-like family protein	0.111
4088	UGT85A4	UDP-glucosyl transferase 85A4	0.279
38856	CCR1	glycine-rich RNA-binding protein 8	0.336
17956	AT2G01510	pentatricopeptide repeat-containing protein	0.489
37474	AT4G12750	homeodomain-like transcriptional regulator	0.490
27425	AT4G15990	uncharacterized protein	0.381

Table 2.1 (cont'd)

Feature #	Gene Symbol	Description	Fold Change
20195	AT5G46610	aluminum activated malate transporter family protein	0.319
13702	AT1G34575	FAD-binding and BBE domain-containing protein	0.390
38924	PATL1	patellin-1	0.421
36473	AT4G18670	Leucine-rich repeat (LRR) family protein	0.366
10982	AT1G21130	Indole glucosinolate O-methyltransferase 4	0.262
21465	AT4G37483	uncharacterized protein	0.362
14518	AT5G11412	RNA-binding (RRM/RBD/RNP motifs) family protein	0.366
11607	PRR2	pinoresinol reductase 2	0.296
22903	AT3G50140	uncharacterized protein	0.328
13870	CRK30	pentatricopeptide repeat-containing protein	0.256
13844	FLS2	protein ACCELERATED CELL DEATH 6	0.215
31154	AT4G29580	cytidine/deoxycytidylate deaminase family protein	0.299
34109	AT1G22110	structural constituent of ribosome	0.381
16278	TRFL3	protein TRF-like 3	0.313
16165	SDG25	histone methyltransferase SDG25	0.437
26094	AT1G53110	binding partner of acd11 1	0.365
21896	AT1G21510	uncharacterized protein	0.472
45000	AT1G78460	SOUL heme-binding protein	0.271
31924	PRR7	pseudo-response regulator 7	0.430
18885	AT2G43740	Mannose-binding lectin superfamily protein	0.210
43985	ZIF1	zinc induced facilitator 1 proetin	0.486
25062	AT1G74940	uncharacterized protein	0.172
30477	AT3G26580	uncharacterized protein	0.424
19406	TMT1	tonoplast monosaccharide transporter1	0.481
41917	AT4G04078	uncharacterized protein	0.410
33794	AT4G26530	fructose-bisphosphate aldolase 5	0.114
12764	AT2G19130	G-type lectin S-receptor-like serine/threonine-protein kinase	0.327

Table 2.2 Functional annotation of upregulated genes. ES = enrichment score.

#	ES	Ontologies	Genes
1	1.98	metal ion binding; cation binding; zinc binding; ion binding	sip1, tps13, pub18, cml37, at5g43040, at1g33480, at4g05030, at5g52760, enodl15, at2g24030, at3g47660, fer4, at1g54530, zat7, ppa2, at3g46080, enodl13, enh1, dof1
2	1.29	response to organic substance; response to endogenous stimulus; response to hormone stimulus	at2g26690, tar2, hva22b, wrky46, zat7, at5g10990, at3g46080, myb9, at5g51190, dof1
3	0.90	response to chitin; response to carbohydrate stimulus; transcription factor activity; DNA binding;	wrky46, at2g26690, chr17, asl9, zat7, tar2, chr40, sep2, at3g46080, hva22b, myb9, hsfc1, at5g51190, dof1, at5g10990
4	0.89	ZnF_C2H2; Zinc, C2H2-like; zinc ion binding	at2g24030, zat7, at3g46080, at3g47660, pub18, at5g43040, at1g33480, dof1
5	0.83	Glucose/ribitol dehydrogenase; short-chain dehydrogenase/reductase SDR; NAD(P)-binding domain	at3g26770, at2g47130, at1g07450, fer4, sdh1-1
6	0.71	Flower, reproductive structure, seed, & fruit development	fer4, tar2, lea4-5, at3g15670, sep2, rab28
7	0.58	metal ion transport; cation transport; ion transport	fer4, at4g05030, at5g52760
8	0.48	extracellular region; signal peptide; secreted; glycoprotein	at1g54000, rxf26, pdf1, ralfl15, at1g48100, lcr53, at4g20650, at5g19230, enodl13, at3g20270
9	0.41	intrinsic to membrane; transmembrane; membrane; transport	enodl15, ups4, at2g26690, pra1.b5, at5g19230, hva22b, at1g33480, pip2;5, enodl13, at1g68650, mlo5, dogt1, sdh1-1
10	0.25	topological domain-Extracellular; transmembrane region; topological domain-cytoplasmic	ups4, pra1.b5, hva22b, at1g33480, pip2;5, mlo5, dogt1
11	0.16	chloroplast part; plastid part; chloroplast; plastid	sip1, ups4, at1g76620, fer4, cml37, at5g55570, sep2, at2g41040, enh1
12	0.12	ATP binding; adenyl ribonucleotide binding; phosphorylation	at3g53380, sip1, ups4, chr17, chr40, sdh1-1, at3g28600, ppa2, at3g18950

Table 2.3 Functional annotation of downregulated genes. ES = enrichment score.

#	ES	Ontologies	Genes
1	1.559	response to: abiotic stimulus, light stimulus, red or far red light; intracellular signaling cascade	prr7, at3g19850, kti1, nac019, wag1, asn1, ccr1, din10, pil2, elf4, maf5, ebf2, pls
2	1.170	sugar-hydrogen symporter activity; sugar transmembrane transporter activity; integral to membrane	zif1, tmt1, erd6, crk30, at1g75140, fls2
3	0.897	protein serine/threonine kinase activity; enzyme linked receptor protein signaling pathway	sd1-29, at5g01950, crk30, tmt1, at1g34575, ebf2, fls2, at4g39270, at2g19130, at5g39020, at4g18670, wag1, patl1, asn1, ugt85a4, erd6, ccr1, at1g75140, at5g11412, din10, st2a
4	0.436	phosphoprotein; transmembrane region; vacuole; transport	tmt1, patl1, ccr1, at1g75140, erd6, fls2, crk30, at5g39020, zif1
5	0.356	response to: organic substance, endogenous stimulus, hormone stimulus	hsd1, ebf2, pls, asn1, erd6, st2a
6	0.173	transcription regulation; transcription factor activity; nucleus; DNA binding	prr7, prr2, nac019, nac047, pil2, at4g12750, maf5, ebf2
7	0.002	metal ion, transition metal ion, cation :binding	at4g29580, at5g16230, at3g29410, cyp78a7

Table 2.4 Genes of the coexpressed gene network.

ID	GeneSymbol	Description	LogFC	p Value
1	WRKY40	WRKY transcription factor 40	3.51	0.185
2	BAP1	BON association protein 1	2.18	0.288
3	AT3G02840	uncharacterized protein	3.92	0.135
4	STZ	zinc finger protein STZ/ZAT10	3.89	0.144
5	ERF13	ethylene-responsive transcription factor 13	3.59	0.088
6	BCS1	cytochrome BC1 synthesis	2.02	0.055
7	CML37	calcium-binding protein CML37	2.63	0.002
8	WRKY46	WRKY transcription factor 46	1.58	0.018
9	AT3G10930	uncharacterized protein	4.21	0.169
10	DIC2	NF-X1-type zinc finger protein NFXL2	3.89	0.346
11	MYB15	myb domain protein 15	2.92	0.146
12	AT5G51190	ethylene-responsive transcription factor ERF105	2.64	0.035
13	AT1G61340	F-box stress induced 1	1.07	0.280
14	AT5G52760	copper transport family protein	1.76	0.005
15	RRTF1	ethylene-responsive transcription factor ERF109	4.08	0.158
16	AT1G35210	uncharacterized protein	2.36	0.152
17	ZAT7	zinc finger protein ZAT7	1.67	0.004
18	WRKY18	WRKY DNA-binding protein 18	1.47	0.442
19	AT3G46080	C2H2-type zinc finger family protein	1.52	0.008
20	AT5G45630	uncharacterized protein	2.99	0.027
21	AT5G19230	GPI-anchored glycoprotein membrane precursor	1.41	0.033
22	AT1G20823	RING-H2 finger protein ATL80	1.22	0.338

Table 2.5 Functional annotation of the coexpressed gene network. ES = enrichment score.

#	ES	Ontologies	Genes
1	3.29	response to chitin; response to carbohydrate stimulus; DNA-binding region WRKY; DNA-binding region AP2/ERF; ethylene-mediated signaling pathway	rrtf1, at1g20823, erf13, wrky46, zat7, at3g46080, stz, myb15, wrky18, wrky40, at5g51190, bap1
2	1.00	Zinc finger, C2H2-type; zinc ion binding; metal ion binding; ion binding; transition metal ion binding	zat7, at3g46080, stz, at1g20823, cml37, at5g52760

REFERENCES

REFERENCES

Aranega-Bou P, de la O Leyva M, Finiti I, García-Agustín P, González-Bosch C (2014) Priming of plant resistance by natural compounds. Hexanoic acid as a model. Frontiers in Plant Science **5**: 488

Arneth A, Monson RK, Schurgers G, Niinemets Ü, Palmer PI (2008) Why are estimates of global terrestrial isoprene emissions so similar (and why is this not so for monoterpenes)? **8**: 4605–4620

Banerjee A, Sharkey TD (2014) Methylerythritol 4-phosphate (MEP) pathway metabolic regulation. Natural Product Reports **31**: 1043–1055

Banerjee A, Wu Y, Banerjee R, Li Y, Yan H, Sharkey TD (2013) Feedback inhibition of deoxy-d-xylulose-5-phosphate synthase regulates the methylerythritol 4-phosphate pathway. Journal of Biological Chemistry **288**: 16926–16936

Behnke K, Ehlting B, Teuber M, Bauerfeind M, Louis S, Hänsch R, Polle A, Bohlmann J, Schnitzler J-P (2007) Transgenic, non-isoprene emitting poplars don't like it hot: Thermotolerance in isoprene emission knock-down mutants of poplar. The Plant Journal **51**: 485–499

Behnke K, Kaiser A, Zimmer I, Brüggemann N, Janz D, Polle A, Hampp R, Hänsch R, Popko J, Schmitt-Kopplin P, et al (2010a) RNAi-mediated suppression of isoprene emission in poplar transiently impacts phenolic metabolism under high temperature and high light intensities: a transcriptomic and metabolomic analysis. Plant Molecular Biology **74**: 61–75

Behnke K, Kleist E, Uerlings R, Wildt J, Rennenberg H, Schnitzler J-P (2009) RNAi-mediated suppression of isoprene biosynthesis in hybrid poplar impacts ozone tolerance. Tree Physiology **29**: 725–736

Behnke K, Loivamäki M, Zimmer I, Rennenberg H, Schnitzler J-P, Louis S (2010b) Isoprene emission protects photosynthesis in sunfleck exposed Grey Poplar. Photosynthesis Research **104**: 5–17

Bilger W, Rolland M, Nybakken L (2007) UV screening in higher plants induced by low temperature in the absence of UV-B radiation. Photochemical & Photobiological Sciences **6**: 190–195

Bolstad BM, Irizarry RA, Åstrand M, Speed TP (2003) A comparison of normalization methods for high density oligonucleotide array data based on variance and bias. Bioinformatics **19**: 185–193

Campos ML, Kang J-H, Howe GA (2014) Jasmonate-triggered plant immunity. Journal of Chemical Ecology **40**: 657–675

Christie PJ, Alfenito MR, Walbot V (1994) Impact of low-temperature stress on general phenylpropanoid and anthocyanin pathways: Enhancement of transcript abundance and anthocyanin pigmentation in maize seedlings. Planta **194**: 541–549

Conrath U, Beckers GJM, Flors V, García-Agustín P, Jakab G, Mauch F, Newman M-A, Pieterse CMJ, Poinssot B, Pozo MJ, et al (2006) Priming: getting ready for battle. Molecular Plant-Microbe Interactions **19**: 1062–1071

Eulgem T, Rushton PJ, Robatzek S, Somssich IE (2000) The WRKY superfamily of plant transcription factors. Trends in Plant Science **5**: 199–206

Farmer EE, Ryan CA (1990) Interplant communication: airborne methyl jasmonate induces synthesis of proteinase inhibitors in plant leaves. Proceedings of the National Academy of Sciences of the United States of America **87**: 7713–7716

Fehsenfeld F, Calvert J, Fall R, Goldan P, Guenther AB, Hewitt CN, Lamb B, Liu S, Trainer M, Westberg H, et al (1992) Emissions of volatile organic compounds from vegetation and the implications for atmospheric chemistry. Global Biogeochemical Cycles **6**: 389–430

Fortunati A, Barta C, Brilli F, Centritto M, Zimmer I, Schnitzler J-P, Loreto F (2008) Isoprene emission is not temperature-dependent during and after severe drought-stress: a physiological and biochemical analysis. The Plant Journal **55**: 687–697

Franceschini A, Szklarczyk D, Frankild S, Kuhn M, Simonovic M, Roth A, Lin J, Minguez P, Bork P, von Mering C, et al (2013) STRING v9.1: protein-protein interaction networks, with increased coverage and integration. Nucleic Acids Research **41**: D808–D815

Ghirardo A, Wright LP, Bi Z, Rosenkranz M, Pulido P, Rodríguez-Concepción M, Niinemets Ü, Brüggemann N, Gershenzon J, Schnitzler J-P (2014) Metabolic flux analysis of plastidic isoprenoid biosynthesis in poplar leaves emitting and nonemitting isoprene. Plant Physiology **165**: 37–51

Girón-Calva PS, Molina-Torres J, Heil M (2012) Volatile dose and exposure time impact perception in neighboring plants. Journal of Chemical Ecology **38**: 226–228

González-Cabanelas D, Wright LP, Paetz C, Onkokesung N, Gershenzon J, Rodríguez-Concepción M, Phillips MA (2015) The diversion of 2-C-methyl-d-erythritol-2,4-cyclodiphosphate from the 2-C-methyl-d-erythritol 4-phosphate pathway to hemiterpene glycosides mediates stress responses in *Arabidopsis thaliana*. The Plant Journal **82**: 122–137

Guenther AB, Hewitt CN, Erickson D, Fall R, Geron C, Graedel T, Harley P, Klinger L, Lerdau M, Mckay WA, et al (1995) A global model of natural volatile organic compound emissions. Journal of Geophysical Research: Atmospheres **100**: 8873–8892

Guenther AB, Jiang X, Heald CL, Sakulyanontvittaya T, Duhl T, Emmons LK, Wang X (2012) The Model of Emissions of Gases and Aerosols from Nature version 2.1 (MEGAN2.1): an extended and updated framework for modeling biogenic emissions. Geoscientific Model Development **5**: 1503–1560

Heil M (2014) Herbivore-induced plant volatiles: targets, perception and unanswered questions. New Phytologist **204**: 297–306

Heil M, Lion U, Boland W (2008) Defense-inducing volatiles: in search of the active motif. Journal of Chemical Ecology **34**: 601–604

Hemm MR, Rider SD, Ogas J, Murry DJ, Chapple C (2004) Light induces phenylpropanoid metabolism in *Arabidopsis* roots. The Plant Journal **38**: 765–778

Huang DW, Sherman BT, Tan Q, Collins JR, Alvord WG, Roayaei J, Stephens R, Baseler MW, Lane HC, Lempicki RA (2007) The DAVID Gene Functional Classification Tool: a novel biological module-centric algorithm to functionally analyze large gene lists. Genome Biology **8**: R183

Jardine KJ, Monson RK, Abrell L, Saleska SR, Arneth A, Jardine A, Ishida FY, Serrano AMY, Artaxo P, Karl T, et al (2012) Within-plant isoprene oxidation confirmed by direct emissions of oxidation products methyl vinyl ketone and methacrolein. Global Change Biology **18**: 973–984

Khandelwal A, Elvitigala T, Ghosh B, Quatrano RS (2008) *Arabidopsis* transcriptome reveals control circuits regulating redox homeostasis and the role of an AP2 transcription factor. Plant Physiology **148**: 2050–2058

Kinsella RJ, Kahari A, Haider S, Zamora J, Proctor G, Spudich G, Almeida-King J, Staines D, Derwent P, Kerhornou A, et al (2011) Ensembl BioMarts: a hub for data retrieval across taxonomic space. Database **2011**: bar030–bar030

Lai L, Liberzon A, Hennessey J, Jiang G, Qi J, Mesirov JP, Ge SX (2012) AraPath: a knowledgebase for pathway analysis in *Arabidopsis*. Bioinformatics **28**: 2291–2292

Laothawornkitkul J, Paul ND, Vickers CE, Possell M, Taylor JE, Mullineaux PM, Hewitt CN (2008) Isoprene emissions influence herbivore feeding decisions. Plant, Cell & Environment **31**: 1410–1415

Leyva A, Jarillo JA, Salinas J, Martinez-Zapater JM (1995) Low temperature induces the accumulation of phenylalanine ammonia-lyase and chalcone synthase mRNAs of *Arabidopsis thaliana* in a light-dependent manner. Plant Physiology **108**: 39–46

Lichtenthaler HK, Schwender J, Disch A, Rohmer M (1997) Biosynthesis of isoprenoids in higher plant chloroplasts proceeds via a mevalonate-independent pathway. FEBS Letters **400**: 271–274

Li Z, Ratliff EA, Sharkey TD (2011) Effect of temperature on postillumination isoprene emission in oak and poplar. Plant Physiology **155**: 1037–1046

Loivamäki M, Louis S, Cinege G, Zimmer I, Fischbach RJ, Schnitzler J-P (2006) Circadian rhythms of isoprene biosynthesis in Grey Poplar leaves. Plant Physiology **143**: 540–551

Loivamäki M, Mumm R, Dicke M, Schnitzler J-P (2008) Isoprene interferes with the attraction of bodyguards by herbaceous plants. Proceedings of the National Academy of Sciences of the United States of America **105**: 17430–17435

Loreto F, Delfine S (2000) Emission of isoprene from salt-stressed *Eucalyptus globulus* leaves. Plant Physiology **123**: 1605–1610

Loreto F, Mannozzi M, Maris C, Nascetti P, Ferranti F, Pasqualini S (2001) Ozone quenching properties of isoprene and its antioxidant role in leaves. Plant Physiology **126**: 993–1000

Loreto F, Schnitzler J-P (2010) Abiotic stresses and induced BVOCs. Trends in Plant Science **15**: 154–166

Loreto F, Velikova V (2001) Isoprene produced by leaves protects the photosynthetic apparatus against ozone damage, quenches ozone products, and reduces lipid peroxidation of cellular membranes. Plant Physiology **127**: 1781–1787

Magnani E, Sjölander K, Hake S (2004) From endonucleases to transcription factors: evolution of the AP2 DNA binding domain in plants. The Plant Cell **16**: 2265–2277

Merico D, Isserlin R, Stueker O, Emili A, Bader GD (2010) Enrichment Map: a network-based method for gene-set enrichment visualization and interpretation. PLoS ONE **5**: e13984

Miller B, Oschinski C, Zimmer W (2001) First isolation of an isoprene synthase gene from poplar and successful expression of the gene in *Escherichia coli*. Planta **213**: 483–487

Mizoi J, Shinozaki K, Yamaguchi-Shinozaki K (2012) AP2/ERF family transcription factors in plant abiotic stress responses. Biochimica et Biophysica Acta - Gene Regulatory Mechanisms **1819**: 86–96

Monson RK, Fall R (1989) Isoprene emission from aspen leaves. Influence of environment and relation to photosynthesis and photorespiration. Plant Physiology **90**: 267–274

Moura JCMS, Bonine CAV, De Oliveira Fernandes Viana J, Dornelas MC, Mazzafera P (2010) Abiotic and biotic stresses and changes in the lignin content and composition in plants. Journal of Integrative Plant Biology **52**: 360–376

Nakano T, Suzuki K, Fujimura T, Shinshi H (2006) Genome-wide analysis of the ERF gene family in *Arabidopsis* and rice. Plant Physiology **140**: 411–432

Nanbu T, Shimada J, Kobayashi M, Hirano K, Koh T, Machino M, Ohno H, Yamamoto M, Sakagami H (2013) Anti-UV activity of lignin-carbohydrate complex and related compounds. In Vivo **27**: 133–139

Pääkkönen E, Seppänen S, Holopainen T, Kokko H, Kärenlampi S, Kärenlampi L, Kangasjärvi J (1998) Induction of genes for the stress proteins PR-10 and PAL in relation to growth, visible injuries and stomatal conductance in birch (*Betula pendula*) clones exposed to ozone and/or drought. New Phytologist **138**: 295–305

De Paepe A, Vuylsteke M, Van Hummelen P, Zabeau M, Van Der Straeten D (2004) Transcriptional profiling by cDNA-AFLP and microarray analysis reveals novel insights into the early response to ethylene in *Arabidopsis*. The Plant Journal **39**: 537–559

Rasmann S, De Vos M, Casteel CL, Tian D, Halitschke R, Sun JY, Agrawal AA, Felton GW, Jander G (2012) Herbivory in the previous generation primes plants for enhanced insect resistance. Plant Physiology **158**: 854–863

Rosenstiel T, Ebbets A, Khatri W, Fall R, Monson R (2004) Induction of poplar leaf nitrate reductase: A test of extrachloroplastic control of isoprene emission rate. Plant Biology **6**: 12–21

Rosenstiel T, Potosnak M, Griffin K, Fall R, Monson R (2003) Increased CO_2 uncouples growth from isoprene emission in an agriforest ecosystem. Nature **421**: 256–259

Sanadze GA (2004) Biogenic isoprene (a review). Russian Journal of Plant Physiology **51**: 729–741

Schnitzler J-P, Louis S, Behnke K, Loivamäki M (2010) Poplar volatiles - biosynthesis, regulation and (eco)physiology of isoprene and stress-induced isoprenoids. Plant Biology **12**: 302–316

Shang Y, Yan L, Liu Z-Q, Cao Z, Mei C, Xin Q, Wu F-Q, Wang X-F, Du S-Y, Jiang T, et al (2010) The Mg-chelatase H subunit of *Arabidopsis* antagonizes a group of WRKY transcription repressors to relieve ABA-responsive genes of inhibition. The Plant Cell **22**: 1909–1935

Sharkey TD, Gray DW, Pell HK, Breneman SR, Topper L (2013) Isoprene synthase genes form a monophyletic clade of acyclic terpene synthases in the tps-B terpene synthase family. Evolution **67**: 1026–1040

Sharkey TD, Loreto F (1993) Water stress, temperature, and light effects on the capacity for isoprene emission and photosynthesis of kudzu leaves. Oecologia **95**: 328–333

Sharkey TD, Singsaas E (1995) Why plants emit isoprene. Nature **374**: 769–769

Shiojiri K, Ozawa R, Matsui K, Sabelis MW, Takabayashi J (2012) Intermittent exposure to traces of green leaf volatiles triggers a plant response. Scientific Reports **2**: 378

Shulaev V, Silverman P, Raskin I (1997) Airborne signalling by methyl salicylate in plant pathogen resistance. Nature **385**: 718–721

Silver G, Fall R (1995) Characterization of aspen isoprene synthase, an enzyme responsible for leaf isoprene emission to the atmosphere. Journal of Biological Chemistry **270**: 13010–13016

Singsaas EL, Lerdau M, Winter K, Sharkey TD (1997) Isoprene increases thermotolerance of isoprene-emitting species. Plant Physiology **115**: 1413–1420

Springob K, Nakajima J, Yamazaki M, Saito K (2003) Recent advances in the biosynthesis and accumulation of anthocyanins. Natural Product Reports **20**: 288–303

Steyn WJ, Wand SJE, Holcroft DM, Jacobs G (2002) Anthocyanins in vegetative tissues: a proposed unified function in photoprotection. New Phytologist **155**: 349–361

Subramanian A, Tamayo P, Mootha VK, Mukherjee S, Ebert BL, Gillette MA, Paulovich A, Pomeroy SL, Golub TR, Lander ES, et al (2005) Gene set enrichment analysis: A knowledge-based approach for interpreting genome-wide expression profiles. Proceedings of the National Academy of Sciences of the United States of America **102**: 15545–15550

Suzuki N, Rizhsky L, Liang H, Shuman J, Shulaev V, Mittler R (2005) Enhanced tolerance to environmental stress in transgenic plants expressing the transcriptional coactivator Multiprotein Bridging Factor 1c. Plant Physiology **139**: 1313–1322

Tanaka K, Hanaoka M (2013) The early days of plastid retrograde signaling with respect to replication and transcription. Frontiers in Plant Science **3**: 301

Tang Y, Li M, Wang J, Pan Y, Wu F-X (2015) CytoNCA: A cytoscape plugin for centrality analysis and evaluation of protein interaction networks. Biosystems **127**: 67–72

Terry GM, Stokes NJ, Hewitt CN, Mansfield TA (1995) Exposure to isoprene promotes flowering in plants. Journal of Experimental Botany **46**: 1629–1631

Thwe AA, Kim Y, Li X, Kim YB, Park N-I, Kim HH, Kim S-J, Park SU (2014) Accumulation of phenylpropanoids and correlated gene expression in hairy roots of Tartary Buckwheat under light and dark conditions. Applied Biochemistry and Biotechnology **174**: 2537–2547

Vanderauwera S, Zimmermann P, Rombauts S, Vandenabeele S, Langebartels C, Gruissem W, Inzé D, Breusegem FV (2005) Genome-wide analysis of hydrogen peroxide-regulated gene expression in *Arabidopsis* reveals a high light-induced transcriptional cluster involved in anthocyanin biosynthesis. Plant Physiology **139**: 806–821

Velikova V, Ghirardo A, Vanzo E, Merl J, Hauck SM, Schnitzler J-P (2014) Genetic manipulation of isoprene emissions in poplar plants remodels the chloroplast proteome. Journal of Proteome Research **13**: 2005–2018

Velikova V, Várkonyi Z, Szabó M, Maslenkova L, Nogues I, Kovács L, Peeva V, Busheva M, Garab G, Sharkey TD, et al (2011) Increased thermostability of thylakoid membranes in isoprene-emitting leaves probed with three biophysical techniques. Plant Physiology **157**: 905–916

Vickers CE, Gershenzon J, Lerdau MT, Loreto F (2009a) A unified mechanism of action for volatile isoprenoids in plant abiotic stress. Nature Chemical Biology **5**: 283–291

Vickers CE, Possell M, Cojocariu CI, Velikova VB, Laothawornkitkul J, Ryan A, Mullineaux PM, Nicholas Hewitt C (2009b) Isoprene synthesis protects transgenic tobacco plants from oxidative stress. Plant, Cell & Environment **32**: 520–531

Vogel MO, Gomez-Perez D, Probst N, Dietz K-J (2012) Combinatorial signal integration by APETALA2/Ethylene Response Factor (ERF)-transcription factors and the involvement of AP2-2 in starvation response. International Journal of Molecular Sciences **13**: 5933–5951

Wang D, Amornsiripanitch N, Dong X (2006) A genomic approach to identify regulatory nodes in the transcriptional network of systemic acquired resistance in plants. PLoS Pathogens **2**: e123

Warde-Farley D, Donaldson SL, Comes O, Zuberi K, Badrawi R, Chao P, Franz M, Grouios C, Kazi F, Lopes CT, et al (2010) The GeneMANIA prediction server: biological network integration for gene prioritization and predicting gene function. Nucleic Acids Research **38**: W214–W220

Way DA, Ghirardo A, Kanawati B, Esperschütz J, Monson RK, Jackson RB, Schmitt-Kopplin P, Schnitzler J-P (2013) Increasing atmospheric CO_2 reduces metabolic and physiological differences between isoprene- and non-isoprene-emitting poplars. New Phytologist **200**: 534–546

Way DA, Schnitzler J-P, Monson RK, Jackson RB (2011) Enhanced isoprene-related tolerance of heat- and light-stressed photosynthesis at low, but not high, CO_2 concentrations. Oecologia **166**: 273–282

Weise SE, Aung K, Jarou ZJ, Mehrshahi P, Li Z, Hardy AC, Carr DJ, Sharkey TD (2012) Engineering starch accumulation by manipulation of phosphate metabolism of starch. Plant Biotechnology Journal **10**: 545–554

Wessler SR (2005) Homing into the origin of the AP2 DNA binding domain. Trends in Plant Science **10**: 54–56

Wilkinson MJ, Owen SM, Possell M, Hartwell J, Gould P, Hall A, Vickers C, Nicholas Hewitt C (2006) Circadian control of isoprene emissions from Oil Palm (*Elaeis guineensis*). The Plant Journal **47**: 960–968

Xiao Y, Savchenko T, Baidoo EEK, Chehab WE, Hayden DM, Tolstikov V, Corwin JA, Kliebenstein DJ, Keasling JD, Dehesh K (2012) Retrograde signaling by the plastidial metabolite MEcPP regulates expression of nuclear stress-response genes. Cell **149**: 1525 – 1535

Xiong L, Schumaker KS, Zhu J-K (2002) Cell signaling during cold, drought, and salt stress. The Plant Cell **14**: S165–S183

Ye J, Coulouris G, Zaretskaya I, Cutcutache I, Rozen S, Madden TL (2012) Primer-BLAST: A tool to design target-specific primers for polymerase chain reaction. BMC Bioinformatics **13**: 134

Yonekura-Sakakibara K, Nakayama T, Yamazaki M, Saito K (2008) Modification and stabilization of anthocyanins. *In* C Winefield, K Davies, K Gould, eds, Anthocyanins. Springer New York, pp 169–190

Yong Qian XQ (2014) Lignin: a nature-inspired sun blocker for broad-spectrum sunscreens. Green Chemistry **17**: 320–324

Zebelo SA, Matsui K, Ozawa R, Maffei ME (2012) Plasma membrane potential depolarization and cytosolic calcium flux are early events involved in tomato (*Solanum lycopersicon*) plant-to-plant communication. Plant Science **196**: 93–100

Zhang Y, Wang L (2005) The WRKY transcription factor superfamily: its origin in eukaryotes and expansion in plants. BMC Evolutionary Biology **5**: 1

Zhong GV, Burns JK (2003) Profiling ethylene-regulated gene expression in *Arabidopsis thaliana* by microarray analysis. Plant Molecular Biology **53**: 117–131

Chapter 3

Biophysical and Physiological Investigation of ROS Quenching and Membrane Remodeling by Isoprene

Abstract

Isoprene protects plant leaves from abiotic stress but two hypothesized molecular mechanisms, quenching of reactive oxygen species and membrane modification, have been difficult to test. In *Arabidopsis thaliana* leaves, exposure to methyl vinyl ketone, a product of reactive oxygen species quenching by isoprene, caused an accumulation of H_2O_2. Isoprene prevented the increase in H_2O_2 in methyl vinyl ketone treated leaves but did not reduce H_2O_2 in unstressed leaves. Isoprene prevented the induction of expression of several genes caused by methyl vinyl ketone but did not reduce their expression in unstressed leaves. On the other hand, isoprene appeared to cause membrane thickening, often suggested as a mechanism of volatile anesthetics. Membrane thickness was monitored using the channel forming antibiotic gramicidin in a reconstituted membrane system. In the presence of isoprene, gramicidin channel lifetimes were significantly reduced, indicating an effect on this proteinaceous probe. The effect of isoprene on membrane fluidity was also tested using the fluorescent molecular probe perylene. Isoprene did not cause a measurable change in vesicle fluidity in these experiments. These results support some effects similar to that of volatile anesthetics, not reactive oxygen species quenching, as the primary mode by which isoprene induces thermoprotection in plants. Membrane dynamics could also explain the ozone tolerance provided by isoprene.

Introduction

A number of hypotheses about the benefits plants may gain from synthesizing isoprene have been advanced. These include 1. thermotolerance, especially tolerance of short high temperature episodes (Sharkey and Singsaas, 1995; Velikova et al., 2011), 2. protection against oxidative stress (Loreto et al., 2001; Loreto and Velikova, 2001; Vickers et al., 2009a; Vickers et al., 2009b; Jardine et al., 2012), 3. release of carbon inadvertently diverted to the methylerythritol pathway, 4. a flowering stimulus (Terry et al., 1995), 5. interaction with terpene signals between plants and insects (Laothawornkitkul et al., 2008; Loivamäki et al., 2008). Most reports focus on the first two effects and lump these together as tolerance of abiotic stress.

Several deleterious effects of abiotic stress are ameliorated by isoprene: (i) the loss of photosynthetic capacity (Sharkey and Singsaas, 1995; Loreto and Velikova, 2001) (ii) the accumulation of reactive oxygen species (ROS) and lipid oxidation products (Velikova et al., 2005; Behnke et al., 2010) and (iii) the induction of cell death (Sharkey et al., 2001; Velikova et al., 2005). However, the mechanism of these effects is controversial. Two hypotheses for the molecular mechanism of isoprene action are direct quenching of ROS (Loreto and Velikova, 2001; Velikova et al., 2004) and changes in membrane dynamics (Sharkey, 1996; Siwko et al., 2007; Behnke et al., 2010). Oxidative stress damages membranes and membrane damage can lead to oxidative stress, linking these two mechanisms (Velikova et al., 2012).

The quenching of ROS is the mechanism often invoked for isoprene protection against abiotic stress (Vickers et al., 2009a; Jardine et al., 2012). The double bonds of isoprene are considered ideal targets for ROS quenching but isoprene reactions with ROS produce cytotoxic

compounds (Doyle et al., 2004; Karl et al., 2010). Reaction products including the conjugated carbonyl methyl vinyl ketone (MVK) (Paulson et al., 1992a; Paulson et al., 1992b) in highly stressed isoprene emitting plants has been interpreted as evidence of isoprene oxidation inside plant cells (Jardine et al., 2012), although production of MVK by membrane lipid degradation is also possible (Kai et al., 2012). More and more, ROS are being viewed as important signaling molecules that normally vary in amount in order to signal changes in gene expression to counter environmental stress (Foyer and Shigeoka, 2010; Munne-Bosch et al., 2012). In this view ROS are generally adaptive even though a positive feedback loop can be created in which a small amount of ROS-induced membrane damage can increase ROS production causing additional membrane damage eventually leading to cell death (Zoeller et al., 2012). Such a mechanism in thylakoids likely underlies the hypersensitive response (Göhre et al., 2012). While this positive feedback system is likely be beneficial to plants under some circumstances, it may be inadvertently activated by the heat-stress-induced alteration of membrane properties (Fig. 3.1).

Reactive oxygen species refers to a family of molecules with varying properties and reaction specificities. The superoxide radical and hydroxyl radical are likely to be more reactive than hydrogen peroxide or ozone. Singlet oxygen ($^1O_2$) has been shown to be the primary source of damage to polyunsaturated fatty acids under photosynthetic conditions regardless of the starting form of ROS (Triantaphylidès et al., 2008). In plants, $^1O_2$ is primarily produced in chloroplasts by photosensitization at the PSII reaction center and in the light harvesting antennas, but may also be produced by phytoalexins in response to pathogenic stress (Triantaphylidès and Havaux, 2009). It can be detoxified by physical quenching, for example by carotenoids, and chemical reaction mechanisms. Only chemical detoxification produces oxidized byproducts of

the quencher. Physical quenching of $^1O_2$ is much faster than the chemical reaction for most compounds important in ROS protection. The combined quenching and reaction rate of $^1O_2$ by isoprene has been measured at $\sim 20*10^3$ M^{-1} s^{-1} (Frimer, 1985). By comparison, the quenching rate of $^1O_2$ by β-carotene, lutein, and violaxanthin has been measured at $\sim 10*10^9$ M^{-1} s^{-1} (Triantaphylidès and Havaux, 2009). Thus, at equimolar concentration with carotenoids, isoprene will quench only one in one million molecules of $^1O_2$.

Several in vivo studies have suggested that isoprene interacts with membranes. Removing endogenous isoprene production from poplar causes an alteration in the ratio of saturated and unsaturated lipids (Way et al., 2013). Transgenic, isoprene emitting Arabidopsis have been shown to have more heat stable light harvesting complex II arrays than non emitting plants and a slower relaxation of the electrochromic shift that indicates slower leakage of charge across the thylakoid membrane (Velikova et al., 2011). In vivo studies have been useful for characterizing the physiological effects of isoprene on membranes, but have not produced a molecular scale understanding of the mechanism of action of isoprene. Also, given the possibility for a mutually reinforcing cycle of altered membrane dynamics and ROS formation, it is difficult to unambiguously determine the extent to which isoprene is affecting both processes from in vivo studies alone.

There are several aspects of membrane biophysics that could be affected by isoprene. Most often membrane viscosity changes are associated with temperature changes (Pearcy, 1978; Berry and Björkman, 1980; Raison et al., 1982). However, several other effects are possible. These include alteration in the thickness of the membrane. Membrane thickness can change in response to some treatments (Murakami and Packer, 1970; Johnson et al., 2011). Membranes,

such as the thylakoid membrane, that contain many proteins must maintain the appropriate hydrophobic depth to optimize the function of the membrane embedded proteins (Montecucco et al., 1982; Andersen and Koeppe, 2007). Membrane thickness can also affect movement of small molecules across the membrane (Paula et al., 1996). Diffusion of small neutral molecules depends on them dissolving in the hydrophobic membrane interior while small charged molecules such as potassium ions and protons likely pass through transient pores in the membrane (Paula et al., 1996). Other membrane effects include lateral organization. Small molecules can have large effects on critical points that allow separation of membranes into macromolecular domains (Veatch, 2007; Honerkamp-Smith et al., 2009). The presence of cholesterol in animal cell plasma membranes can lead to lipid rafts (Veatch et al., 2008).

In this study the likelihood of ROS quenching versus membrane stabilization as the mechanism for stopping the membrane damage-ROS cycle was explored. The consequences of chemical interaction of isoprene with ROS was tested. In addition, the effect of isoprene on membrane dynamics was assessed using gramicidin A, a probe of membrane hydrophobic thickness, and perylene, a flourescent probe of membrane viscosity. The biggest effect was a reduction of the gramacidn A channel lifetime similar to what is seen with volatile anesthetics. Membrane thickness or other effects similar to volatile anesthetics appeared to be the most likely explanation of the molecular mechanism underpinning the abiotic stress protection by isoprene.

Materials and methods

Double bond estimation (in collaboration with Dr Ziru Li)

Compounds typically found in membranes were assumed to have the following number of double bonds: isoprene, 2; carotenoids (lutein and β-carotene), 11; chlorophyll a and b (phytyl tail only), 1; quinones (plastoquinone and ubiquinone), 9. A fresh weight to area ratio of 245 g m^{-2} (determined from average of 10 fresh poplar leaves) was used for converting between units reported in literature (Chapman and Barber, 1986; Demmig et al., 1987). The amount of isoprene inside a leaf was estimated from post illumination isoprene emission (Li et al., 2011).

Methyl vinyl ketone treatment

Mature *Arabidopsis thaliana* rosettes (Columbia ecotype) were placed in air-tight containers in near-darkness at room temperature and exposed to 20 µL L^{-1} isoprene and/or MVK for 3 hours. After treatment, leaf samples were collected with a 1.5cm diameter leaf punch, placed in microcentrifuge tubes containing a steel ball and flash frozen in liquid nitrogen. Samples were stored at -80 °C until used. Frozen samples were ground at 30 shakes s^{-1} for 30 s in a Retsch MM301 mill. For measurement of H_2O_2, the tissue powder was extracted with 400 µL of 6 mM trichloroacetic acid solution. Tissue powder was pelleted by a 15 min, 12,000 x g spin at 4 °C, and the supernatant was assayed for H_2O_2 content using an Invitrogen Amplex® Red Hydrogen Peroxide Assay kit. Assays were performed in 96-well Costar® 3912 plates (Corning Inc.

Corning, New York). After the addition of sample to the assay medium, plates were shaken and placed in darkness for 30 min prior to fluorescence measurement with a Molecular Devices SpectraMax M2 operating at 550 nm excitation and 590 nm emission. H_2O_2 content was calculated from catalase-labile fluorescence using an H_2O_2 standard curve. H_2O_2 contents were normalized to the leaf area. For comparison with other work, an empirically determined ratio of 163 g m^{-2} was used for conversion to fresh weight. The procedures used for mRNA extraction, cDNA synthesis, and quantitative reverse transcription polymerase chain reaction during the analysis of Glutathione-S-Transferase 1 (*GST1*) and Pathogenesis-Related 4 (*PR4*) transcript levels were as previously described (Weise et al., 2012). Measured transcript levels were normalized using the Actin2 housekeeping gene.

Gramicidin single channel lifetime

Gramicidin experiments were conducted using an Ionovation Compact electrophysiology chamber and a HEKA EPC10 USB amplifier. Bilayers were formed across 100 μm apertures in a Teflon sheet by painting lipid over the aperture. This was followed by repeatedly raising and lowering the aqueous solvent surface on both sides of the sheet past the aperture by pipetting. Chamber wells contained 1.8 mL of volume on either side of the Teflon sheet, and were filled with 1.5 mL KCl solution. Bilayers were formed from an 80/20 mixture of egg-yolk phosphatidylcholine/phosphatidylethanolamine bathed in 1 M KCl and monitored with 100 mV voltage. Isoprene, lipids, cholesterol, and gramicidin A were purchased from Sigma and used without further purification. The PE and PC used were not characterized for acyl chain

composition; lipid and cholesterol mixing ratios were calculated assuming two desaturations per lipid molecule and an average acyl chain length of 17 (Milinsk et al., 2003). Gramicidin A ethanol stock solutions were prepared weekly from powder and daily diluted down to a 100 fM working concentration. 1 M KCl solution was prepared using filter sterilization, aliquoted into 40 mL volumes, and stored at -20 °C until use; excess aliquot volume was discarded at the end of each day. Isoprene was added directly to the solution in sufficient amount to give a 2000 µL L^{-1} gas phase concentration and mixed for 5 min prior to measurement. The electrophysiology stage was enclosed by a 10x26x44 cm^3 Faraday cage. Heating was provided by a thermostat-controlled electrical heating strip. Air temperature inside of the Faraday cage was monitored using a thermocouple. All bilayers were allowed to thermally equilibrate for 20 min prior to measurements. Traces were recorded with Patchmaster v2x71 software in voltage clamp mode. Individual traces were analyzed to determine the lifetime of single channels. Lifetime histograms with 10 µs resolution were analyzed for statistical significance using an unpaired, one-tailed Mann-Whitney-Wilcoxon ranked sums test. In the cholesterol experiment, channel events were combined across temperature ranges prior to ranked sums testing. Channel survival was fitted to a single exponential logarithmic decay function to obtain τ:

$$y = Ae^{T/\tau} \quad , \qquad \text{Eq. 1}$$

where T is time in seconds. Fits were constrained to unity at time zero.

Perylene anisotropy decay

Lipids were obtained from Avanti and used without further purification. Upon arrival, lipids were

aliquoted under anaerobic conditions to 100 μL vials with Teflon septums and stored as 25 mg mL^{-1} chloroform solutions at -20 °C until use. Perylene powder was obtained from Sigma-Aldrich and used without further purification. Perylene was stored as a 100 μg ml^{-1} chloroform stock solution. Upon use, lipids and perylene were mixed in a 290:1 molar ratio, and the chloroform solvent was evaporated under a dry nitrogen stream. Tris buffer (10 mM, pH 7.8), was added to give a final sample lipid concentration of 1 mg ml^{-1}. Samples were processed through five freeze-thaw-vortex cycles to ensure complete mixing. Each cycle consisted of a 5 min immersion in liquid nitrogen followed by a 5 min incubation in a 60 °C water bath and a 2 min vortex. When not prepared the morning of experiments, lipids were prepared the night prior and stored overnight at -80 °C at the last freeze step. Vesicles were formed by extruding the lipid solutions 11 times at room temperature through a 400 nm polycarbonate membrane filter using a mini-extruder (Avanti Polar Lipids Inc.). Dynamic light scattering characterizations of vesicle preparations were performed using a Malvern Zetasizer operating at 632.8 nm. Vesicle preparations were diluted ten-fold prior to measurement. Measurements were performed at 25 °C.

The fluorescence anisotropy decay kinetics of vesicle-embedded perylene was monitored with a time correlated single photon counting system. The features of the system have been described previously (Pillman and Blanchard, 2010). The perylene was excited by a vertically polarized dye laser operating at 440 nm using stilbene 420 dye, and the subsequent fluorescence was measured at 475 nm. Liquid isoprene was added to the sample cuvette and the solution was allowed to equilibriate for 20 min prior to the start of measurements. Cuvettes were capped with adhesive-coated foil to prevent the evaporative loss of isoprene. At least 15 min was allowed for

thermal equilibration between individual measurements. Acquisitions at a condition were conducted over the course of 30 min and consisted of six 5 min acquisitions to allow for detection of temporal drift. Each acquisition was individually processed and fitted. Parallel and perpendicular fluorescence decay transients were aligned based on the temporal location of the maximum of the response function of each channel. Channel bias was corrected for by tail matching the decays at ~8 ps. Anisotropy was calculated using the induced optical anisotropy function:

$$R(t) = \frac{I_{\parallel}(t) - I_{\perp}(t)}{I_{\parallel}(t) + 2I_{\perp}(t)} \quad , \qquad \text{Eq. 2}$$

where $I_{\parallel}(t)$ and $I_{\perp}(t)$ are the fluorescence emission intensities parallel and perpendicular to the vertically polarized excitation pulse. The resulting anisotropy decay curves were fitted using Origin 8 software. Fit parameters for individual acquisitions were pooled for statistical analysis. For the transition dipole moment that was pumped and probed (S_1-S_0), the model for perylene reorientation as a prolate rotor is:

$$R(t) = 0.4e^{-6D_z t} \qquad \text{Eq. 3}$$

The model for perylene reorientation as an oblate rotor is:

$$R(t) = 0.1e^{-(2D_x + 4D_z)t} + 0.3e^{-6D_x t} \qquad \text{Eq. 4}$$

In the model equations, D_x and D_z are the Cartesian components of the rotational diffusion constant (Jiang and Blanchard, 1994). Data fitting to the prolate rotor model was by a first-order decay function.

$$R(t) = Ae^{-t/\tau} \qquad \text{Eq. 5}$$

Data fitting to the oblate rotor model was by a constrained second-order decay function,

$$R(t) = Ae^{-t/\tau_2} + 3\mathrm{Ae}^{-t/\tau_1} \quad , \qquad \text{Eq. 6}$$

where constraints were "A" between 10^{-4} and 0.2, "τ_1" between 20 and 5000, "τ_2" between 1 and 1000, and "τ_1" between 1.33 and 20 multiples of "τ_2". Adjusted R-squared was used to determine best fit between the two models. For the single-exponential decays that characterized my data, the Debye-Stokes-Einstein equation was used to calculate viscosity (Koan and Blanchard, 2006).

$$\tau_{OR} = \frac{\eta V f}{k_B T S} \qquad \text{Eq. 7}$$

τ_{OR} is the anisotropy decay time constant, η is viscosity, V is the hydrodynamic volume of perylene, *f* is a solvent-solute frictional interaction coefficient, k_B is the Boltzmann constant, T is the absolute temperature, and S is a shape factor to account for non-spherical shape of perylene. The hydrodynamic volume of perylene is 225 $Å^3$, and the shape factor is 0.7. The translational diffusion coefficient, D_T, was estimated using the Stokes-Einstein equation,

$$D_T = \frac{k_B T}{6 \pi R \eta} \quad , \qquad \text{Eq. 8}$$

where R is the radius of perylene. R was calculated from the hydrodynamic volume of perylene, 225 $Å^3$, by assuming a spherical shape, yielding R = 3.77 Å.

Results

ROS quenching and methyl vinyl ketone toxicity

ROS quenching as a mechanism of isoprene action is attractive because of the double bonds in isoprene. Photosynthetic leaves have a large number of molecules with double bonds and

protecting these against destruction by ROS could help leaves tolerate abiotic stress. The size of the alternative ROS sink provided by isoprene can be estimated. Carotenoids (known ROS quenchers) are estimated to provide 800 times more double bonds than isoprene (Table 3.1). Chlorophylls, quinones, and fatty acids would all contribute even more double bonds, making the presence of isoprene double bonds much less than 0.1% of the total inside a photosynthesizing cell.

The carbon and energy efficiency of isoprene quenching of ROS can also be estimated. Reported emission rates of MVK are about 10% of emission rates of isoprene meaning 90% of isoprene molecules are lost to the atmosphere before interacting with ROS inside a leaf. Given six carbons are required to make one isoprene molecule, plus 20 ATP and 14 NADPH, the cost of quenching one ROS molecule is 60 carbons, 200 ATP, and 140 NADPH.

Protection against ROS damage by chemical reaction of ROS with scavenger molecules requires that the products of the reaction be less toxic than the ROS itself. Since the presence of MVK has been taken as evidence of ROS scavenging by isoprene, isoprene and MVK were tested for their effects on oxidative stress indicators. Mature Arabidopsis rosettes were treated for 3 hr with 20 μL L^{-1} isoprene and MVK in a double factorial fashion. To support ROS quenching as the mechanism of action it is expected that isoprene would reduce stress indicators while MVK would have no effect or itself be protective.

The levels of hydrogen peroxide were tested in each of the four conditions of my two-factor design (Fig. 3.2). The control and isoprene-treated condition showed identical hydrogen peroxide levels of 12 nmol g^{-1} FW. In the MVK-treated plants, a significant increase in H_2O_2 levels was detected, increasing to ~18 nmol g^{-1} FW. The addition of isoprene to the MVK

treatment prevented the MVK-induced increase in H_2O_2 levels. If this decrease were due to quenching of ROS by isoprene, a similar decrease in H_2O_2 would be expected to occur between the control and isoprene condition.

Michael-addition acceptors such as MVK also affect gene expression levels. The transcript levels of two MVK-responsive genes, pathogenesis related 4 (*PR4*) and glutathione S-transferase 1 (*GST1*), were tested with quantitative reverse transcription polymerase chain reaction. The expression pattern of both of these genes closely tracked the pattern of H_2O_2 (Fig. 3.3). Transcript levels in the control and isoprene treated plants were identical at ~0.008 transcripts per ACT2. MVK treatment again caused an increase in the reporters, this time to a level of ~0.03 transcripts per ACT2. The magnitude of this increase was substantially larger, at ~4 fold, than the increase observed in H_2O_2, ~1.5 fold. Once again, the addition of isoprene to the MVK treatment prevented the MVK-induced increase in reporter gene expression levels. While there was statistically no difference between the control and MVK+ISP conditions, the expression levels of both genes trended upwards in the MVK+ISP condition.

Perturbation of membrane-embedded proteins

Isoprene was tested for the capacity to affect membranes by assessing gramicidin single-channel lifetimes, which are responsive to bilayer hydrophobic thickness. Channel lifetimes were tested at room temperature in a black lipid membrane composed of an 80/20 mixture of phosphatidylcholine/phosphatidylethanolamine derived from egg yolk. A total of 371 and 567 distinct single-channel events were analyzed in the absence and presence of isoprene,

respectively. Conversion of the collection of single-channel lifetimes into a survival histogram yields a curve that can be fit by a single exponential decay function. The survival histograms for gramicidin A single-channel events in the presence and absence of isoprene are shown in Figure 3.4. Single exponential decay fits are shown as dotted lines. In the presence of isoprene, gramicidin channels persisted for a significantly shorter period of time ($p=1.69*10^{-5}$), possibly indicating an expansion of the hydrophobic thickness of the bilayer.

This result, though suggestive, was the result of measurements taken at a single temperature and membrane composition, and may not be representative of the effects of isoprene in all membrane conditions. The range of tested conditions was increased by modulating the membrane temperature and modulating the membrane composition by the inclusion of cholesterol. Cholesterol was chosen because it is widely used in planar bilayer-lipid membrane experiments, it easily forms bilayers, and it produces large effects on bilayer properties. A temperature range from 30 to 50 °C and cholesterol content of 20 mol% were used in these experiments. The data were processed as in the first set of experiments and their survival histograms fit to single-exponential decay functions. τ is positively correlated to gramicidin channel lifetime and may be used as a proxy for the survival histogram. A plot of τ as a function of temperature and cholesterol presence revealed several trends (Fig. 3.5). Isoprene caused modest declines in channel lifetimes at lower temperatures while a larger decrease was observed at 45 °C. Cholesterol caused a large absolute decrease in channel lifetimes at 40 °C. In the presence of 20 mol% cholesterol, isoprene caused a larger decrease in channel lifetimes at 30 °C and 35 °C. At 45 °C channel lifetimes were short regardless of the presence of isoprene. At 50 °C isoprene lengthened channel lifetimes in both the presence and absence of cholesterol.

Interestingly, the effect of cholesterol on membrane thickness in the absence of isoprene was reversed at high and low temperatures. Over all of the single channel events from the temperature range from 30-45 °C channel lifetimes are significantly reduced in the presence of isoprene. p-value = .0452 and 1.27E-27 without and with cholesterol, respectively. Channel events from 50 °C were not included in the Mann-Whitney-Wilcoxon test.

Isoprene does not alter membrane fluidity

The impact of isoprene on the reorientation kinetics of bilayer membrane-embedded perylene was assessed in a series of lipids: distearoylphosphatidylcholine (DSPC), 1-stearoyl-2-oleoylphosphatidylcholine (SOPC), and 1-stearoyl-2-linoleoylphosphatidylcholine (SLPC). Vesicles were formed from (50/50 mol%) DSPC:SOPC, (100 mol%) SOPC, (50/50 mol%) SOPC:SLPC, and (100 mol%) SLPC. Vesicle preparations were characterized for size distributions by dynamic light scattering, and found to be slightly less than the nominal extrusion diameter of 400 nm (Fig 3.6). Perylene reorientation kinetics were assessed at 5 °C intervals from 30-45 °C.

The resulting perylene anisotropy decay kinetics were best fit by a first-order decay (Fig. 3.7), indicating that perylene was acting as a prolate rotor. From the recovered time constants the membrane viscosity and the perylene translational diffusion coefficient were calculated. The recovered viscosities ranged from 10-30 cP (Table 3.2), well within the range expected for a bilayer membrane environment, indicating stable bilayer formation. Interestingly, the viscosity measured in vesicles formed from lipid mixtures was significantly higher than that for vesicles

formed from pure lipid. No effect of isoprene was seen on the bilayer viscosity or on the translational diffusion coefficient across any of the temperature and lipid combinations (Fig. 3.7).

Discussion

The results reported here support the alteration of membrane dynamics, as demonstrated by gramicidin A channel lifetimes, as the molecular mechanism of action of isoprene. The alternative ROS quenching mechanism was evaluated and found to be inadequate in several ways. First, the concentration of double bonds in isoprene is much less than the concentration of double bonds in carotenoids and other molecules (Table 3.1). Second, emission ratios of MVK and isoprene indicate that at least 90% of synthesized isoprene, and often times more, escapes from plants without interacting with ROS making the energetic cost of chemical detoxification of ROS with isoprene enormous. Third, isoprene does not reduce the levels of H_2O_2 and message level of stress responsive genes in unstressed leaves, rather, it prevents their increase when leaves are stressed. Fourth, the interaction of isoprene with ROS leads to the formation of toxic breakdown products. These data are consistent with two interpretations: (i) little isoprene is converted to cytotoxic products during abiotic stress and (ii) isoprene is acting by an indirect mechanism to *prevent* ROS formation, rather than by direct chemical quenching of ROS after it is formed. This is consistent with the view that ROS inside cells plays a critical role in information exchange and are not simply deleterious molecules that should always be quenched (Foyer and Noctor, 2011).

The membrane hypothesis

The membrane hypothesis of isoprene action emerged based on the lipophyllicity of isoprene (Sharkey and Singsaas, 1995). Functional assays indicate that processes occurring in thylakoid membranes are stabilized by isoprene (Velikova et al., 2011; Beckett et al., 2012) but the mechanism of this stabilization is unknown. Molecular dynamics indicates that isoprene will reside primarily in the mid-plane of the membrane bilayer (Siwko et al., 2007). This is notable because of the relatively low mass density of the bilayer midplane, and the enhanced conformational freedom and decreased order of acyl chains in this region. Isoprene is not alone in this behavior, however, as the bilayer midplane is the preferred location for many membrane-embedded, biological molecules (Hauß et al., 2002; Hauß et al., 2005). This raises the question of what molecular characteristics make isoprene effective. For the protection of photosynthesis, there is a double bond requirement (Sharkey et al., 2001). The other prominent feature of isoprene, branching of the carbon backbone, was not important. This suggests that the enhanced volume or the polar character of pi bonds is important for the function of isoprene; the reason for this remains unclear.

Perturbation of gramicidin A channel lifetimes

This possibility was probed in these studies using measurements of the channel lifetime of individual gramicidin A channels. The gramicidin family of peptides was selected because they are well studied; their channel lifetimes are generally accepted to be primarily responsive to

membrane hydrophobic thickness (Kelkar and Chattopadhyay, 2007; Kim et al., 2012). The gramicidin channel-forming dimer possesses a hydrophobic length shorter than the depth of a typical bilayer (~40 Å). Bending of the lipid bilayer to match the hydrophobic length of the dimer adds to the free energy of channel formation, decreasing channel stability and lifetime. Bilayer expansion exacerbates the hydrophobic mismatch, shortening channel lifetimes.

The results are consistent with isoprene causing bilayer expansion under a range of physiologically relevant temperatures and in the presence and absence of cholesterol. The effect of isoprene in reducing channel lifetimes in the absence of cholesterol was most pronounced at 45 °C, consistent with the role of isoprene as a thermoprotectant in this temperature range. At extreme temperatures of 50 °C, isoprene did not reduce gramicidin A channel lifetimes. This is consistent with the view that isoprene exerts protective effects at moderately high temperatures of 38-45 °C, where the emission rate is maximal (Monson et al., 2012). Interestingly, at low temperatures, gramicidin channel lifetime was significantly more isoprene-sensitive in the presence of cholesterol. Previous studies have shown that the efficacy of volatiles on gramicidin A channels is affected by cholesterol (Lundbaek et al., 1996; Weinrich et al., 2009), and have generally attributed this to cholesterol-induced stiffening of membranes. Cholesterol inclusion can cause changes in the area-per-lipid and hydrophobic thickness of a membrane, which can consequently alter intra-membrane solute partitioning (Smith et al., 1981; Nezil and Bloom, 1992; Lundbaek et al., 1996; Hung et al., 2007). The data in the present study suggest that at lower temperatures cholesterol increased the area-per-lipid and thinned bilayers, resulting in an increased membrane partitioning of isoprene. Reversal of this effect at higher temperatures is consistent with previous findings (Ipsen et al., 1990). While thylakoids are sterol-free, their high

protein density may cause distortions in the bulk lipid phase that mimic sterol-induced alterations. The fact that the expansive effect of isoprene was seen in both of the lipid conditions suggests that this result is applicable to a much larger range of membrane conditions, including those conditions found within thylakoid membranes.

Perylene anisotropy decay

In the membrane fluidity studies, the recovery of a single exponential anisotropy decay in the perylene studies is important for the interpretation of the experimental results. Past studies have found perylene to exhibit double-exponential anisotropy decay kinetics when embedded in DMPC vesicles (Pillman and Blanchard, 2010), and have interpreted this to indicate that the perylene probe is residing preferentially in the bilayer midplane. In alkane solvents, however, the effective rotor shape of perylene is known to be sensitive to the solvent chain length (Jiang and Blanchard, 1994). It is possible that the use of 18-carbon acyl chain lipids in the present study causes a similar shift from oblate to prolate rotor shape, indicating that perylene intercalated within the acyl-chains themselves. Given that isoprene is midplane localized, this intra-chain orientation may have contributed to the lack of effect. However, this result still suggests that fluidity alteration, if it occurs, is below the detection limit of the system, and is unlikely to be as significant an effect as the expansion of the hydrophobic thickness.

Translation of membrane effects to physiological thermotolerance

There are a few modes by which expansion of the thylakoid membrane could in turn cause thermal protection of the photosynthetic apparatus. Generally, protection could be mediated by bulk lipid effects or by more specific protein effects. In the bulk lipid phase membrane bilayer expansion might prevent pore formation. Transient pore formation is related to membrane thickness with thicker membranes reducing ion movement through transient pores (Paula et al., 1996). Hydrophilic pores form through a gradual invasion of water molecules (Fig. 3.8). This can lead to acyl chain interdigitation and monolayer formation. Once water can form a continuous channel through the bilayer, lipid headgroups can reorient forming a stabilized pore. Isoprene, by increasing the mass density in the midplane, could prevent water chain formation.

Besides pore formation, membrane thickness could modulate the function of membrane-embedded proteins (Andersen and Koeppe, 2007). Lipid-protein interactions are especially important for electron transport chains such as those of respiration and photosynthesis. Membrane thickness can have significant effects on electron transport chain components (Montecucco et al., 1982). Isoprene is known to enhance the temperature stability of light harvesting complex II supercomplexes (Velikova et al., 2011). Aggregation of light harvesting complex II during induction of non-photochemical quenching that protects against stress damage has been associated with localized changes in membrane thickness (Johnson et al., 2011). Isoprene, by altering the thickness of the bulk lipid phase of the thylakoid membrane, could increase the hydrophobic mismatch between light harvesting complex II supercomplexes and their surrounding lipid environment. This mismatch would tend to enhance the aggregation of

light harvesting complex II arrays, preventing their breakdown at high temperature and explaining at a molecular scale the results of Velikova et al. 2011.

The membrane-based effects of isoprene need not be limited to the thylakoid, and the prevention of programmed cell death like symptoms (Sharkey et al., 2001) may be more easily explained by invoking effects on extra-plastidic membranes. Many membranes are involved in cell death signaling and ROS production, and it is possible to hypothesize effects of isoprene on any of these membranes. Plasma membranes, for example, are sites of apoplast-targeted ROS production and Ca^{2+} influx in response to pathogens (Torres, 2006). The outer mitochondrial membrane and endoplasmic reticulum are involved in cell death signaling in response to biotic and abiotic stress. Mitochondrial membrane permeabilization is a significant step in programmed cell death in *Arabidopsis thaliana* (Yao et al., 2004). By simple bilayer expansion, isoprene could exert effects on any of these processes.

Our results and analysis indicate that ROS quenching is unlikely to be an important mechanism for isoprene protection against abiotic stress and may even be deleterious. The alternative, that isoprene dissolves in the membrane and thereby strengthens it at moderately high temperature or when oxidative stress begins to damage a membrane, is supported. Specifically, these results suggest that this strengthening comes as a result of an increase in the hydrophobic thickness, rather than a decrease in fluidity. This thickening could protect photosynthesis through a decrease in the rate of pore formation or through the alteration of lipid-protein hydrophobic matching. Additional in vivo studies are needed to correlate these general membrane changes to specific physiological processes in thylakoid membranes.

Acknowledgments

I thank Shelagh Ferguson-Miller and Michael Feig for helpful discussions. This material is based upon work supported by the National Science Foundation under Grant No. 0950574. My travel to Germany was supported by the iGRAD-Plant graduate exchange program IRTG 1525, which is funded by the Deutsche Forschungsgemeinschaft and the Michigan State University Graduate School.

APPENDIX

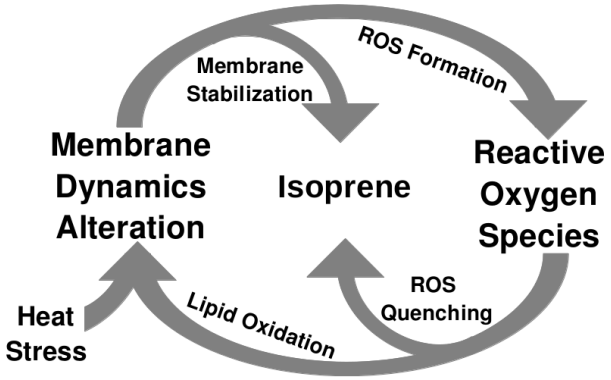

Figure 3.1 Schematic representation of the lipid oxidation/ROS production feedback cycle. The cycle may be initiated by heat stress, and isoprene may break the membrane damage/ROS production cycle by stabilizing damaged membranes or by ROS quenching. Modified from Velikova et al., 2012.

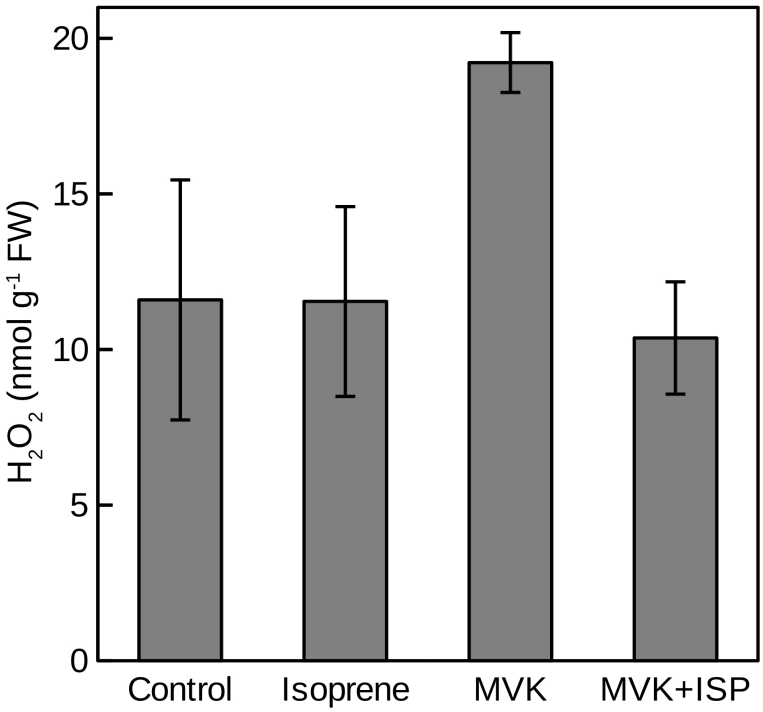

Figure 3.2 Hydrogen peroxide content of *Arabidopsis thaliana* leaves following isoprene (ISP) and/or methyl vinyl ketone (MVK) treatment. Isoprene prevents the accumulation of MVK-induced hydrogen peroxide but does not lower background levels of hydrogen peroxide. Error bars represent the standard errors of the means, n=6.

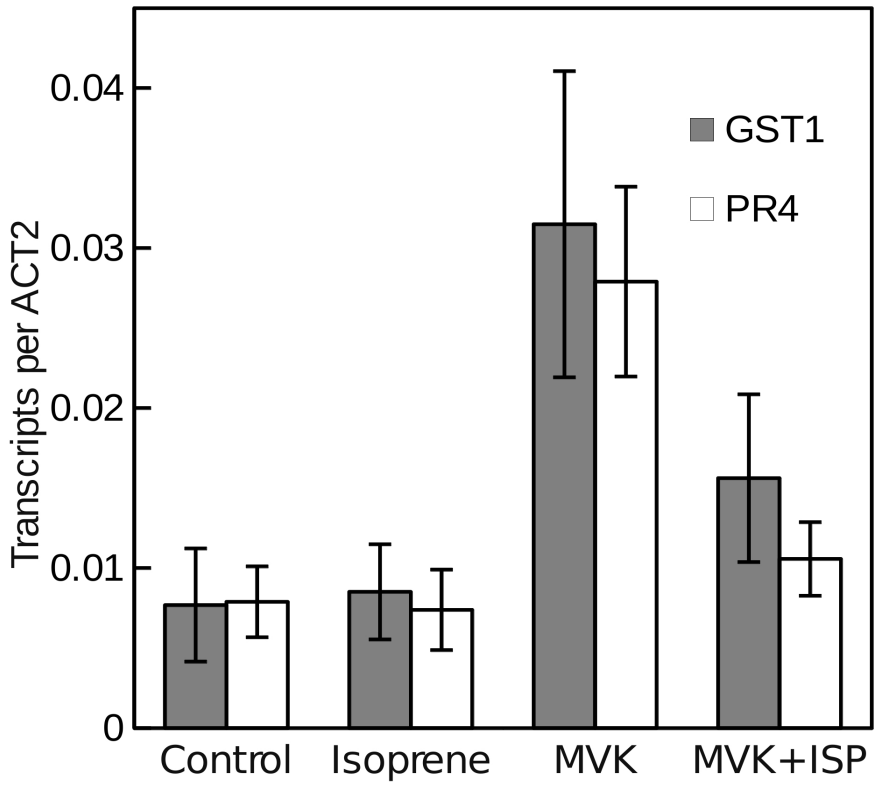

Figure 3.3 Transcript levels of methyl vinyl ketone responsive genes in *Arabidopsis thaliana* leaves following isoprene (ISP) and/or methyl vinyl ketone (MVK) treatment. Isoprene prevented a majority of the MVK-induced increase in GST1 and PR4 expression. relative to ACT2 transcript level. Error bars represent the standard errors of the means, n=6.

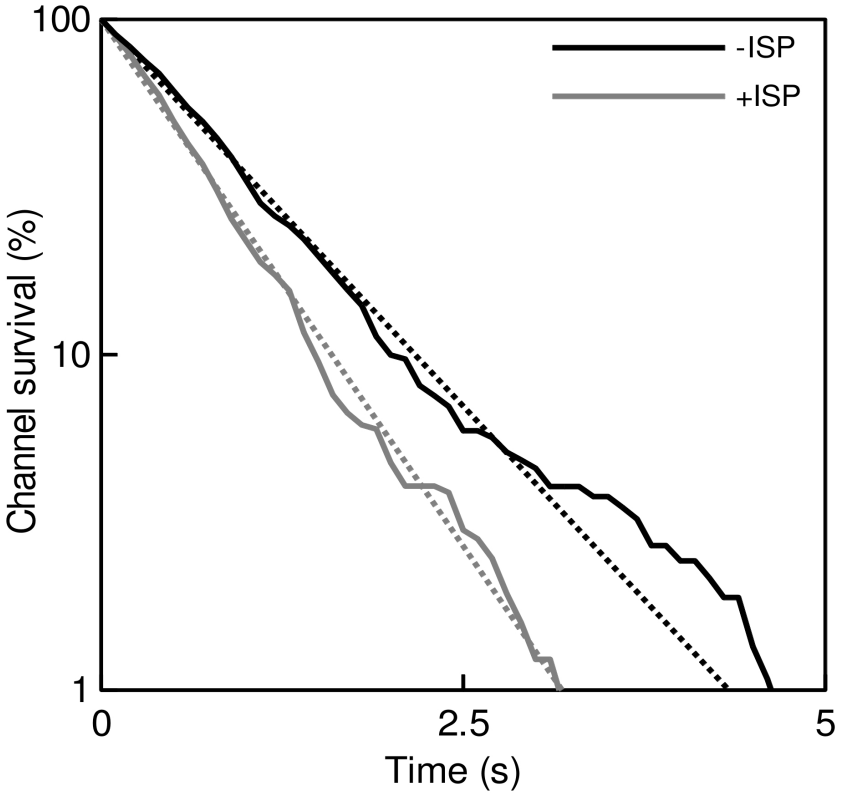

Figure 3.4 Survival of gramicidin A channels following formation. Channels were embedded in cholesterol-free membranes at room temperature (~25 °C).

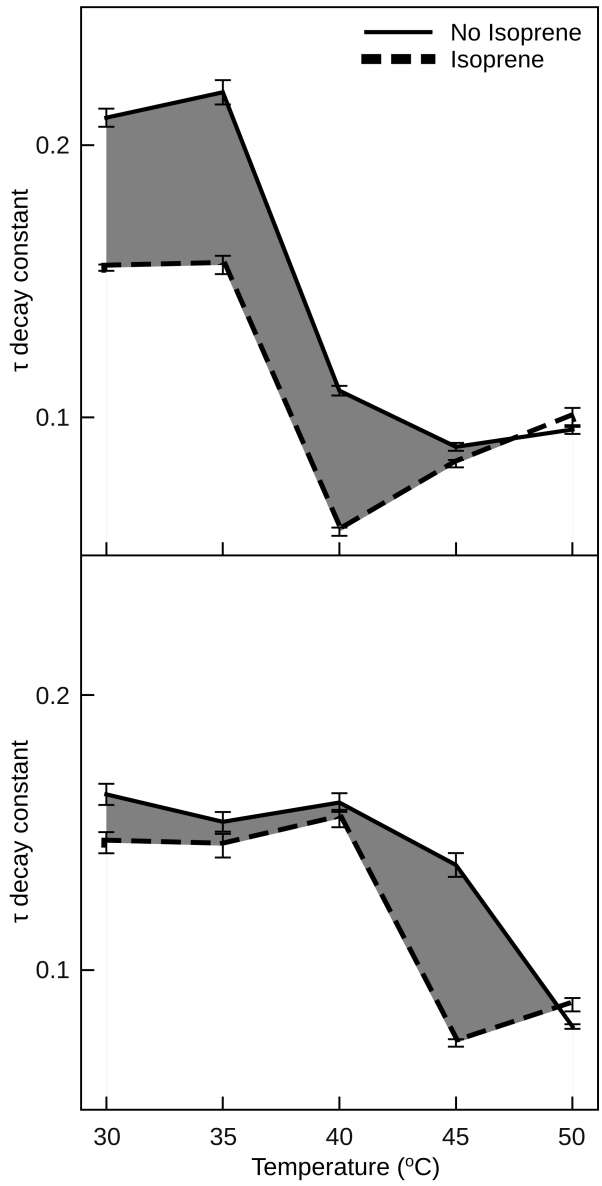

Figure 3.5 τ decay constants of gramicidin A channels. The top panel is from cholesterol-free membranes and the bottom pannel is from membranes containing 20 mol% cholesterol. Solid grey lines represent the absence of isoprene, dashed grey lines represent the presence of isoprene, the darkened area represents the difference between the two datasets. Error bars represent ± three times the standard error of the fit. In the cholesterol-lacking membranes, the τ value at 35 °C in the without isoprene series is an average of measurements taken on two different membranes. The τ values from a cholesterol-free membrane at 50 °C were found to be outliers, and the measurement was repeated. Only τ values from the second membrane are shown.

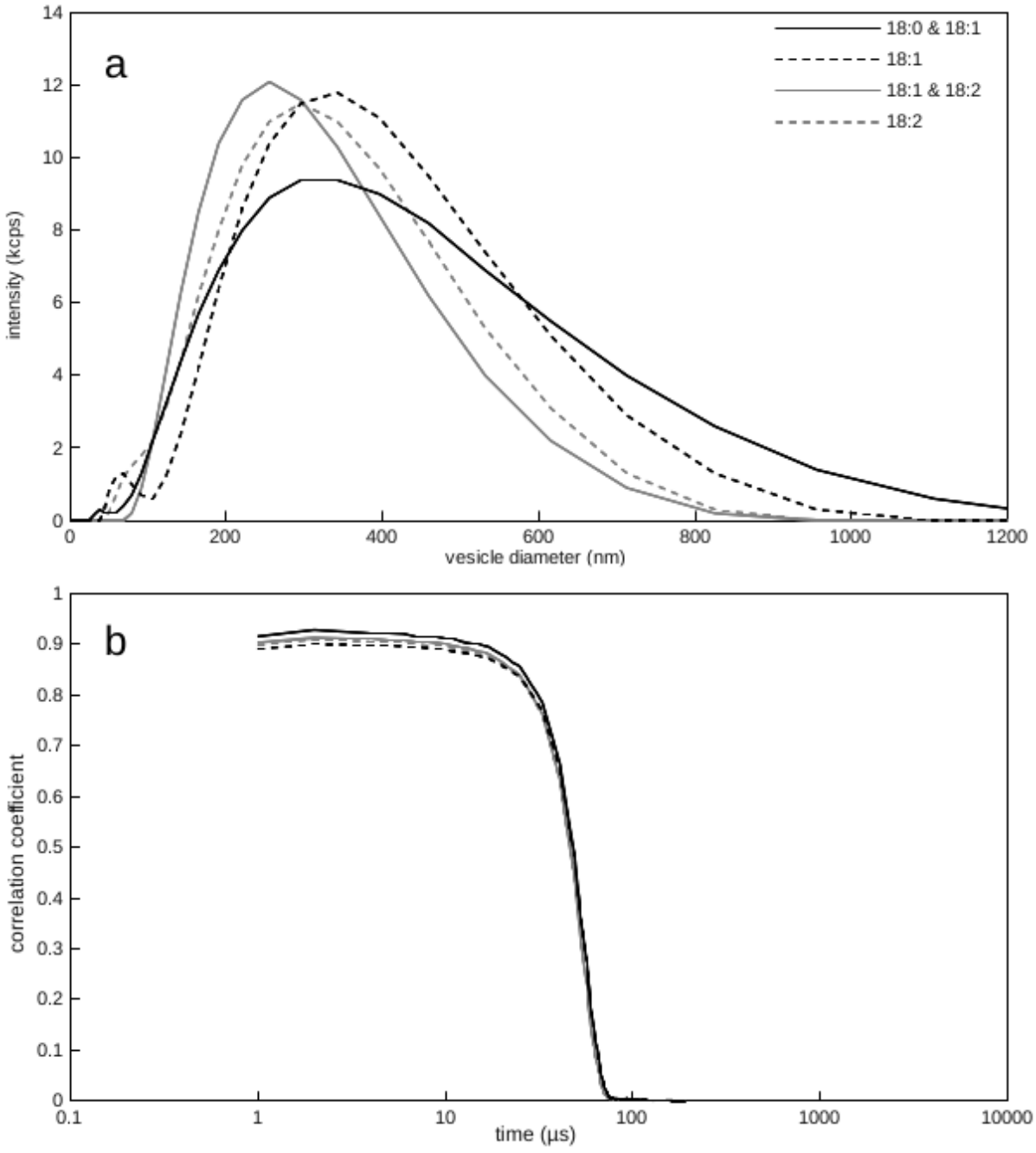

Figure 3.6 Dynamic light scattering characterization of vesicles used in perylene studies (a) Experimental size distributions for vesicles composed of 1:1 DSPC:1-stearoyl-2-oleoyl PC (black solid line), 1-stearoyl-2-oleoyl PC (black dashed line), 1:1 1-stearoyl-2-oleoyl PC:1-stearoyl-2-linoleoyl PC (grey solid line), and 1-stearoyl-2-linoleoyl PC (grey dashed line). (b) Experimental correlation functions associated with the same samples.

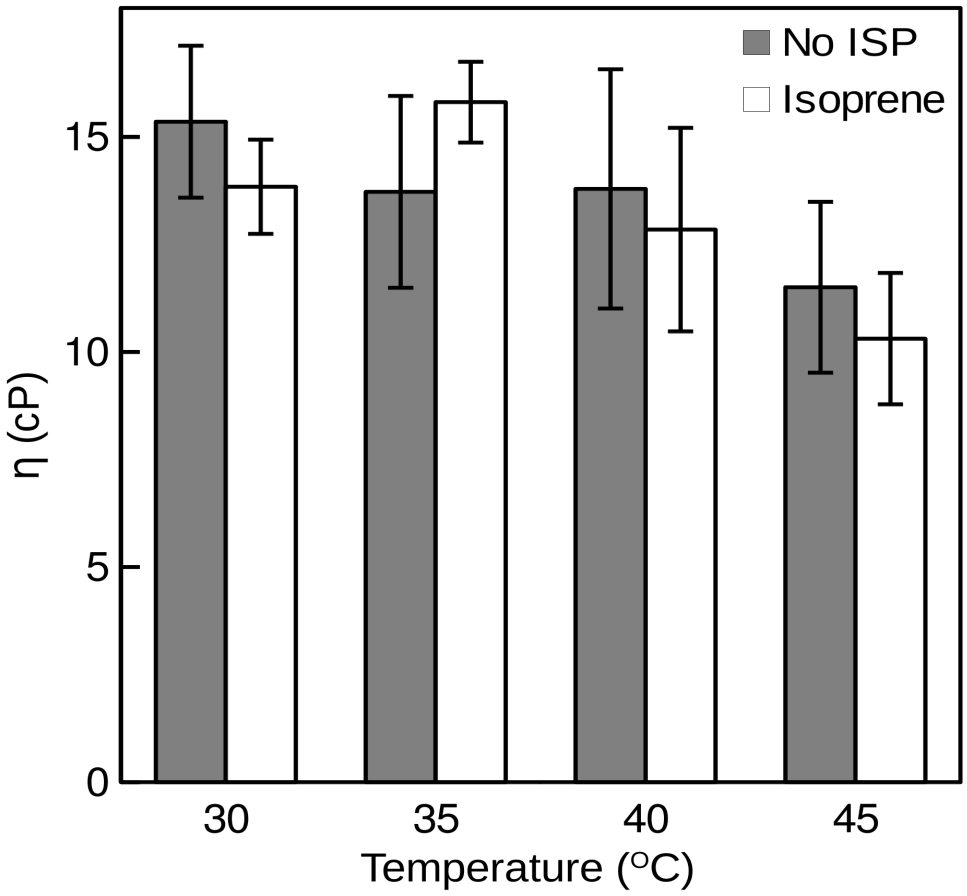

Figure 3.7 Viscosity of 1-stearoyl-2-linoleoyl-phosphatidylcholine vesicles. Isoprene did not significantly alter the viscosity of the membrane at the midplane under any of the conditions tested. Error bars represent the standard errors of the means, n=6.

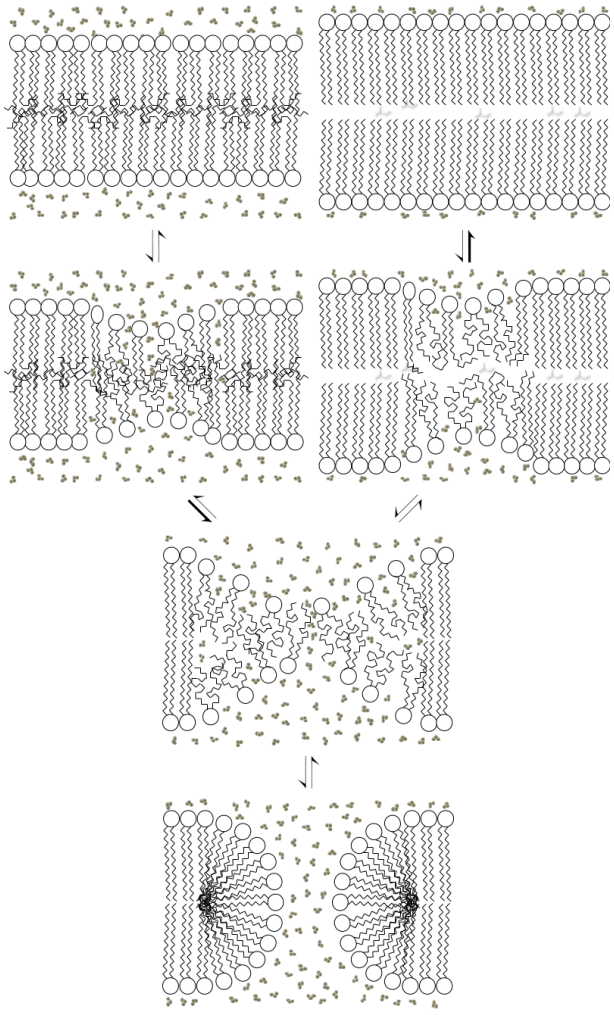

Figure 3.8 Model of bilayer expansion mediated inhibition of pore formation. Pore formation initiates from invagination of one or both monolayers. Upon reaching a critical threshold of invagination, acyl chain interdigitation induces monolayer formation. Water chain-led headgroup invagination completes formation of the hydrophilic pore. Isoprene may expand bilayers by ordering acyl chains, preventing monolayer interdigitation, and increasing medial separation of monolayer lipids. Isoprene may also decrease intercalation of water molecules, and subsequent water chain formation.

Table 3.1 Number of double bonds contributed by different compounds in a leaf. Isoprene contributes few double bonds compared to dedicated reactive oxygen species quenchers.

Compound	Double Bonds (μmol m^{-2})
Isoprene	3
Carotenoids	2387
Chlorophyll a	5376
Chlorophyll b	605
Quinines	116

Table 3.2 Membrane physical parameters measured by perylene orientation anisotropy decay. DB index refers to the number of double bonds, on average, per lipid. The double bond index of 1:1 DSPC:1-stearoyl-2-oleoylphosphatidylcholine was 0.5, of 1-stearoyl-2-oleoylphosphatidylcholine was 1, of 1:1 1-stearoyl-2-oleoyl PC:1-stearoyl-2-linoleoylphosphatidylcholine 1.5, and of 1-stearoyl-2-linoleoylphosphatidylcholine was 2. Negative and positive signs following physical parameters indicate measures in the absence and presence of isoprene, respectively.

DB Index	T(°C)	τ_{OR},- (ps)	η- (cP)	D_T,- (μm2 s-1)	τ_{OR},+ (ps)	η+ (cP)	D_T,+ (μm2 s-1)
0.5	30	1359±40	25±1	23±1	1447±90	27±2	22±1
0.5	35	1461±99	28±2	22±1	1438±47	27±1	22±1
0.5	40	1379±30	26±1	23±1	1422±97	27±2	23±2
0.5	45	1542±34	30±1	21±.5	1336±71	26±1	24±1
1	30	858±109	16±2	41±8	870±39	16±1	37±2
1	35	675±80	13±2	51±8	753±92	14±2	45±7
1	40	669±84	13±2	51±8	710±90	14±2	48±7
1	45	483±40	9±1	68±6	676±100	13±2	54±12
1.5	30	1106±86	21±2	29±3	919±90	17±2	36±3
1.5	35	907±35	17±1	35±1	963±83	18±2	34±3
1.5	40	908±113	17±2	37±5	760±128	15±2	47±7
1.5	45	905±77	18±2	36±3	864±88	17±2	38±4
2	30	825±95	15±2	41±5	744±59	14±1	44±4
2	35	726±118	14±2	49±9	836±50	16±1	38±2
2	40	718±145	14±3	53±11	668±123	13±2	56±12
2	45	589±102	12±2	62±12	528±78	10±2	69±15

REFERENCES

REFERENCES

Andersen OS, Koeppe RE (2007) Bilayer thickness and membrane protein function: an energetic perspective. Annual Review of Biophysics and Biomolecular Structure **36**: 107–130

Beckett M, Loreto F, Velikova V, Brunetti C, Di Ferdinando M, Tattini M, Calfapietra C, Farrant JM (2012) Photosynthetic limitations and volatile and non-volatile isoprenoids in the poikilochlorophyllous resurrection plant *Xerophyta humilis* during dehydration and rehydration: Photosynthesis, isoprenoids and drought. Plant, Cell & Environment **35**: 2061–2074

Behnke K, Loivamäki M, Zimmer I, Rennenberg H, Schnitzler J-P, Louis S (2010) Isoprene emission protects photosynthesis in sunfleck exposed Grey Poplar. Photosynthesis Research **104**: 5–17

Berry J, Björkman O (1980) Photosynthetic response and adaptation to temperature in higher-plants. Annual Review of Plant Physiology and Plant Molecular Biology **31**: 491–543

Chapman DJ, Barber J (1986) Analysis of plastoquinone-9 levels in appressed and non-appressed thylakoid membrane regions. Biochimica et Biophysica Acta - Bioenergetics **850**: 170–172

Demmig B, Winter K, Krüger A, Czygan F-C (1987) Photoinhibition and zeaxanthin formation in intact leaves: a possible role of the xanthophyll cycle in the dissipation of excess light energy. Plant Physiology **84**: 218–224

Doyle M, Sexton KG, Jeffries H, Bridge K, Jaspers I (2004) Effects of 1,3-butadiene, isoprene, and their photochemical degradation products on human lung cells. Environmental Health Perspectives **112**: 1488–1495

Foyer CH, Noctor G (2011) Ascorbate and glutathione: the heart of the redox hub. Plant Physiology **155**: 2–18

Foyer CH, Shigeoka S (2010) Understanding oxidative stress and antioxidant functions to enhance photosynthesis. Plant Physiology **155**: 93–100

Frimer AA (1985) Singlet O_2. CRC Press, Boca Raton, Fla.

Göhre V, Jones AM, Sklenár J, Robatzek S, Weber AP (2012) Molecular crosstalk between PAMP-triggered immunity and photosynthesis. Molecular Plant-Microbe Interactions **25**: 1083–1092

Hauß T, Dante S, Dencher NA, Haines TH (2002) Squalane is in the midplane of the lipid bilayer: implications for its function as a proton permeability barrier. Biochimica et Biophysica Acta - Bioenergetics **1556**: 149–154

Hauß T, Dante S, Haines TH, Dencher NA (2005) Localization of coenzyme Q10 in the center of a deuterated lipid membrane by neutron diffraction. Biochimica et Biophysica Acta - Bioenergetics **1710**: 57–62

Honerkamp-Smith AR, Veatch SL, Keller SL (2009) An introduction to critical points for biophysicists; observations of compositional heterogeneity in lipid membranes. Biochimica et Biophysica Acta - Biomembranes **1788**: 53–63

Hung W-C, Lee M-T, Chen F-Y, Huang HW (2007) The condensing effect of cholesterol in lipid bilayers. Biophysical Journal **92**: 3960–3967

Ipsen JH, Mouritsen OG, Bloom M (1990) Relationships between lipid membrane area, hydrophobic thickness, and acyl-chain orientational order. The effects of cholesterol. Biophysical Journal **57**: 405–412

Jardine KJ, Monson RK, Abrell L, Saleska SR, Arneth A, Jardine A, Ishida FY, Serrano AMY, Artaxo P, Karl T, et al (2012) Within-plant isoprene oxidation confirmed by direct emissions of oxidation products methyl vinyl ketone and methacrolein. Global Change Biology **18**: 973–984

Jiang Y, Blanchard GJ (1994) Rotational diffusion dynamics of perylene in n-alkanes. Observation of a solvent length-dependent change of boundary condition. The Journal of Physical Chemistry **98**: 6436–6440

Johnson MP, Brain APR, Ruban AV (2011) Changes in thylakoid membrane thickness associated with the reorganization of photosystem II light harvesting complexes during photoprotective energy dissipation. Plant Signaling & Behavior **6**: 1386–1390

Kai H, Hirashima K, Matsuda O, Ikegami H, Winkelmann T, Nakahara T, Iba K (2012) Thermotolerant cyclamen with reduced acrolein and methyl vinyl ketone. Journal of Experimental Botany **63**: 4143–4150

Karl T, Harley P, Emmons L, Thornton B, Guenther A, Basu C, Turnipseed A, Jardine K (2010) Efficient atmospheric cleansing of oxidized organic trace gases by vegetation. Science **330**: 816–819

Kelkar DA, Chattopadhyay A (2007) The gramicidin ion channel: A model membrane protein. Biochimica et Biophysica Acta - Biomembranes **1768**: 2011–2025

Kim T, Lee KI, Morris P, Pastor RW, Andersen OS, Im W (2012) Influence of hydrophobic mismatch on structures and dynamics of gramicidin A and lipid bilayers. Biophysical Journal **102**: 1551–1560

Koan MM, Blanchard GJ (2006) Gauging the effect of impurities on lipid bilayer phase transition temperature. The Journal of Physical Chemistry B **110**: 16584–16590

Laothawornkitkul J, Paul ND, Vickers CE, Possell M, Taylor JE, Mullineaux PM, Hewitt CN (2008) Isoprene emissions influence herbivore feeding decisions. Plant, Cell & Environment **31**: 1410–1415

Li Z, Ratliff EA, Sharkey TD (2011) Effect of temperature on postillumination isoprene emission in oak and poplar. Plant Physiology **155**: 1037–1046

Loivamäki M, Mumm R, Dicke M, Schnitzler J-P (2008) Isoprene interferes with the attraction of bodyguards by herbaceous plants. Proceedings of the National Academy of Sciences of the United States of America **105**: 17430–17435

Loreto F, Mannozzi M, Maris C, Nascetti P, Ferranti F, Pasqualini S (2001) Ozone quenching properties of isoprene and its antioxidant role in leaves. Plant Physiology **126**: 993–1000

Loreto F, Velikova V (2001) Isoprene produced by leaves protects the photosynthetic apparatus against ozone damage, quenches ozone products, and reduces lipid peroxidation of cellular membranes. Plant Physiology **127**: 1781–1787

Lundbaek JA, Birn P, Girshman J, Hansen AJ, Andersen OS (1996) Membrane stiffness and channel function. Biochemistry **35**: 3825–3830

Milinsk MC, Murakami AE, Gomes STM, Matsushita M, de Souza NE (2003) Fatty acid profile of egg yolk lipids from hens fed diets rich in n-3 fatty acids. Food Chemistry **83**: 287–292

Monson RK, Grote R, Niinemets Ü, Schnitzler J-P (2012) Modeling the isoprene emission rate from leaves. New Phytologist **195**: 541–559

Montecucco C, Smith GA, Dabbeni-sala F, Johannsson A, Galante YM, Bisson R (1982) Bilayer thickness and enzymatic activity in the mitochondrial cytochrome *c* oxidase and ATPase complex. FEBS Letters **144**: 145–148

Munne-Bosch S, Queval G, Foyer CH (2012) The impact of global change factors on redox signaling underpinning stress tolerance. Plant Physiology **161**: 5–19

Murakami S, Packer L (1970) Protonation and chloroplast membrane structure. The Journal of Cell Biology **47**: 332–351

Nezil FA, Bloom M (1992) Combined influence of cholesterol and synthetic amphiphillic peptides upon bilayer thickness in model membranes. Biophysical Journal **61**: 1176 – 1183

Paula S, Volkov AG, Van Hoek AN, Haines TH, Deamer DW (1996) Permeation of protons, potassium ions, and small polar molecules through phospholipid bilayers as a function of membrane thickness. Biophysical Journal **70**: 339–348

Paulson SE, Flagan RC, Seinfeld JH (1992a) Atmospheric photooxidation of isoprene part I: The hydroxyl radical and ground state atomic oxygen reactions. International Journal of Chemical Kinetics **24**: 79–101

Paulson SE, Flagan RC, Seinfeld JH (1992b) Atmospheric photooxidation of isoprene part II: The ozone-isoprene reaction. International Journal of Chemical Kinetics **24**: 103–125

Pearcy R (1978) Effect of growth temperature on fatty-acid composition of leaf lipids in *Atriplex-lentiformis*-(torr)-wats. Plant Physiology **61**: 484–486

Pillman HA, Blanchard GJ (2010) Effects of ethanol on the organization of phosphocholine lipid bilayers. The Journal of Physical Chemistry B **114**: 3840–3846

Raison J, Pike C, Berry J (1982) Growth temperature-induced alterations in the thermotropic properties of *Nerium oleander* membrane lipids. Plant Physiology **70**: 215–218

Sharkey TD (1996) Isoprene synthesis by plants and animals. Endeavour **20**: 74–78

Sharkey TD, Chen X, Yeh S (2001) Isoprene increases thermotolerance of fosmidomycin-fed leaves. Plant Physiology **125**: 2001–2006

Sharkey TD, Singsaas E (1995) Why plants emit isoprene. Nature **374**: 769–769

Siwko ME, Marrink SJ, de Vries AH, Kozubek A, Schoot Uiterkamp AJM, Mark AE (2007) Does isoprene protect plant membranes from thermal shock? A molecular dynamics study. Biochimica et Biophysica Acta - Biomembranes **1768**: 198–206

Smith R, Porter E, Miller K (1981) The solubility of anesthetic-gases in lipid bilayers. Biochimica et Biophysica Acta **645**: 327–338

Terry GM, Stokes NJ, Hewitt CN, Mansfield TA (1995) Exposure to isoprene promotes flowering in plants. Journal of Experimental Botany **46**: 1629–1631

Torres MA (2006) Reactive oxygen species signaling in response to pathogens. Plant Physiology **141**: 373–378

Triantaphylidès C, Havaux M (2009) Singlet oxygen in plants: production, detoxification and signaling. Trends in Plant Science **14**: 219–228

Triantaphylidès C, Krischke M, Hoeberichts FA, Ksas B, Gresser G, Havaux M, Van Breusegem F, Mueller MJ (2008) Singlet oxygen is the major reactive oxygen species involved in photooxidative damage to plants. Plant Physiology **148**: 960–968

Veatch SL (2007) From small fluctuations to large-scale phase separation: Lateral organization in model membranes containing cholesterol. Seminars in Cell & Developmental Biology **18**: 573–582

Veatch SL, Cicuta P, Sengupta P, Honerkamp-Smith A, Holowka D, Baird B (2008) Critical fluctuations in plasma membrane vesicles. ACS Chemical Biology **3**: 287–293

Velikova V, Edreva A, Loreto F (2004) Endogenous isoprene protects *Phragmites australis* leaves against singlet oxygen. Physiologia Plantarum **122**: 219–225

Velikova V, Pinelli P, Pasqualini S, Reale L, Ferranti F, Loreto F (2005) Isoprene decreases the concentration of nitric oxide in leaves exposed to elevated ozone: Rapid report. New Phytologist **166**: 419–426

Velikova V, Sharkey TD, Loreto F (2012) Stabilization of thylakoid membranes in isoprene-emitting plants reduces formation of reactive oxygen species. Plant Signaling & Behavior **7**: 139–41

Velikova V, Várkonyi Z, Szabó M, Maslenkova L, Nogues I, Kovács L, Peeva V, Busheva M, Garab G, Sharkey TD, et al (2011) Increased thermostability of thylakoid membranes in isoprene-emitting leaves probed with three biophysical techniques. Plant Physiology **157**: 905–916

Vickers CE, Gershenzon J, Lerdau MT, Loreto F (2009a) A unified mechanism of action for volatile isoprenoids in plant abiotic stress. Nature Chemical Biology **5**: 283–291

Vickers CE, Possell M, Cojocariu CI, Velikova VB, Laothawornkitkul J, Ryan A, Mullineaux PM, Nicholas Hewitt C (2009b) Isoprene synthesis protects transgenic tobacco plants from oxidative stress. Plant, Cell & Environment **32**: 520–531

Way DA, Ghirardo A, Kanawati B, Esperschütz J, Monson RK, Jackson RB, Schmitt-Kopplin P, Schnitzler J-P (2013) Increasing atmospheric CO_2 reduces metabolic and physiological differences between isoprene- and non-isoprene-emitting poplars. New Phytologist **200**: 534–546

Weinrich M, Rostovtseva TK, Bezrukov SM (2009) Lipid-dependent effects of halothane on gramicidin channel kinetics: a new role for lipid packing stress. Biochemistry **48**: 5501–5503

Weise SE, Aung K, Jarou ZJ, Mehrshahi P, Li Z, Hardy AC, Carr DJ, Sharkey TD (2012) Engineering starch accumulation by manipulation of phosphate metabolism of starch. Plant Biotechnology Journal **10**: 545–554

Yao N, Eisfelder BJ, Marvin J, Greenberg JT (2004) The mitochondrion - an organelle commonly involved in programmed cell death in *Arabidopsis thaliana*. The Plant Journal **40**: 596–610

Zoeller M, Stingl N, Krischke M, Fekete A, Waller F, Berger S, Mueller MJ (2012) Lipid profiling of the *Arabidopsis* hypersensitive response reveals specific lipid peroxidation and fragmentation processes: biogenesis of pimelic and azelaic acid. Plant Physiology **160**: 365–378

Chapter 4

The Intramembrane Concentration of Isoprene

Abstract

The concentration of isoprene in the thylakoid membrane of rapidly emitting plants is unknown. This concentration is important for determining what effects isoprene might be having on the thylakoid membrane. In this study I determined the intramembrane concentration of isoprene using a combination of gas exchange techniques and gas chromatography fatty acid methyl ester analysis. Concentrations in both synthetic vesicles and isolated thylakoids were determined, and found to be roughly two orders of magnitude lower than had previously been predicted. This result was in agreement with ab initio calculations based on the octanol water partitioning coefficient of isoprene. This suggests that the physiological concentration of isoprene is too low to affect the dynamics of thylakoid lipids.

Introduction

The concentration of a solute in a membrane determines the magnitude of effects on the constituent lipids. Thus, the intramembrane concentration of isoprene is an important consideration for determining if isoprene causes membrane expansion or acyl chain ordering to a large enough degree to protect the thylakoid membrane from heat stress. Previous studies have demonstrated that at least several mole percent of solutes need to be embedded in membranes in order for any significant bilayer effects to occur (Cantor, 1997). The concentration of isoprene in membranes has been estimated previously in order to inform molecular dynamics simulations, and such concentrations were found to be feasible (Siwko et al., 2007). Siwko et al state that "Based on the nominal concentration of isoprene in air within leaves of ~ 20 ppm and the partition constant of isoprene in octanol one would predict an isoprene:lipid ratio of approximately 1:200". The authors used this estimate as the basis for a molecular dynamics simulation study of the effects of 20 and 43 mol% isoprene on dimyristoylphosphatidylcholine (DMPC) bilayers. Siwko et al demonstrated that 20 mol% of isoprene in DMPC bilayers caused a decrease in the acyl chain order parameter equivalent to a decrease in temperature of 10 K.

The prediction method that Siwko et al refer to is based on the observation that on a volume basis, the concentration of lipophilic compounds dissolved in membranes is close to but generally slightly less than their concentration in octanol (Simon and Gutknecht, 1980). This slight decrease in solubility in interfacial regions was attributed to the partial ordering of acyl chains in a bilayer, which has been predicted to cause solute exclusion (Marqusee and Dill, 1986). Based on the theoretical work by Marqusee and Dill, this effect is most pronounced at the

bilayer surface, and least pronounced in the bilayer midplane. The partitioning of solutes in lipid bilayers thus follows a gradient, with the highest concentration of solute occurring in the bilayer midplane. Also from the work of Marqusee and Dill, bilayer curvature was predicted to decrease solute partitioning relative to planar bilayers. This effect was attributed to the mechanical coupling of surface area to the bilayer volume in vesicles, a coupling that does not exist for planar bilayers. This effect is slight, and was predicted to only come significantly into play with vesicles having radii of 100 angstroms or less (Simon et al., 1982).

Membranes with high surface density were predicted to exclude solute more forcefully than membranes with low surface density. Surface density is effectively the inverse of area per lipid. Thus, for bilayers with a high area per lipid, partitioning is predicted to be greater (Deyoung and Dill, 1988). This is likely due to the increased chain ordering that occurs in membranes with increasing surface densities. Decreasing the temperature through the main transition phase leads to increased surface density and a decrease in the partition coefficient (Simon et al., 1979). Inclusion of cholesterol leads to an increase in surface density and decreased solute partitioning. Also, more disordered lipids tend to take up more solute than well-ordered lipids (Miller et al., 1977). The area per lipid of a membrane increases with increasing levels of lipid unsaturation and decreases upon the inclusion of sterols (Deyoung and Dill, 1990). The thylakoid membrane lacks sterols and contains a high level of acyl desaturation, suggesting that it could have a very high area per lipid and a high solute partitioning capacity.

In this study I developed a simple and sensitive technique for measuring intramembrane isoprene. Using this method I was able to determine the mole % of isoprene in vesicles composed of dimyristoylphosphatidylcholine (DMPC), as well as thylakoid membranes,

equilibrated to a gas phase concentration of 20 μL L^{-1}. I found the concentration of isoprene in each case to be several orders of magnitude lower than previously believed. This result was corroborated by a simple calculation from first principles. This suggests that modulation of the bulk lipid phase is not the mechanism by which isoprene induces thermotolerance.

Materials and methods

Gas exchange, equilibration and gas stripping apparatus

Isoprene was mixed to a nominal concentration of 20 μL L^{-1} in nitrogen using Mass-Flo® controllers (model #1479A, MKS Instruments, Andover, MA, USA) before passing to the equilibration apparatus (Fig. 4.1). This apparatus consisted of midget impingers (Chemglass CG-1820) that had been modified with septa to allow for sampling and were linked in sequence. Linkages between equilibration chambers were made using quarter inch Bev-A-Line tubing. For the measurement in DMPC, gases were bubbled through both solutions for two hours prior to sampling. Thylakoids foamed excessively using this method and were instead stirred. Gases were passed over top of the solution in this case and the equilibration time was increased to twelve hours. To mitigate sample evaporation, nitrogen was humidified before mixing with isoprene and passing to the equilibration chambers. Samples were injected into a gas stripping chamber connected to a Fast Isoprene Sensor (Hills-Scientific, Boulder, CO, USA). The gas-stripping chamber was connected to the Fast Isoprene Sensor using quarter inch stainless steel tubing fastened with Swagelok fittings. The stripping chamber was similar to a previously published

design (Smith et al., 1981). It was composed of a quarter inch diameter sealing tube with a medium fritted glass disc in the base (Chemglass CG-202-02). This was modified on either end to allow for connection to gas tubing, and a septum-covered port was added to allow for sample introduction. Added samples rested on top of the fritted disc, and air was bubbled through from below. For the plastid samples, a small amount of antifoam agent was added to suppress bubbling. The antifoam was tested and did not give off additional isoprene. Gas samples washed out in under 30 seconds (Fig. 4.2). Aqueous samples caused a peak with a long tail, however, complete washout of isoprene still occurred in under 60 seconds (Fig. 4.3). The total amount of isoprene in an injected sample was determined by integration of the area under a curve.

Gas exchange calculations

The Fast Isoprene Sensor supplies data as counts per second. A calibration curve was used to convert the counts per second data to the concentration of isoprene in incoming air, as nL L^{-1}. This was converted to moles of isoprene by multiplying by the number of moles of air drawn into the Fast Isoprene Sensor sample port during the measurement interval. 22.4 L $mole^{-1}$ was used as a conversion constant for converting between volume and moles of air. This constant comes from the ideal gas equation, assuming standard temperature and pressure. Summation of isoprene under the entire area of a washout peak gave the total isoprene dissolved in an aqueous sample. The stripping chamber could only support a flow rate of 50-150 mL min^{-1}, while the Fast Isoprene Sensor drew 400 mL min^{-1} from the sample line. The flow deficit was made up by drawing room air downstream of the stripping chamber. The background additions of isoprene

from room air were negligible, and were ignored. The gas phase concentration of isoprene in the equilibration apparatus was determined by sampling the head space of either of the equilibration chambers, which had identical concentrations of isoprene. To account for variation between runs, the concentration of isoprene in lipid bilayers was linearly scaled to a gaseous standard state of 20 μL L^{-1}.

Thylakoid and vesicle preparation

Vesicles of DMPC 100 nm in diameter were prepared using the extrusion method. Thylakoids were isolated from spinach leaves using differential and isopycnic centrifugation, and then washed several times to remove residual percoll. Chlorophyll content of the thylakoid solutions was quantified in ethanol extract using the optical density at 654 nm and a specific absorbance coefficient of 39.8 (Wintermans and Mots, 1965).

Thylakoid lipid quantification

The lipid concentration of the DMPC vesicle solution was controlled and therefore known. For estimation of the content of lipid of the thylakoid samples, the chlorophyll/lipid mass ratio was taken as unity (Janero and Barrnett, 1981; Droppa et al., 1990; Kóta et al., 2002). This estimate was confirmed using gas chromatography quantification of fatty acid methyl esters (GC-FAME). For GC-FAME analysis, thylakoid samples were flash frozen in liquid nitrogen and lyophilized to dryness. Tri-15:0-triacylglycerol was added as an internal standard and samples were then

directly transmethylated. Transmethylated samples were run on an Agilent 6820 gas chromatograph equipped with a flame ionization detector and a DB-23 column.

Results

Fast Isoprene Sensor measurement of isoprene

The amount of additional isoprene dissolved in the lipid containing solution, relative to the buffer solution, was compared to the amount of lipid in the sample to determine the intramembrane isoprene concentration. A 3.6 mg mL^{-1} DMPC vesicle solution contained 27% more isoprene than its corresponding buffer solution (Fig. 4.3). Chloroplast vesicles at a concentration of 0.87 mg mL^{-1} chlorophyll contained 40% more isoprene than the corresponding buffer solution (Fig. 4.4).

GC-FAME quantification of thylakoid lipid

The peaks from the GC-FAME quantification of thylakoid lipids were well resolved (Fig. 4.5). The presence of early eluting peaks indicated some contamination of the preps, but did not interfere with the integration of the fatty acid peaks. The contamination could stem from residue on the vessels in which the thylakoid samples were stored following isoprene quantification, or from the initial isolation procedure. In addition to thylakoids, fatty acids were extracted from whole leaves. Comparison of the fatty acid ratios shows the expected enrichment of 18:3 lipid in

the thylakoid extracts (Fig. 4.6).

ab initio calculations

The concentration of isoprene in DMPC bilayers equilibrated to a gaseous standard state of 20 μL L^{-1} was estimated from the Henry's constant and octanol-water partitioning coefficient (K_{OW}) of isoprene. Standard temperature and pressure was assumed. The Henry's constant of a substance is the ratio of its concentration in water to its gas phase partial pressure, in a system at equilibrium. At room temperature, the Henry's constant of isoprene is 7780 Pa m^3 mol^{-1}. The K_{OW} of a substance is the ratio of its molar concentration in octanol to its molar concentration in water, in a system at equilibrium. At standard temperature and pressure, the K_{OW} of isoprene is 263. The area per lipid and bilayer thickness of a DMPC bilayer were taken to be 0.63 nm^2 and 3.4 nm, respectively.

The gas phase concentration of isoprene was converted from μL L^{-1} to Pascals by:

$$101{,}325 \text{ Pa air} * \frac{20 \text{ parts isoprene}}{10^6 \text{ parts air}} = 2.02 \text{ Pa isoprene} \qquad \text{Eq. 1}$$

The molar concentration of isoprene in water was calculated by:

$$2.02 \text{ Pa} * \frac{1 \text{ mole}}{7780 \text{ Pa m}^3} = 2.6 * 10^{-4} \frac{\text{moles}}{\text{m}^3} \qquad \text{Eq. 2}$$

The molar concentration of isoprene in a bilayer was calculated by:

$$2.6 * 10^{-4} \frac{\text{moles}}{\text{m}^3} * 263 = 6.83 * 10^{-2} \frac{\text{moles}}{\text{m}^3} \qquad \text{Eq. 3}$$

The number of isoprene molecules per unit volume of bilayer was calculated by:

$$\frac{6.83*10^{-2}\ \text{moles}}{\text{m}^3} * \frac{6.022*10^{23}}{\text{mole}} * \left(\frac{1\ \text{m}}{10^9\ \text{nm}}\right)^3 = \frac{4.11*10^{-5}\ \text{isoprene}}{\text{nm}^3} \quad \text{Eq. 4}$$

The volume per lipid of DMPC in the bilayer was calculated by:

$$0.63\ \text{nm}^2 * \frac{3.4}{2}\ \text{nm} = \frac{1.071\ \text{nm}^3}{1\ \text{DMPC}} \quad \text{Eq. 5}$$

The number of DMPC molecules per unit volume of bilayer was calculated by:

$$\frac{1\ \text{DMPC}}{1.071\ \text{nm}^3} = \frac{.934\ \text{DMPC}}{1\ \text{nm}^3} \quad \text{Eq. 6}$$

The mole percent of isoprene in a DMPC bilayer was calculated by:

$$\frac{4.11*10^{-5}\ \text{isoprene nm}^{-3}}{.934\ \text{DMPC nm}^{-3}} = \frac{1\ \text{isoprene}}{22700\ \text{DMPC}} = .0044\ \text{mol\%\ isoprene} \quad \text{Eq. 7}$$

For thylakoids, the area per lipid and membrane thickness were taken to be 0.66 nm^2 and 2.9 nm, respectively.

Intramembrane isoprene concentration

The mole % of isoprene in DMPC was approximately 50% lower than the value that would be predicted by the octanol water K_{OW} of isoprene (Table 4.1). The partitioning of isoprene into thylakoids was found to be significantly higher. The higher partitioning is expected given the longer chain length and degree of unsaturation of thylakoid lipids.

Discussion

Validity of the method

My method allowed a rapid, moderately accurate measurement of the intramembrane isoprene concentration of DMPC vesicles and thylakoids. Other methods have been used in the past to accomplish this task. Scintillation counting of radiolabeled solutes is common when the solute of interest is not volatile (Deyoung and Dill, 1990). Another common practice is to separate the lipid and aqueous phases by centrifugation prior to counting (Miller et al., 1977; Smith et al., 1981). The amount of solute dissolved in membranes is then normalized to the dry weight of the pellet. A potential drawback to this approach is that no distinction is made between the protein and lipid fraction of the membrane. Other studies have normalized to lipid content by measuring sample phosphate. While possible for DMPC, thylakoid membranes are composed predominantly of galactolipids and contain very little phosphate. Therefore DMPC and thylakoid lipids were quantified by dry lipid weight and GC-FAME analysis, respectively. For volatile compounds, gas chromatography based solute quantification has been used (Miller et al., 1977; Smith et al., 1981). Solute partitioning has even been estimated from neutron diffraction data (White et al., 1981), though this is a less sensitive approach and is thus not suitable for extremely low solute concentrations. The Fast Isoprene Sensor based method that I have used is simple, sensitive, does not require radioactivity, and has modest equipment requirements.

Solute partitioning in biological membranes

I wanted to determine if isoprene can reach concentrations of several mole percent relative to lipids, so the ~10% uncertainty in my measurements is acceptable. However, my method ignores, rather than quantifies, the protein content of the thylakoid membrane. As with most biological membranes, proteins make up the majority surface area (~70%) of thylakoids. However, proteins are tightly compressed relative to the lipid fraction of the membrane. Therefore binding of a significant amount of isoprene to internal pockets seems unlikely. Binding of isoprene to exterior sites is possible, though the abundance of the binding site(s) and/or the affinity for isoprene would need to be high for these to contribute to the measured partitioning. Therefore, while it is appropriate to base the thylakoid measurement solely on the lipid fraction of the membrane, one must also consider that this method produces an upper limit whose accuracy may be affected by the abundance of non-lipid binding sites.

Few studies have directly compared the effect of membrane proteins on solute partitioning. A series of studies observed a ~ two-fold lower binding of the volatile anesthetics butane, thiopental, and halothane in various biological membranes than in their corresponding lipid dispersions (Miller et al., 1977; Korten et al., 1980; Smith et al., 1981). However, these studies normalized the amount of membrane embedded solutes to membrane dry weight and included both the protein and lipid fractions of their biological membrane. The lipid portion of the membrane likely partitions the majority of solutes, so inclusion of the protein component could cause a significant underestimation of the partitioning coefficient. Later studies normalized solute partitioning to the membrane lipid content. A series of studies observed enhanced

partitioning of insecticides to biomembranes relative to corresponding lipid dispersions (Antunes-Madeira and Madeira, 1985; Antunes-Madeira and Madeira, 1986; Antunes-Madeira and Madeira, 1987). The partitioning of chlorpromazine into erthyrocyte ghosts was weaker than the partitioning into pure DMPC vesicles, but greater than partitioning into DMPC vesicles with 10 mol % or more cholesterol (Luxnat and Galla, 1986). Dopamine partitioned less strongly into the biomembranes of sheep caudate nuclei than into liposomes of the corresponding lipid (Palmeira and Oliveira, 1992). The mixed results of these studies suggest that the effect of proteins on solute partitioning is complex and dependent on the molecular characteristics of both the solute and of solvating lipids.

My results demonstrate that the presence of isoprene in thylakoid membranes of rapidly emitting plants is substantially less than previously predicted (Siwko et al., 2007). At such low concentrations, isoprene is unlikely to be acting through modification of the bulk lipid phase. Small solutes typically must be present at a few mole % or higher to cause significant lipid bilayer alteration (Miller, 1985; Cantor, 1999; Hauet et al., 2003). Even at these concentrations, there is some debate within the field of general anesthesia about whether the effects on membranes are large enough to mediate physiological changes. Many researchers now favor a protein binding based mechanism (Franks, 2008; Sear, 2009). Isoprene may exert its function by binding to specific membrane proteins.

Acknowledgements

I thank Scott Bankroff for assistance in the design and manufacture of the equilibration and gas

stripping apparatus; Professor John Ohlrogge and Dr. Dylan Kosma for helpful discussions regarding FAME; and Dr. Henrik Tjellström for analysis of thylakoid samples.

APPENDIX

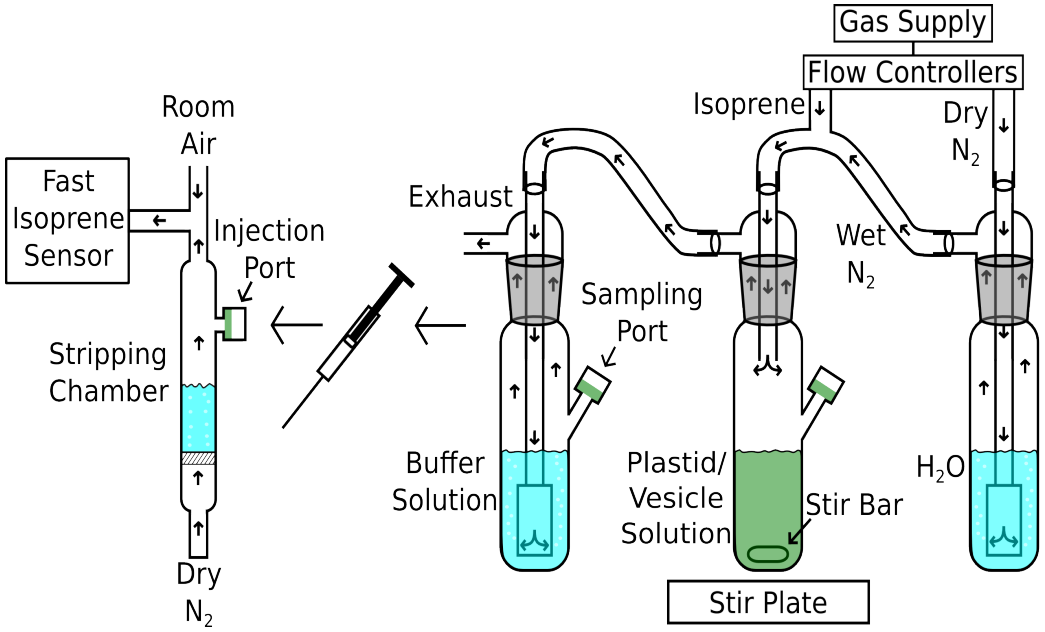

Figure 4.1 Measurement apparatus. The system was composed of a stripping chamber and two linked equilibration chambers. Gas and liquid samples from the equilibration chambers were sampled using a gas tight Hamilton syringe and then injected into the gas-stripping chamber.

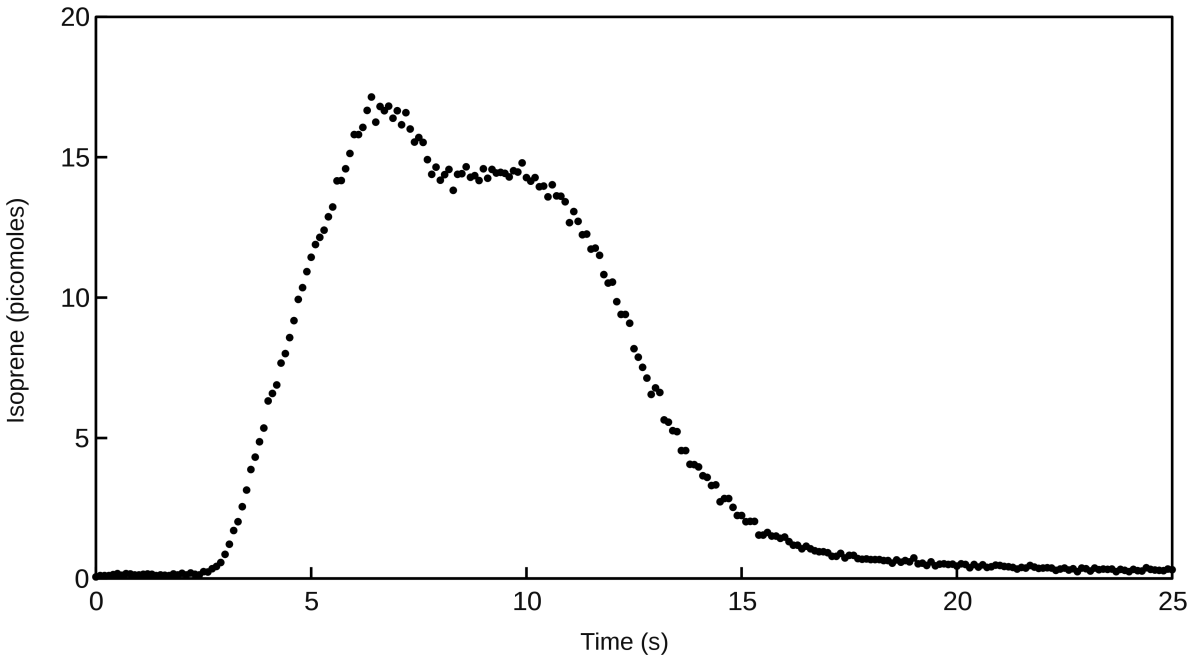

Figure 4.2 Trace of a two milliliter head space sample. Each point corresponds to one tenth of a second, with the zero time point arbitrarily designated. The y-axis corresponds to the number of picomoles of isoprene passing into the Fast Isoprene Sensor in a tenth of a second. The area under each curve corresponds to the amount of dissolved isoprene in a sample.

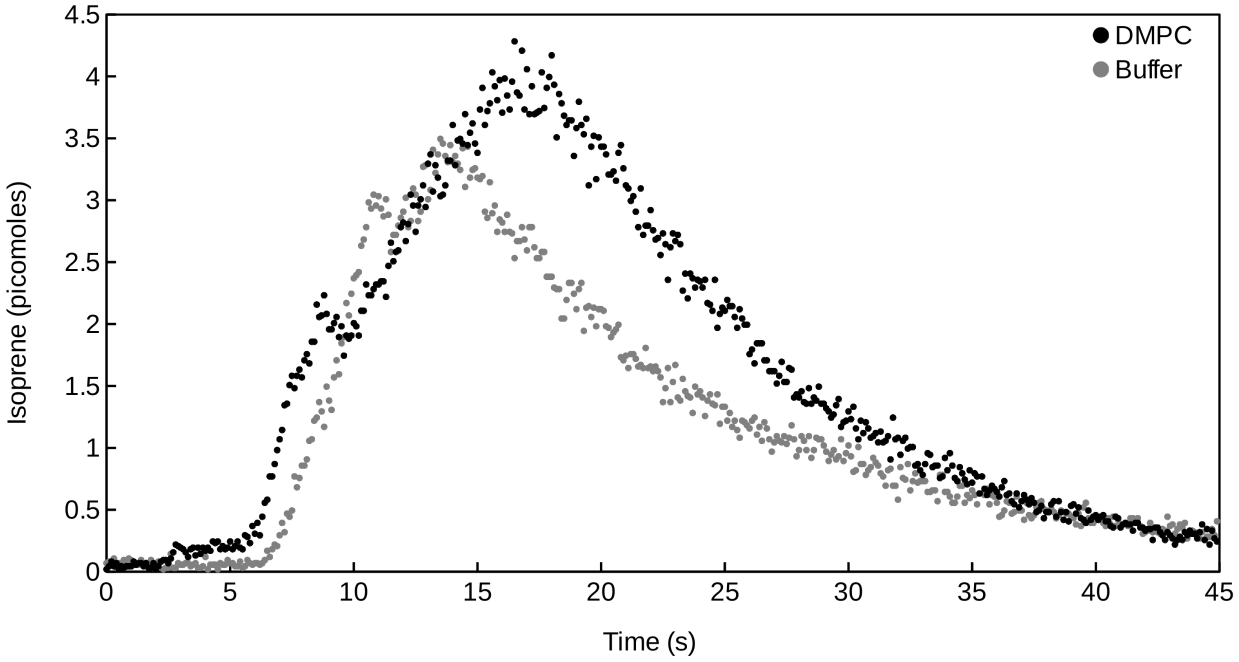

Figure 4.3 Typical trace from quantification of isoprene dissolved in DMPC vesicles. Both sample were two milliliters in volume. Each point corresponds to one tenth of a second, with the zero time point arbitrarily designated for each curve. The y-axis corresponds to the number of picomoles of isoprene passing into the Fast Isoprene Sensor in a tenth of a second. The area under each curve corresponds to the amount of dissolved isoprene in a sample. The shoulders in the rising edge of each curve are caused by subtle variation in the speed of individual injections.

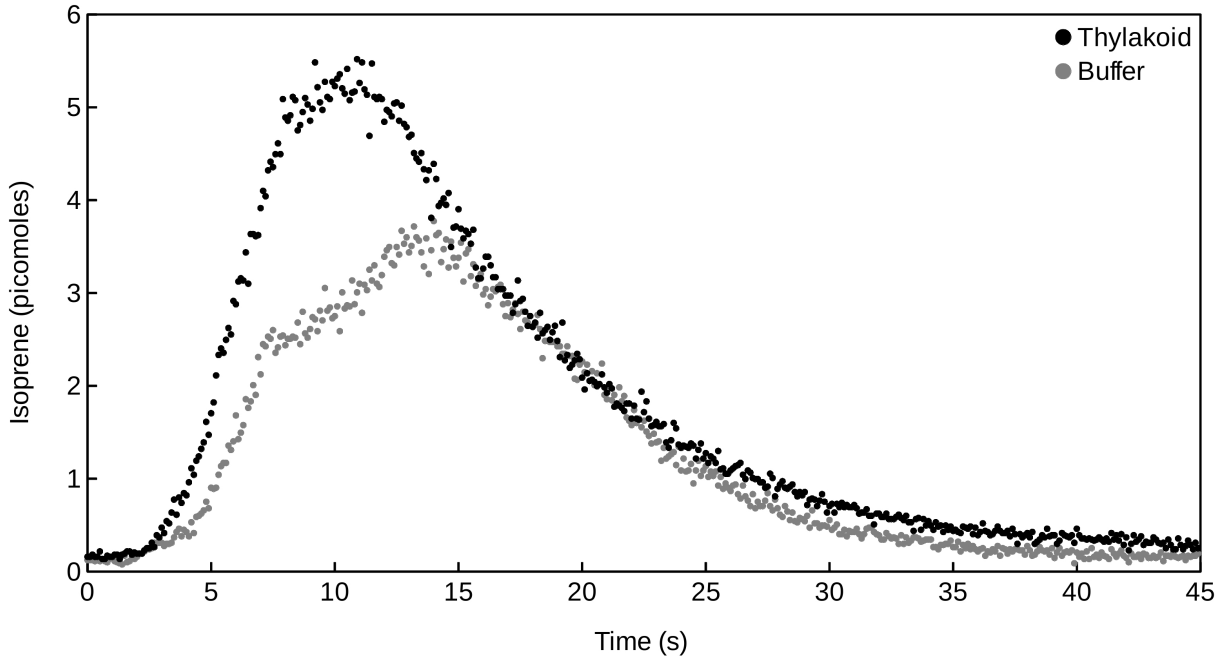

Figure 4.4 Typical trace from quantification of isoprene dissolved in chloroplast vesicles. Each point corresponds to one tenth of a second, with the zero time point arbitrarily designated for each curve. The y-axis corresponds to the number of picomoles of isoprene passing into the Fast Isoprene Sensor in a tenth of a second. The area under each curve corresponds to the amount of dissolved isoprene in a sample. Perturbations in the rising edge of each curve are caused by variation in the speed of individual injections.

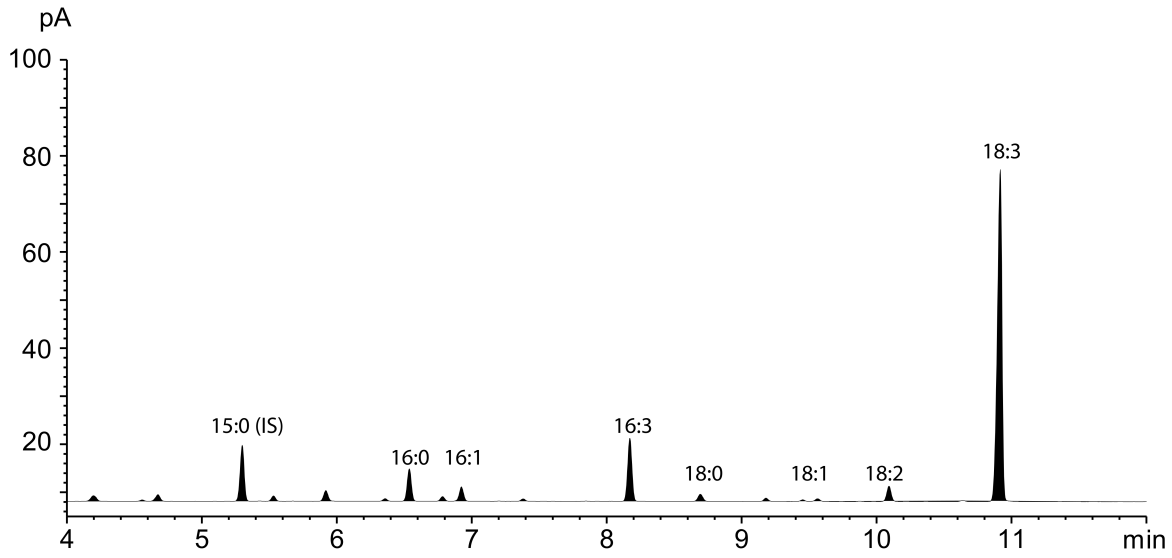

Figure 4.5 Gas chromatograph from FAME quantification of thylakoid lipids. The y-axis is current, in picoamperes, from the gas-chromatograph flame ionization detector. The x-axis is time after sample injection. Peaks corresponding to individual acyl chains are denoted by the chain length and the degree of unsaturation. 15:0 is the internal standard. The peaks eluting prior to the internal standard are due to a sample contaminant whose source and nature are unknown. The area under individual peaks corresponds to the amount of that lipid species.

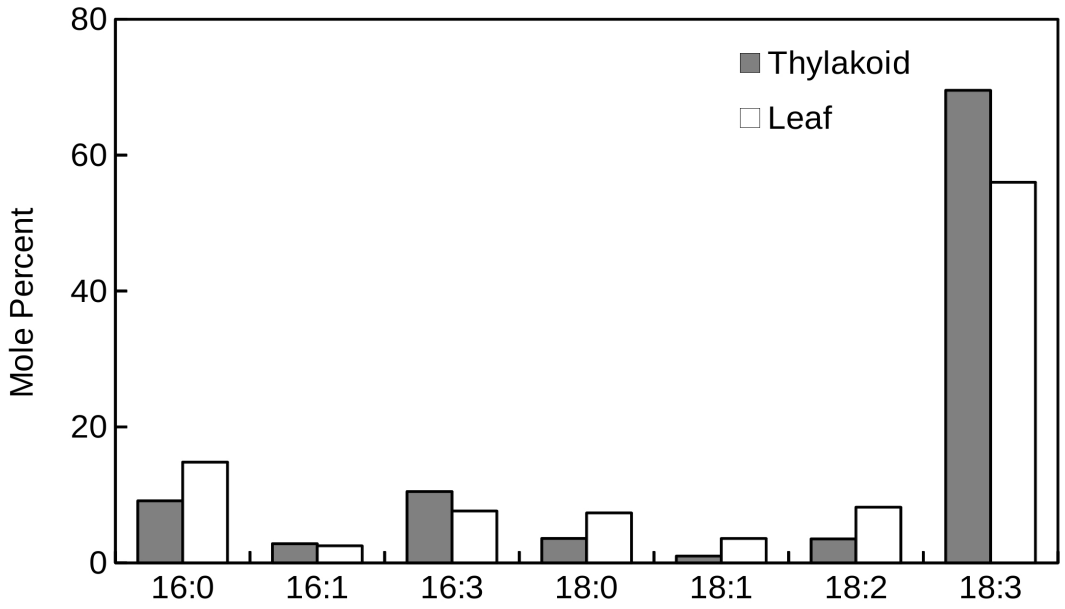

Figure 4.6 Fatty acid composition of isolated thylakoids and spinach leaves. From a single technical replicate in which the samples were directly transmethylated. The increased percentage of 18:3 lipid is indicative of thylakoid enrichment.

Table 4.1 Intramembrane isoprene content at 20 µL L^{-1} gas phase equivalent concentration. Isoprene concentrations are given as the number of isoprene molecules per million lipid molecules. The "$[ISP]_{Measured}$" and "Partitioning coefficient" columns provide experimentally determined physical parameters, while the "$[ISP]_{Calculated}$" column is based on the octanol-water partitioning coefficient of isoprene.

System	$[ISP]_{measured}$	$[ISP]_{calculated}$	Partitioning coefficient
DMPC	20.5±3.8	44.0	122.3
Thylakoid	64.4±7.2	39.3	429.8

REFERENCES

REFERENCES

Antunes-Madeira M, Madeira V (1985) Partition of lindane in synthetic and native membranes. Biochimica et Biophysica Acta **820**: 165–172

Antunes-Madeira M, Madeira V (1986) Partition of DDT in synthetic and native membranes. Biochimica et Biophysica Acta **861**: 159–164

Antunes-Madeira M, Madeira V (1987) Partition of malathion in synthetic and native membranes. Biochimica et Biophysica Acta **901**: 61–66

Cantor RS (1997) The lateral pressure profile in membranes: a physical mechanism of general anesthesia. Biochemistry **36**: 2339–2344

Cantor RS (1999) Lipid composition and the lateral pressure profile in bilayers. Biophysical Journal **76**: 2625–2639

Deyoung L, Dill KA (1988) Solute partitioning into lipid bilayer-membranes. Biochemistry **27**: 5281–5289

Deyoung L, Dill KA (1990) Partitioning of nonpolar solutes into bilayers and amorphous n-alkanes. The Journal of Physical Chemistry **94**: 801–809

Droppa M, Masojidek J, Horvath G (1990) Changes of the polypeptide composition in thylakoid membranes during differentiation. Zeitschrift Fur Naturforschung C-a Journal of Biosciences **45**: 253–257

Franks NP (2008) General anaesthesia: from molecular targets to neuronal pathways of sleep and arousal. Nature Reviews Neuroscience **9**: 370–386

Hauet N, Artzner F, Boucher F, Grabielle-Madelmont C, Cloutier I, Keller G, Lesieur P, Durand D, Paternostre M (2003) Interaction between artificial membranes and enflurane, a general volatile anesthetic: DPPC-enflurane interaction. Biophysical Journal **84**: 3123–3137

Janero D, Barrnett R (1981) Cellular and thylakoid-membrane phospholipids of *Chlamydomonas reinhardtii* 137+. Journal of Lipid Research **22**: 1126–1130

Korten K, Sommer T, Miller K (1980) Membrane-composition modulates thiopental partitioning in bilayers and biomembranes. Biochimica et Biophysica Acta **599**: 271–279

Kóta Z, Horváth LI, Droppa M, Horváth G, Farkas T, Páli T (2002) Protein assembly and heat stability in developing thylakoid membranes during greening. Proceedings of the National Academy of Sciences of the United States of America **99**: 12149–12154

Luxnat M, Galla H (1986) Partition of chlorpromazine into lipid bilayer-membranes - the effect of membrane-structure and composition. Biochimica et Biophysica Acta **856**: 274–282

Marqusee J, Dill KA (1986) Solute partitioning into chain molecule interphases - monolayers, bilayer-membranes, and micelles. Journal of Chemical Physics **85**: 434–444

Miller K, Hammond L, Porter E (1977) The solubility of hydrocarbon gases in lipid bilayers. Chemistry and Physics of Lipids **20**: 229–241

Miller KW (1985) The nature of the site of general anesthesia. International Review of Neurobiology **27**: 1–61

Palmeira CM, Oliveira CR (1992) Partitioning and membrane disordering effects of dopamine antagonists: Influence of lipid peroxidation, temperature, and drug concentration. Archives of Biochemistry and Biophysics **295**: 161–171

Sear JW (2009) What makes a molecule an anaesthetic? Studies on the mechanisms of anaesthesia using a physicochemical approach. British Journal of Anaesthesia **103**: 50–60

Simon S, Gutknecht J (1980) Solubility of carbon-dioxide in lipid bilayer-membranes and organic-solvents. Biochimica et Biophysica Acta **596**: 352–358

Simon S, McDaniel R, McIntosh T (1982) Interaction of benzene with micelles and bilayers. The Journal of Physical Chemistry **86**: 1449–1456

Simon S, Stone W, Bennett P (1979) Can regular solution theory be applied to lipid bilayer membranes? Biochimica et Biophysica Acta **550**: 38–47

Siwko ME, Marrink SJ, de Vries AH, Kozubek A, Schoot Uiterkamp AJM, Mark AE (2007) Does isoprene protect plant membranes from thermal shock? A molecular dynamics study. Biochimica et Biophysica Acta - Biomembranes **1768**: 198–206

Smith R, Porter E, Miller K (1981) The solubility of anesthetic-gases in lipid bilayers. Biochimica et Biophysica Acta **645**: 327–338

White S, King G, Cain J (1981) Location of hexane in lipid bilayers determined by neutron-diffraction. Nature **290**: 161–163

Wintermans JFGM, Mots AD (1965) Spectrophotometric characteristics of chlorophylls a and b and their phenophytins in ethanol. Biochimica et Biophysica Acta - Biophysics including Photosynthesis **109**: 448 – 453

Chapter 5

Conclusions and Future Directions

Introduction and conclusions

The membrane hypothesis was proposed upon discovery of isoprene-induced thermotolerance of photosynthesis, and has remained relatively unchanged during the subsequent two decades (Sharkey and Singsaas, 1995). This hypothesis is not universally accepted, and the main alternative hypothesis, that isoprene quenches cellular reactive oxygen species, has stood for over a decade (Loreto and Velikova, 2001). Neither of these hypotheses had been previously subjected to rigorous quantitative analysis in terms of the amount of isoprene present in a membrane under physiological conditions. With some theoretical considerations involving biochemical and biophysical constants and the quantity of isoprene in living cells, I have called both hypotheses into question. In chapter two I profiled the transcriptional changes induced by isoprene in the non-emitting plant *Arabidopsis thaliana*. The results in chapter two of this thesis suggest that isoprene acts as a signaling molecule in plants. The results in chapters three and four suggest that isoprene does not contribute significantly to ROS quenching nor to the modulation of the acyl-lipid bilayer portion of the thylakoid membrane. Given that the ROS and membrane hypotheses now seem non-viable, a new mechanistic hypothesis for isoprene action needs to be proposed. Binding of isoprene to proteins seems like a viable alternative hypothesis.

Binding to proteins would seem to provide a better explanation for the results presented in chapter 3 of this thesis. In that chapter, isoprene altered the dynamics of gramicidin A channels, but failed to modify the kinetics of perylene reorientation. I had interpreted this to indicate that isoprene was causing membrane thickening but not altering membrane fluidity. This explanation seems untenable in light of the results presented in chapter 4. Indeed, even at the

relatively high concentrations (2000 μL L^{-1}) used in those studies, the intramembrane concentration of isoprene would be expected to reach only ~0.5 mol% relative to lipid. It is possible that a direct interaction of isoprene with gramicidin A caused alteration of the channel dynamics. A series of studies observed that 1-chloro-1,2,2-trifluorocyclobutane, a volatile anesthetic, modified gramicidin A channel kinetics (Tang et al., 1999), but did so without causing any structural changes (Tang et al., 2002). Molecular dynamics simulations also revealed that halothane significantly altered gramicidin channel dynamics (Tang and Xu, 2002), but that the closely related nonimmobilizer hexafluoroethane had no effect on channel dynamics (Liu et al., 2005). This difference in dynamics alteration was attributed to a differing tendency for interaction with tryptophan residues situated at the lipid water interface, a consequence of the intramembrane distribution of halothane and hexafluorethane towards the lipid-water interface and the bilayer midplane, respectively. The putative midplane localization of isoprene would suggest that it is altering channel kinetics by a mechanism dissimilar to that of halothane.

Future directions

Small molecule binding to proteins

It is striking how closely our thinking about the mechanism of action of isoprene has mirrored the history of the distantly related field of volatile anesthetics (Lugli et al., 2009). At the turn of the 20th century a now famous correlation between the lipophilicity and potency of anesthetics was independently observed by two researchers (Overton, 1901; Meyer, 1906), the so-called

Meyer-Overton correlation. Later investigators in the first half of the 20th century proposed that anesthetic effects might be mediated by interactions with the oil-like portion of proteins. Ether and chloroform were observed to decrease the luminescence of marine bacteria (Harvey, 1915), though the mechanism by which this occurred went unappreciated at the time. This result was later seized upon in the study of luciferase inhibition by halothane (Adey et al., 1975; Franks and Lieb, 1984). In the 1970s, with the advent of techniques for the production and characterization of synthetic membranes, intense focus on the lipid portion of membranes developed. Effects were observed to be small and inconsistent between different anesthetics, which eventually caused the field to move back to protein-based mechanisms. This long history of reversal has been well reviewed (Eckenhoff and Johansson, 1997; Campagna et al., 2003; Sonner et al., 2003; Rudolph and Antkowiak, 2004).

The location and nature of the anesthetic binding sites in target proteins is a topic of active research, however, there are some general trends to observe that may point the way forward for the isoprene field. It has been hypothesized that binding to small hydrophobic cavities would be most energetically favorable (Eckenhoff and Johansson, 1997). Cavities could be located at protein-protein interfaces (Hubbard and Argos, 1994), at protein-lipid interfaces (Lemmon and Engelman, 1994), as well as within the hydrophobic cores of individual proteins (Rashin et al., 1986; Hubbard et al., 1994; Brunori et al., 2000). Cavities within proteins are destabilizing (Eriksson et al., 1992a), and the binding of hydrophobic molecules to these sites can promote structural integrity (Eriksson et al., 1992b). However, even for these sites, binding is likely to be low-affinity and non-specific. The multiplicity of these sites in any given protein could have a cumulative effect that promotes structural stabilization even at low ligand

concentrations. In support of this view, recent molecular dynamics simulations have shown that isoflurane is capable of binding to multiple sites in the nicotinic acetylcholine receptor (Brannigan et al., 2010). Multiple propofol binding sites were also identified in a γ-aminobutyric acid type A receptor using a photoreactive propofol analog (Jayakar et al., 2014).

An estimate of the affinity of isoprene for an ideal internal hydrophobic cavity would be beneficial as a coarse validation for this hypothesis. This might seem possible to a casual observer. During the last half-century, amazing advances have been made in our understanding of how physico-chemical forces govern protein folding and ligand binding (Dill, 1990; Dill and MacCallum, 2012). The weak binding of hydrophobic molecules to proteins is a consequence of the inability of these molecules to form electrostatic interactions. Attraction is a result of the hydrophobic effect and weak van der Waals interactions.

Unfortunately, de novo prediction of ligand binding affinities is not a trivial task, and requires sophisticated molecular dynamics simulations (Boresch et al., 2003; Clark et al., 2009; Deng and Roux, 2009). A few studies have measured the affinity of small molecules to hydrophobic cavities with varying properties. Binding of halothane and chloroform to the hydrophobic interior cavity of a four-α-helix bundle was observed to increase as a consequence of alanine → valine mutations (Manderson et al., 2003). This effect was attributed to an increase in cavity hydrophobicity and improved ligand:cavity shape complementarity as a result of the substitutions. Another set of studies (Morton et al., 1995; Morton and Matthews, 1995) characterized the binding affinity of various ligands to T4 lysozyme cavity mutants (Eriksson et al., 1992a; Eriksson et al., 1992b). The binding affinity was observed to be poorly correlated to the solvent-transfer free energy of the ligands (Morton et al., 1995). I know of no simple method

for calculation of the upper-limit of isoprene affinity for protein docking sites. However, protein stabilization occurs in response to low nanomolar concentrations of some anesthetics (Eckenhoff and Johansson, 1997). Isoprene may reach aqueous concentrations of several hundred nanomolar in highly emitting plants, therefore a protein-stabilizing effect of isoprene seems plausible. The efforts of isoprene researchers in the near future might be best spent finding target proteins to which the binding of isoprene could be directly tested.

Identifying proteinaceous targets of isoprene

Many methods exist for the prediction and detection of ligand:protein interactions, including transcriptional profiling, genetic manipulation, biochemical characterization, affinity purification, and predictive modeling (Schenone et al., 2013). However, some of these approaches fail for weak ligand binding such as isoprene is likely to have. In the study of the mechanism of action of anesthetics, the search for protein targets was greatly aided by knowledge of the physiological effects of anesthetics. This allowed the action of individual anesthetics to be traced to various parts of the central nervous system, and the pool of potential protein targets culled accordingly. Targets were further reduced by focusing efforts on plasma membrane localized receptors and ion channels. These proteins are collectively responsible for creating the action potentials that mediate central nervous system function. Still, neuronal membranes contain many receptors and channels, and many studies were needed to sift through the multitude of potential binding sites. Some ion channels were found to be generally insensitive to anesthetics. Others were sensitive, but only at doses that are not physiologically

relevant (Franks and Lieb, 1994). Over time a small number of protein families have emerged as anesthetic binding sites (Franks, 2008).

A similar course of study seems likely to occur in the study of isoprene. Luckily, the problem of protein identification would seem to be less challenging, given the putative localization of isoprene action to the thylakoid membrane. An interdisciplinary approach combining proteomics and bioinformatics determined that thylakoid membranes contain only 154 different proteins (Friso, 2004). As isoprene protects the photosynthetic apparatus from heat damage, and not all of these 154 proteins are directly involved in the photosynthetic electron transport chain, the number of potential targets is likely to be even lower than this. Based on literature evidence, a few proteins would already seem to pose obvious targets. Two studies have suggested that isoprene enhances the heat stability of light harvesting complex II (Velikova et al., 2011; Pollastri et al., 2014). Velikova et al also reported that isoprene decreased the proton efflux rate, which could suggest an effect on the ATP synthase complex. An increase in the temperature of peak luminescence of PSII was also observed, but was not rapidly affected by the presence or absence of isoprene. The authors concluded that the change in thermoluminescence was due to changes in the thylakoid structure that were induced only by the long-term presence of isoprene.

One study that directly tested the effect of isoprene on the stability of thylakoid proteins failed to see an effect (Logan et al., 1999). The authors utilized differential scanning calorimetry to monitor whole-thylakoid protein denaturation. Protein denaturation occurred at temperatures in excess of 50 °C, and isoprene was observed to have no effect on this thermal profile. This should not be taken as conclusive evidence that isoprene is not binding to proteins, as the measurements were performed on the entire ensemble of thylakoid proteins. The effects of

isoprene on individual proteins may therefore have been obscured by averaging of the effects of many proteins. The differential thermogram was also conducted to temperatures that far exceeded the physiologically relevant range of thylakoids in nature, at which proteins were irreversibly denatured. A calorimetric approach is more likely to identify effects of isoprene if conducted upon single proteins across a physiologically relevant temperature range.

Future perspectives and open questions

It may be decades before a detailed mechanism of action is established for isoprene. While this pace of progress may seem slow in comparison to the current rate of progress in many fields of biological research, it is relatively in step with the rate of determination of mechanisms of anesthesia. The complete solution to this question will require an interdisciplinary approach. It is not sufficient to demonstrate that isoprene may bind to and/or stabilize proteins in the thylakoid transport chain. These physicochemical effects must also be correlated to the induction of photosynthetic thermotolerance by isoprene. It is here that a more thorough and detailed understanding of the effects of isoprene on the photosynthetic electron transport chain would be indispensable. There are some conflicting reports in the literature, and a consensus needs to be reached.

Some of these discrepancies may be due to species and/or environment-specific effects of isoprene. In the past, species-specific effects have been viewed as unlikely, given that isoprene was believed to operate in the acyl lipid bilayer, which would confer limited binding specificity. If isoprene indeed binds to proteins, species-specific effects become more plausible, as relatively

small sequence changes could conceivably alter binding sites. Condition-specific effects could arise due to the decreased function of certain parts of photosynthesis under certain conditions. For example, if isoprene indeed stabilizes the light harvesting complex II arrays against thermal denaturation, it is plausible that its thermoprotective effects will only be realized under conditions in which the arrays are fully complexed and operating at full capacity. Such would be the situation for dark acclimated plants with arrays configured around photosystem II. In such a situation, the biophysical protection afforded by isoprene could be confined to a relatively narrow window following a dark → light transition. This would be consistent with the hypothesis that isoprene is an adaptation to rapidly fluctuating light and temperature conditions (Sharkey et al., 2008).

It is presumptive to believe that all of the functions of isoprene have been identified. For example, it remains to be seen whether the induction of gene expression by isoprene is a direct result of isoprene binding to proteins or to some other unidentified function. Perhaps isoprene acts as a so-called “line-active molecule”, intercalating into specific lateral interfaces in the membrane (Muddana et al., 2012; Palmieri et al., 2014). Line active molecules are known to alter membrane domain stability, and a recent molecular dynamics study observed that simple aliphatic molecules partition to the interface between ordered and disordered domains (Barnoud et al., 2014). However, this partitioning promoted lipid mixing, which would seem counter to the role of isoprene as a thermoprotectant. Another question is whether the function of isoprene is limited to proteins embedded in the thylakoid membrane or if isoprene may also be binding to and altering the function of soluble proteins. Anesthesia-induced gene expression changes have been recognized within the last decade (Sakamoto et al., 2005; Kobayashi et al., 2007), and the

field is only beginning to consider the mechanisms by which these changes might occur (Ren et al., 2008; Pekny et al., 2014).

During the course of my graduate studies, the isoprene field has continued to accumulate physiological evidence for the role of isoprene in thermotolerance. This approach offers diminishing returns in determining the mechanism of action of isoprene. In order for the field to make significant additional progress, it will be necessary to migrate from such observation-oriented research to the testing of specific biophysical hypotheses. This will require a different skillset in future isoprene researchers. Experimental and computational biophysics is likely to be where the majority of findings are derived. Whole-leaf physiological characterization of the effects of isoprene will still be necessary of course, but will be increasingly used to validate discoveries made at the protein level. My graduate work has played the small but necessary role of eliminating a quantitatively non-viable mechanism from the consideration of the field.

REFERENCES

REFERENCES

Adey G, Wardley-Smith B, White D (1975) Mechanism of inhibition of bacterial luciferase by anaesthetics. Life Sciences **17**: 1849–1854

Barnoud J, Rossi G, Marrink SJ, Monticelli L (2014) Hydrophobic compounds reshape membrane domains. PLoS Computational Biology **10**: e1003873

Boresch S, Tettinger F, Leitgeb M, Karplus M (2003) Absolute binding free energies: a quantitative approach for their calculation. The Journal of Physical Chemistry B **107**: 9535–9551

Brannigan G, LeBard DN, Hénin J, Eckenhoff RG, Klein ML (2010) Multiple binding sites for the general anesthetic isoflurane identified in the nicotinic acetylcholine receptor transmembrane domain. Proceedings of the National Academy of Sciences of the United States of America **107**: 14122–14127

Brunori M, Vallone B, Cutruzzolà F, Travaglini-Allocatelli C, Berendzen J, Chu K, Sweet RM, Schlichting I (2000) The role of cavities in protein dynamics: crystal structure of a photolytic intermediate of a mutant myoglobin. Proceedings of the National Academy of Sciences of the United States of America **97**: 2058–2063

Campagna JA, Miller KW, Forman SA (2003) Mechanisms of actions of inhaled anesthetics. New England Journal of Medicine **348**: 2110–2124

Clark M, Meshkat S, Wiseman JS (2009) Grand canonical free-energy calculations of protein−ligand binding. Journal of Chemical Information and Modeling **49**: 934–943

Deng Y, Roux B (2009) Computations of standard binding free energies with molecular dynamics simulations. The Journal of Physical Chemistry B **113**: 2234–2246

Dill KA (1990) Dominant forces in protein folding. Biochemistry **29**: 7133–7155

Dill KA, MacCallum JL (2012) The protein-folding problem, 50 years on. Science **338**: 1042–1046

Eckenhoff RG, Johansson JS (1997) Molecular interactions between inhaled anesthetics and proteins. Pharmacological Reviews **49**: 343–368

Eriksson A, Baase W, Zhang X, Heinz D, Blaber M, Baldwin E, Matthews B (1992a) Response of a protein-structure to cavity-creating mutations and its relation to the hydrophobic effect. Science **255**: 178–183

Eriksson AE, Baase WA, Wozniak JA, Matthews BW (1992b) A cavity-containing mutant of T4 lysozyme is stabilized by buried benzene. Nature **355**: 371–373

Franks N, Lieb W (1994) Molecular and cellular mechanisms of general-anesthesia. Nature **367**: 607–614

Franks NP (2008) General anaesthesia: from molecular targets to neuronal pathways of sleep and arousal. Nature Reviews Neuroscience **9**: 370–386

Franks NP, Lieb WR (1984) Do general anaesthetics act by competitive binding to specific receptors? Nature **310**: 599–601

Friso G (2004) In-depth analysis of the thylakoid membrane proteome of *Arabidopsis thaliana* chloroplasts: new proteins, new functions, and a plastid proteome database. The Plant Cell **16**: 478–499

Harvey EN (1915) The effect of certain organic and inorganic substances upon light production by luminous bacteria. Biological Bulletin **29**: 308–311

Hubbard SJ, Argos P (1994) Cavities and packing at protein interfaces. Protein Science **3**: 2194–2206

Hubbard SJ, Gross K-H, Argos P (1994) Intramolecular cavities in globular proteins. Protein Engineering **7**: 613–626

Jayakar SS, Zhou X, Chiara DC, Dostalova Z, Savechenkov PY, Bruzik KS, Dailey WP, Miller KW, Eckenhoff RG, Cohen JB (2014) Multiple propofol-binding sites in a γ-Aminobutyric Acid Type A Receptor (GABAAR) identified using a photoreactive propofol analog. Journal of Biological Chemistry **289**: 27456–27468

Kobayashi K, Takemori K, Sakamoto A (2007) Circadian gene expression is suppressed during sevoflurane anesthesia and the suppression persists after awakening. Brain Research **1185**: 1–7

Lemmon MA, Engelman DM (1994) Specificity and promiscuity in membrane helix interactions. Quarterly Reviews of Biophysics **27**: 157–218

Liu Z, Xu Y, Tang P (2005) Molecular dynamics simulations of C_2F_6 effects on gramicidin A: implications of the mechanisms of general anesthesia. Biophysical Journal **88**: 3784–3791

Logan BA, Anchordoquy TJ, Monson RK, Pan RS (1999) The effect of isoprene on the properties of spinach thylakoids and phosphatidylcholine liposomes. Plant Biology **1**: 602–606

Loreto F, Velikova V (2001) Isoprene produced by leaves protects the photosynthetic apparatus against ozone damage, quenches ozone products, and reduces lipid peroxidation of cellular membranes. Plant Physiology **127**: 1781–1787

Lugli AK, Yost CS, Kindler CH (2009) Anaesthetic mechanisms: update on the challenge of unravelling the mystery of anaesthesia. European Journal of Anaesthesiology **26**: 807–820

Manderson GA, Michalsky SJ, Johansson JS (2003) Effect of four-α-helix bundle cavity size on volatile anesthetic binding energetics. Biochemistry **42**: 11203–11213

Meyer H (1906) The theory of narcosis. The Journal of the American Medical Association **46**: 167–169

Morton A, Baase WA, Matthews BW (1995) Energetic origins of specificity of ligand binding in an interior nonpolar cavity of T4 lysozyme. Biochemistry **34**: 8564–8575

Morton A, Matthews BW (1995) Specificity of ligand binding in a buried nonpolar cavity of T4 lysozyme: Linkage of dynamics and structural plasticity. Biochemistry **34**: 8576–8588

Muddana HS, Chiang HH, Butler PJ (2012) Tuning membrane phase separation using nonlipid amphiphiles. Biophysical Journal **102**: 489–497

Overton CE (1901) Studien über die Narkose. Gustav Fischer, Jena

Palmieri B, Yamamoto T, Brewster RC, Safran SA (2014) Line active molecules promote inhomogeneous structures in membranes: Theory, simulations and experiments. Advances in Colloid and Interface Science **208**: 58–65

Pekny T, Andersson D, Wilhelmsson U, Pekna M, Pekny M (2014) Short general anaesthesia induces prolonged changes in gene expression in the mouse hippocampus. Acta Anaesthesiologica Scandinavica **58**: 1127–1133

Pollastri S, Tsonev T, Loreto F (2014) Isoprene improves photochemical efficiency and enhances heat dissipation in plants at physiological temperatures. Journal of Experimental Botany **65**: 1565–1570

Rashin AA, Iofin M, Honig B (1986) Internal cavities and buried waters in globular proteins. Biochemistry **25**: 3619–3625

Ren Y, Zhang F-J, Xue Q-S, Zhao X, Yu B-W (2008) Bilateral inhibition of γ-Aminobutyric Acid Type A Receptor function within the basolateral amygdala blocked propofol-induced amnesia and activity-regulated cytoskeletal protein expression inhibition in the hippocampus. Anesthesiology **109**: 775–781

Rudolph U, Antkowiak B (2004) Molecular and neuronal substrates for general anaesthetics. Nature Reviews Neuroscience **5**: 709–720

Sakamoto A, Imai J, Nishikawa A, Honma R, Ito E, Yanagisawa Y, Kawamura M, Ogawa R, Watanabe S (2005) Influence of inhalation anesthesia assessed by comprehensive gene expression profiling. Gene **356**: 39–48

Schenone M, Dančík V, Wagner BK, Clemons PA (2013) Target identification and mechanism of action in chemical biology and drug discovery. Nature Chemical Biology **9**: 232–240

Sharkey TD, Singsaas E (1995) Why plants emit isoprene. Nature **374**: 769–769

Sharkey TD, Wiberley AE, Donohue AR (2008) Isoprene emission from plants: why and how. Annals of Botany **101**: 5–18

Sonner JM, Antognini JF, Dutton RC, Flood P, Gray AT, Harris RA, Homanics GE, Kendig J, Orser B, Raines DE, et al (2003) Inhaled anesthetics and immobility: Mechanisms, mysteries, and minimum alveolar anesthetic concentration. Anesthesia and Analgesia **97**: 718–740

Tang P, Hu J, Liachenko S, Xu Y (1999) Distinctly different interactions of anesthetic and nonimmobilizer with transmembrane channel peptides. Biophysical Journal **77**: 739–746

Tang P, Mandal PK, Zegarra M (2002) Effects of volatile anesthetic on channel structure of gramicidin A. Biophysical Journal **83**: 1413–1420

Tang P, Xu Y (2002) Large-scale molecular dynamics simulations of general anesthetic effects on the ion channel in the fully hydrated membrane: The implication of molecular mechanisms of general anesthesia. Proceedings of the National Academy of Sciences of the United States of America **99**: 16035–16040

Velikova V, Várkonyi Z, Szabó M, Maslenkova L, Nogues I, Kovács L, Peeva V, Busheva M, Garab G, Sharkey TD, et al (2011) Increased thermostability of thylakoid membranes in isoprene-emitting leaves probed with three biophysical techniques. Plant Physiology **157**: 905–916